Faculty of Science

Physics Department

For obtaining the Master's Degree in Physics

Option: Nanophysics

Theme:

Study and simulation of phononic crystal waveguides: effect of localized modes in a phononic waveguide.

Presented by :

Berdamane Imad Eddine

Oudache Abderrezak

Jury Members:

Mr. A. BENHAFFAF	MAA, USDB 1	President
Dr. A. AMRANE	MCB, USDB 1	Examiner
Dr. A. HASSEIN-BEY	MCB, USDB 1	Supervisor
A. L. S. HASSEIN-BEY	Phd student, USDB1/CDTA	Co-Supervisor

Blida, September 27th, 2020

Dedication

I am honored to dedicate this work as a sign of recognition and respect:

To my beloved family who stood with me in good and bad, and have shown me the right path in life.

To ≪my very dear mother≫ who have devoted her entire life to build mine and have waited patiently for the fruits of my good education. No dedication can express my respect, eternal love, and consideration for the sacrifices she endured to make me who I am today, that God protects her and surrounds her with his blessing.

To my teacher's for their support and encouragement throughout my journey.

To my dear friends whom i shared with my joy, my smiles and my passion. This in the memory of those good old days.

To all the 2019/2020 Nanophysics promotion without exception.

Abderrezak

Dedication

I dedicate this work with honor as a sign of recognition and respect:

To ≪my dear parents and my grandmother≫ who have sacrificed their time, health and everything they loved for the sake of my success. No dedication can express my appreciation, respect, and consideration for the sacrifices they made to make me who I am today, that God protects them and surrounds them with his blessing.

To my family who was there for me in good and bad.

To my teacher's for their support and encouragement throughout my path.

To my friends who was there for me in my tough times.

To the Nanophysics 2019/2020 promotion without exception.

Imad Eddine

Acknowledgement

ملخص

في آخر 20 سنة، ظهور (البلورات الصوتية) أدى إلى تغير عدة مفاهيم و فتح عدة أبواب في مختلف الميادين، وساعد في تقديم عدة تطبيقات أفادت البشرية و لا زالت هناك عدة أمور لا تزال غامضة و مخفية حتى الان، وبعضها لم تصل لحد التجربة وهناك عدة توقعات في المستقبل القريب.

الهدف من هذا العمل هو إنشاء عدة أشكال نطبق عليها عدة شروط باستعمال COMSOL انطلاقا من الأعمال السابقة في دراسة خصائص البلورات الصوتية، في المحاولة للوصول إلى تقديم نتائج تساعد في فهم المنطقة الممنوعة (Band-gap) و التأثير عليها لإنتاج أدلة موجية للحصول على كفاءات عالية في نقل المعلومات.

الكلمات المفتاحية: بلورات صوتية، أدلة موجية، أوضاع مترجمة، COMSOL.

Abstract

In the last 20 years, the emergence of (phononic crystals) has changed several concepts and opened several doors in various fields, and helped to present several applications that benefit humanity, and there are still many things that are still obscure and unknown until now, and some of them did not reach the point of experience and there are several Expectations in the near future.

the purpose of this work is to create different structures of phononic crystals by applying different conditions using COMSOL, based on previous works on studying the behavior of the PC's, and trying to get new results that helps us to understand more the band-gap behavior and influencing in it, and produce waveguides to obtain high efficiencies in transmitting information with high Q factor.

Key words: phononic crystals, waveguides, localized modes, COMSOL.

Résumé

Au cours des 20 dernières années, l'émergence des (cristaux phononiques) a changé plusieurs concepts et ouvert plusieurs portes dans divers domaines, et a permis de présenter plusieurs applications qui profitent à l'humanité, et il y a encore beaucoup de choses qui sont encore inconnus et obscurs jusqu'à présent, et certains d'entre eux n'ont pas atteint le point d'expérience et il y a plusieurs attentes dans un proche avenir.

Le but de ce travail est de créer différentes structures de cristaux phononiques en appliquant différentes conditions en utilisant COMSOL, basées sur des travaux précédents sur l'étude du comportement des PnCs, et en essayant d'obtenir de nouveaux résultats qui nous aident à mieux comprendre le comportement de la bande interdite influencer en elle , et produire des guides d'ondes pour obtenir des rendements élevés dans la transmission d'informations avec un facteur Q élevé.

Mots clé: cristaux phononiques, guides d'ondes, modes localisés, COMSOL.

Summary

List of figures and tables

General Introduction

Phononic crystals are some of the main structures that helped to push science forward. They have attracted the researchers' attention since the first day they knew the light and this for their features which allows them to fit and adapt in many fields. They serve several uses when a wave propagates through them, such as for example: waveguides and filters (thanks to the famous band-gap), it depends on how and where we want to use them.

It is in this context, that our study aims by carrying on the previous study to make a simple contribution in the context of highlighting basic knowledge, for the modeling and simulation under COMSOL Multiphysics 5.4 of unit-cell, supercell and multi-supercell models, after subjecting them to certain basic phenomena (Dispersion / Transmission) when a wave propagate through them, and see the reactions obtained before and after the addition of corridors. And that to better understand the behavior of these structures and their functioning.

Our work will be divided into five chapters, all of major importance, which we will try to develop as much as possible, along with an introduction, which essentially presents the motivations and context of this study, and a conclusion, in which we have analyzed and synthesized the different results obtained in our work.

The first chapter will focus on the state of art and generalities of phononic crystals and acoustic waves and their functioning mechanism by describing the interaction phenomena between these two. And finally, we concluded the chapter by some applications of these structures.

Thereafter, the second chapter will be devoted to the numerical study of phononic crystals. We will therefore cite the important equations and theorems which enter in the study, such as wave equations, Bloch-Floquet's theorem, Fourier series...

For the third chapter, we will see the simulation steps we had to follow on COMSOL Multiphysics 5.4 for Dispersion phenomena on a unit-cell and a supercell with / without a corridor.

The same goes for the forth chapter, except in this chapter we followed simulation steps on COMSOL Multiphysics 5.4 for Transmission phenomena on multi-super cells with / without a Perfectly Matched Layer for different corridors.

At the end, the concluded results of the previous simulations will be compared and discussed in the fifth and final chapter.

CHAPTER 1: STATE OF ART OF PHONONIC CRYSTALS

1.1. Introduction

In the last 30 years, the propagation of acoustic/elastic waves in the new periodic elastic artificial materials, are named phononic crystals (PC's). PC's have generated growing interest and significant progress. The periodic nature of PC's gives those novel properties that cannot found in bulk materials, also give as the ability to control the propagation of acoustic/elastic waves, PC's made from composite material which has different density and different elastic properties. The various examinations done on PC's have brought about the featuring of huge numbers of their noteworthy acoustic properties; these results show a particular dispersive character to mechanic/acoustic waves, which strongly depend on the choice of material constituting the crystal as well as its "design" and its conception. That is to say the arrangement and spacing between its constituent elements. The main property of this periodic distribution, which has attracted researchers so much, is the existence possibility of frequency intervals where the PC's behave as a barrier for acoustic/elastic waves. These frequency intervals called phononic band-gaps.

The vast majority of the work on dispersive impacts in PC's is of a theoretical nature and based on different complex digital simulation tool. This has permitted researchers to cover a wide scope of phononic frameworks, and to distinguish their physical behavior. The determination of established researchers have even prompted the origination of new structures, which show physical practices coming out of the standard, and which structure another class of materials called "acoustic metamaterials ".

1.2. Brief history and context

The study of the periodic structures begin in the end of the 19th century in 1887 [1] when Lord Rayleigh studied for the first time theoretically the propagation of electromagnetic waves in a unidirectional periodic dielectric medium. He highlighted the existence of prohibited bands, a wavelength range that does not allow the propagation of waves in the structure. Since these first results, the studies on periodic photonic

structures have multiplied, and showed new remarkable properties, with various applications in the fields of optics wave, electronic and optoelectronics [2–5].

The photonic structure has inspired the researchers to invent new class of periodic structures, called phononic crystals (PC's); these structures made from combination of two materials or more with different density and/or different elastic properties. The year 1988 saw the publication of the works of Tamura *et al* [6] who are the first to study the propagation of phonons in super-lattice. They could theoretically show the possibility of a total reflection of the acoustic wave by a super one-dimensional network designed with a succession of two different materials. In 1993, Sigalas and Economou [7,8], as well as Kushwaha *et al* [9,10], put the evidence of the presence of a prohibited band for acoustic waves in a two-dimensional elastically periodic structure. Since that, several theoretical works on PC's have followed for the past two decades, and treating different systems by using a multitude of numerical simulation methods and by emerging these calculation tools, researchers were able to explore the properties of the PC's, and therefore diversify studies on these structures. In the other hand, the experimental works on PC's did not know a good development as the theoretical works and that due to the lack of equipment or implement in order to properly conduct this kind of studies.

Regarding the theoretical part, the PWE method (*Plane Wave Expansion*) was one of the first methods used by researchers in the 90s for the calculation of the PC's band structures, and continues to be used until today [11–13]. The FDTD (*Finite Difference Time Domain*) [14] method is very commune in photonic, it has been used in 2000 by Sigalas and Garcia [15] to determine the transmission coefficient of acoustic waves in three-dimensional phononic structures. This method has shown its efficiency both for the calculation of the transmission coefficient and for the band structure [16–19], other algorithms have also emerged and adapt more efficiency the nature of the phononic structures studied [20]. Finally, the FEM (*Finite Element Method*) [21] method has been used to calculate the dispersing curves as well as the distribution of the displacement field resulting from the interaction of the waves with PC's.

These simulation methods allowed not only exploring a wide range of complex phononic structures but also to discover and highlight remarkable new properties that go beyond the creation of prohibited bands. Indeed, Page *et al* [22], Schriemer *et al* [23] have demonstrated the possibility of having a slowdown in the group speed of the acoustic wave in a very dispersive phononic medium. In 1998, Sigalas [13,24] showed

that a structural defect in the PC's makes it possible to generate the creation of waves reports located in the forbidden bands, which allowed him to set up a first linear waveguide for elastic waves using a PC [25]. Other studies have continuation exploited the phononic forbidden bands to explore the confinement of the elastic waves bands and their guidance in phononic structures with a point defect, linear or angled [26]. Qiu *et al* [27] have shown on the other hand that PC's may have, at certain frequencies, preferential directions of acoustic wave's propagation.

In addition, new artificial phononic structures designed and made the subject of studies on the propagation and diffusion of long acoustic wave with respect to the periodicity of the structures. In 2000, Liu *et al* [28] indeed carried out a new PC, called local resonant phononic crystal (CPRL), capable of opening prohibited bands in the sonic regime using a periodicity much lower than the wavelengths that propagate there. They have shown that their PC behaves like a medium having a negative effective elastic constant, which integrates it into the category of acoustic metamaterials. Since then, several works have emerged and have focused on the study of acoustic metamaterials with an effective density and / or an effective elastic negative constant [29]. Other work has led to the discovery of new phenomena such as, for example, the negative refraction [30] of acoustic waves by a PC, highlighted in 2000 by Pendry [30].

1.3. Propagation of acoustic waves in periodic structures

In this part, we will discuss some main features of the different types of elastic waves in relation to the structures in which they propagate, in order to better understand PC's and their dispersive behavior in acoustic waves.

1.3.1. Acoustic waves

The wave is a disturbance in an elastic structure within a shape of a vibration as a function of time. This vibration of the structure material in relation to the equilibrium can cause a small displacement of this structure, which returns to its balance after the disappearance of the disturbance. This vibratory behavior is due to the competition between the inertia forces and those of the elastic deformation (the restoring force) by acting on the particles of the structure [31]. Knowing that a material adopts a specific

elastic behavior according to the direction of the deformations which it undergoes compared to its orientation and its crystallographic structure, we can say that the characteristics of an acoustic wave depend on the elastic properties and the density of the medium in which it propagates [32]. These waves can exhibit phenomena like diffraction, reflection and interference when they travel with a characteristic acoustic velocity which depends on the structure they're passing through.

Waves can be classified and divided into different groups according to the medium in which they propagate and the characteristics of the propagation, which brings us to the following types:

- If an elastic wave propagates without encountering an obstacle in a homogeneous and isotropic structure of supposedly infinite dimensions in all space directions, it retains its physical properties throughout its course, and these properties will only depend on its polarization whatever the propagation direction is. We are talking then about a **volume wave**. This type of wave itself is made up of two types of waves:

- Longitudinal waves (pressure wave): They're found in all environments (fluids and solids). The displacement is linked to a volume change (compression waves), and it moves within the propagation direction.
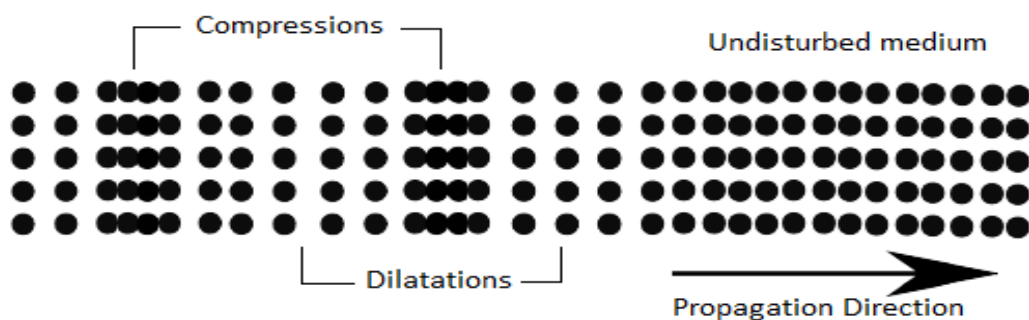
Figure 1.1: Schematic representation of a Longitudinal wave [33].

- Transverse waves (shear waves): They don't exist in non-viscous fluids such as water and air. In solids case, there are always two, which can be degenerated (same velocity, same direction of propagation, but orthogonal polarizations). In this case, the displacement isn't linked to a volume change.
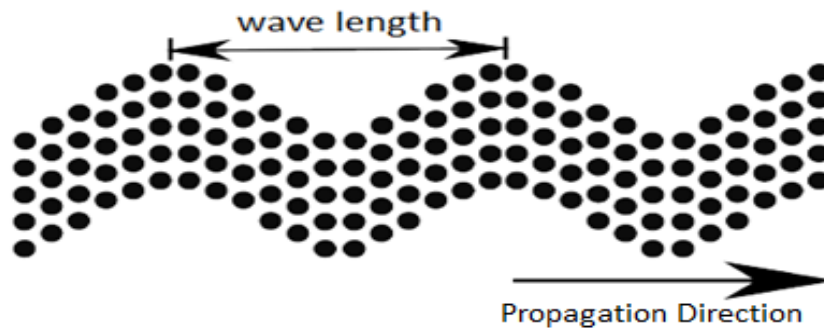
Figure 1.2: Schematic representation of a Transverse wave [33].

In case of an isotropic solid structure, the speed of waves with longitudinal polarization is higher than that of waves with transverse polarization.

- If an elastic wave propagates along a free surface of a medium or along the interface between two different mediums, we are speaking then of a **surface wave** (SAW). The existence of these type of waves was first demonstrated in 1885 by Lord Rayleigh [34]. We distinguish two types of waves in surface waves:

- Rayleigh waves: They exist in fluids and solids. It has an elliptical polarization, and the displacement is linked to a volume variation.
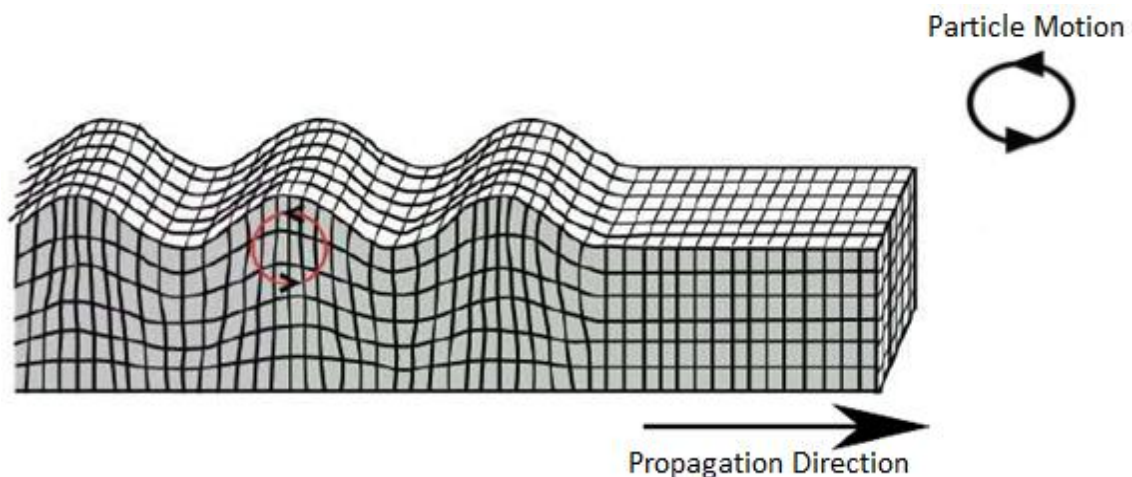
Figure 1.3: Schematic representation of a Rayleigh wave [35].

- Love waves: This type of wave is found particularly in seismology, known as transverse polarized surface waves due to its transverse polarization. Unlike Rayleigh waves, the displacement of these waves isn't linked to a volume variation.
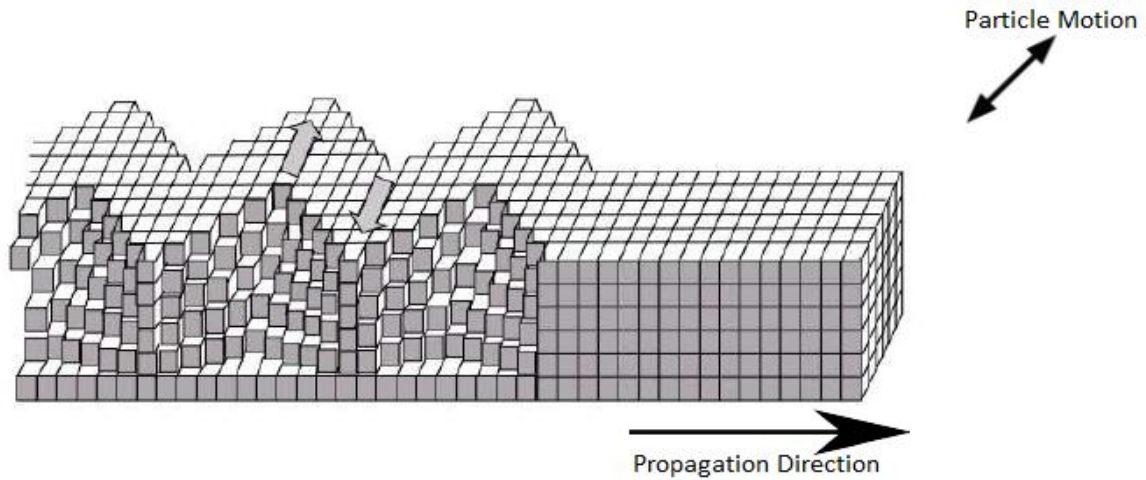
Figure 1.4: Schematic representation of a Love wave [35].

For these two types of waves (Rayleigh and love), the movements amplitude decreases exponentially in depth.

- In 1916, a certain type of wave called **Lamb waves** was discovered by Horace Lamb, who explored the properties of elastic waves and their propagation in an isotropic plate of infinite borders and finite thickness. This solid plate behaves like an elastic waveguide in parallel directions to its free surfaces. The lamb waves appear after the coupling of several surface waves which each propagate on one of the solid plate surfaces. The distance between each surface and another is a few wavelengths (this wavelength is of the same order of magnitude as the plate thickness) [36], which gives rise to lamb waves. In short, we can say that the lamb waves are guided waves which appear after the coupling of the guided surface waves on each side of an isotropic solid plate. In lamb waves we distinguish two modes:

- Symmetrical mode: It's about the lamb waves which have a symmetrical displacement compared to the plane of symmetry which cuts the solid plate in the middle. These modes have a longitudinal polarization.

- <u>Asymmetric mode:</u> It's about the lamb waves which have an asymmetric displacement compared to the plane of symmetry which cuts the solid plate in the middle. These modes have a transverse polarization.
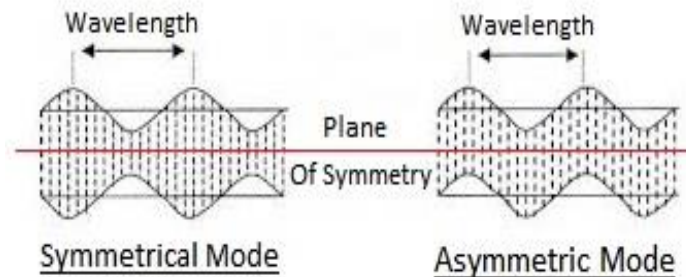
Figure 1.5: Schematic representation of Lamb modes [37].

Finally, we can say that the wave's behavior is related to the environment in which it propagates. Whereas its behavior changes in the boundaries vicinity of the medium in which it propagates, especially when the dimensions of these boundaries become close to the wavelength.

1.3.2. Phononic crystals

Phononic crystals (PC's) are one-two and three dimensional ordered structures composed of at least two materials with different elastic properties (Figure 1.6). These novel synthetic periodic materials are used to control and manipulate the propagation of elastic / acoustic waves in fluids and solids. The periodic nature of PC's and their dispersive behavior gave them novel properties that dragged the attention of scientists and led to many more studies of these crystalline structures. These researches opened the door for several applications such as detection, medical ultrasound imaging...
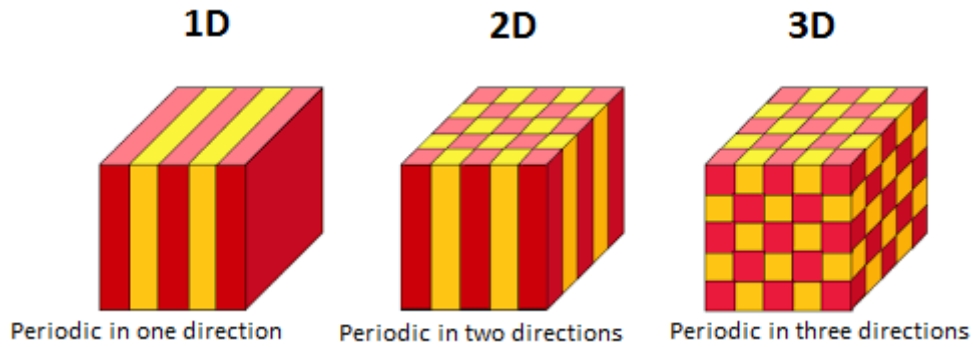
Figure 1.6: Examples of one-two and three dimensional periodic structures [38].

One-dimensional structures are the former models; they have already been studied for a long time and used as dielectric mirrors or optical filters. But, the 2D and 3D PC's has been the subject of most studies in these past years.

For the two-dimensional structures, there are five different types of Bravais lattices (Figure 1.7). These bi-periodic structures are generally composed of dielectric cylinders and they present a simple geometry which facilitates their studies [38].
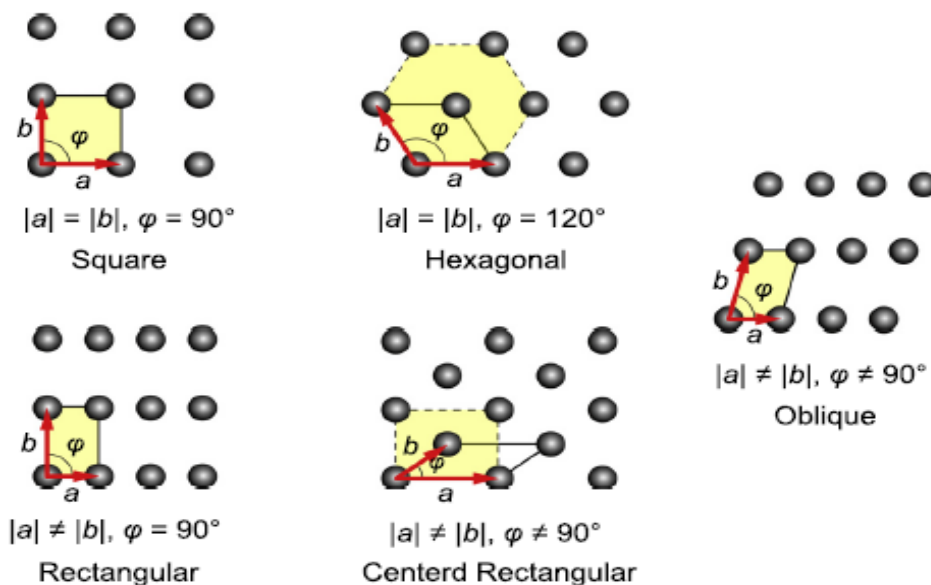
Figure 1.7: Two-dimensional Bravais lattices [39].

And for the three-dimensional structures, they were the first to show the presence of a complete band-gap theoretically in a structure with symmetry cubic face-centered (diamond structure). But the only problem is that these structures are difficult to achieve experimentally.

PC's are considered generally as waveguides or acoustic filters. The filter idea for the audible frequencies was presented as a periodically planted forest. If we remove a row of trees from the periodic structure, the sound can rush into it. As for the frequencies located in a band-gap, the sound can travel without loss in the space provided and it even remains confined there. That explains why the guide sides don't absorb the waves but they act like mirrors that push them out of the periodic structure, and that's why PC's are considered efficient waveguides [33].

1.3.3. Phononic band-gaps

The interaction between PC's and acoustic waves gives the potential existence of band-gaps (Figure 1.8). These are frequency ranges where the phononic crystal behaves as a barrier for acoustic / elastic waves (the penetration of acoustic / elastic waves into the crystal is prohibited). Band-gaps formation is based on Bragg reflections due to the periodicity of the crystal. The propagation of acoustic waves in a medium is generally described by a dispersion relation between frequency (ω) and wave vector (K) [40].
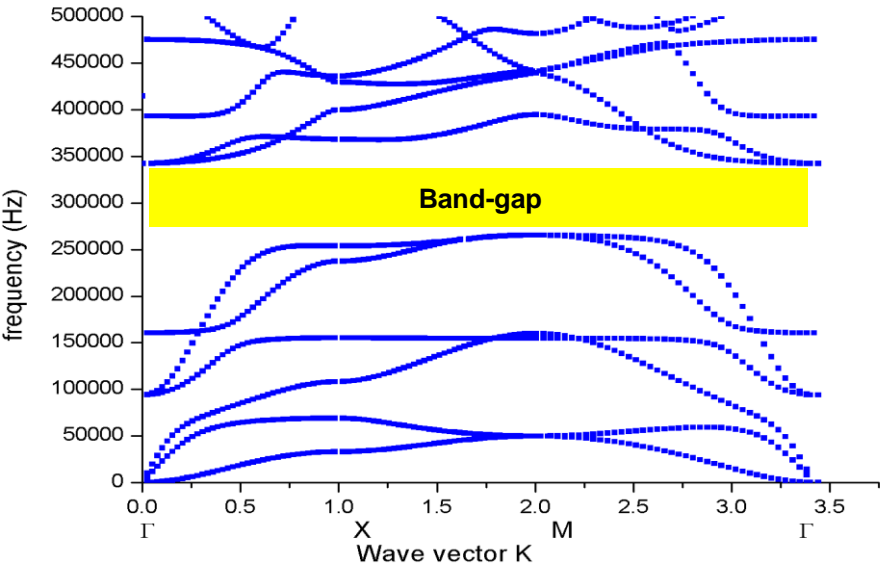
Figure 1.8: Example of phononic crystal band-gap.

Tamura *et al* [6] were among the first to study in detail the Bragg reflection mechanism in a one-dimensional PC (multilayer structure). They have shown that the possibility of having a PC behaving like a barrier for the longitudinal and transverse modes in well defined frequency intervals throughout the first irreducible zone of Brillouin. In addition,

they highlighted a strong attenuation of the waves at these intervals during their transmission in the PC [31].

The geometric parameters that affect the phononic properties are the symmetry of the periodic lattice and the fill factor of the elementary cell. By varying these parameters, we can widen the band-gaps or even make them completely disappear [33]. In 1994, Sigalas and Economou [12] studied a two-dimensional PC at base of a finished thickness plate. They have shown that by varying the plate thickness, they can create a complete band-gap for Lamb waves [31].

The addition of defects to a perfect PC with a phononic band-gap allows for the design of devices like waveguides and cavities to control the propagation of acoustic waves inside the band-gap and to enable novel functionalities in a very compact structure [41].

1.4. Phononic crystals with local resonance (PCLR)

As mentioned before, in 2000, Lui *et al* [42] have implemented new phononic structures with dispersive properties that are out of the ordinary, compared to other classic PC's based on the Bragg mechanism. Indeed, thanks to their structure properties; they have shown that a band-gap can exist for waves having a wavelength much greater than the periodicity of the crystal; which behavior is due to the phenomenon of local resonance. The study started by Lui *et al* [42] was the first real step to create a new class of acoustic materials with unusual behavior, called acoustic metamaterials.

1.4.1. Opening of the prohibited bands by local resonance (LR)

In the PC designed by Liu *et al* [28], the periodicity elements consist of resonators having their own resonance modes which are located at very low frequencies due to the use of very soft material. Each resonator consists of a lead massive heart coated with an elastically very soft elastomer compared to other materials constituting the PC.

These resonators are arranged periodically following a simple cubic structure in an epoxy matrix (Figure 1.9).

| Resonator | Phononic crystal |
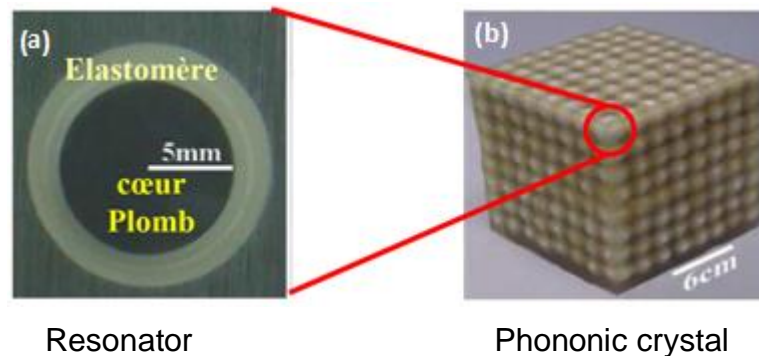
Figure 1.9: (a) Spherical resonator consisting of a lead core coated with a very soft elastomer. (b) Three-dimensional phononic crystal with local resonance [28].

The elastomer-lead assembly behaves as a spring system linked to a mass, thus forming a resonator having resonant modes specific to very low frequencies. The principle of opening the prohibited bands in this type of structures rests on the coupling between the resonance modes of the resonators (localized modes) and the volume modes, which propagate in the PC. When an elastic wave propagate in a phononic medium with a frequency corresponds to the frequency of resonator, these latter interact with it. Under certain conditions, coupling leads to attenuation of the wave. This resonance mechanism thus allows the creation of localized prohibited bands at very low frequencies, where the wavelengths in the epoxy (the matrix) exceed far the periodicity of the PC. In the structure of the (Figure 1.9), Liu *et al* [28] were able to measure the sonic transmission in the crystal using a source emitting sounds and detector microphones placed on the crystal. Attenuations of the acoustic wave could be detected in the forbidden bands at around 380 and 1350Hz where the wavelength of the longitudinal waves in the epoxy counts 300 times the periodicity of the structure (Figure1.10).
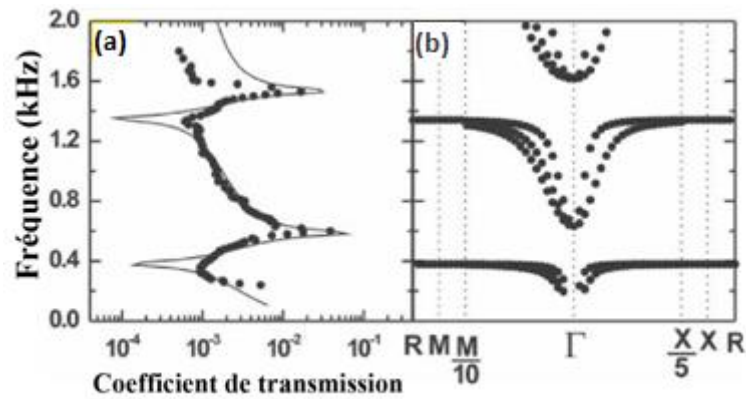
Figure 1.10: Transmission coefficient (a) measured in the PC of (Figure 1.9) as well as the calculated band structure (b) [28].

Other works, mainly theoretical, then focused on the PCLR in developing other three-dimensional structures [43,44]. Likewise, two-dimensional systems based on inclusions of infinite cylinders have been the subject of several studies for LR [31], without forgetting the PCLR in the form of plates for Lamb waves [29]. Wang *et al* [45] have even highlighted the opening of the prohibited bands by LR in a simple one-dimensional structure.

1.4.2. Properties of PCLR

Since the possibility of opening the prohibited bands by the mechanism of local resonance, work on these structures at RL has multiplied, highlighting their particular properties and allowing a better understanding of their vibrational behaviors. So, other theoretical work has emerged concerning new PCLRs made up of resonator arrangements in simple cubic configuration or face centered cubic [43,44]. The condition to open a prohibited band in this case rests essentially on a wise choice of the materials constituting the resonators. Indeed, these latter must contain an elastically very soft material, compared to other materials of the structure. Thus, in another study, Liu *et al* [46] compared two PC's, the first consisting of lead-based resonators coated with a very soft elastomer and incorporated in a silicon matrix, and the second with lead resonators coated with a material with elastic properties very close and incorporated in the same silicon matrix. They have shown that with the first system, they obtain much-localized modes of vibration at resonator level, which generates complete band-gap at

resonance frequencies, which are very low. As for the second PC's, where the elastic behaviors of materials are very close, no resonance is located there, and the band-gap created is due to the Bragg scattering mechanism. As a result, the prohibited bands created by the LR mechanism essentially depend on the much localized resonance modes of resonators. This effect is very visible in the band structure of the PCLR where we can notice the presence of flat modes (Figure 1.10.(b)) in which the frequency does not hardly depends on the wave vector. This implies a zero group speed for these modes, which characterize their wave aspect very localized in the PC's.

Furthermore, this type of prohibited band does not depend on the periodicity or the symmetry of PC's. Indeed, and as an example, we can cite the work of P.Sheng *et al* [43]. The latter studied a structure with LR similar to that of (Figure 1.10.(a)) where the resonators, consisting of a lead core coated with an elastomer, have arranged so as not to respect any periodicity. They have shown that their structure exhibits wave attenuation at around 400Hz. This result has also obtained with a similar PCLR, but with a simple cubic periodic arrangement of the resonators. This independence of the forbidden band of symmetry and periodicity is valid if the resonators are sufficiently spaced apart so that their resonance modes do not interact and thus avoid any coupling in them.

Finally, the PCLRs adopt a behavior, which has attracted so much and still attracts researchers since they can behave under certain configurations and conditions like a medium with negative elastic constant and / or effective density, that we will note respectively k_{eff} and ρ_{eff}. This behavior was underlined by Liu *et al* [28] in their structure presented in (Figure 1.9), which therefore fits into the class of acoustic metamaterials.

1.4.3. Acoustic metamaterials

The name of acoustic metamaterials is given to environments with unusual elastic properties for the propagation of acoustic or elastic waves. The origin of these special mediums comes from the analogy made with optical metamaterials for electromagnetic waves that have long attracted the interest of scientists. The existence idea of this type of artificial mediums dates back to 1968, when Veselago proposed a new material with negative refractive index.

Optical metamaterials are generally structures with resonators in their design, allowing them to behave, on frequency intervals well determined, as a medium with effective permittivity and / or negative permeability [47]. In the case of a simultaneous negativity, we are in the presence of a "double negativity" [47]. This property thus gives these environments remarkable behaviors leading to reverse effects like negative refraction[30] which offers the possibility of manufacture of "super lenses" [30] or "super prism" [48], or creating a reverse Doppler effect [49]. It should be noted, however, that negative refraction can also be created with a photonic crystal without it necessarily having a "double negativity" [50].

By analogy to electromagnetic metamaterials, it became obvious to explore the reproducing possibility of the same remarkable effects for acoustic waves in inventing what we call today acoustic metamaterials. These are periodic structures provided with resonators giving rise to prohibited bands openings. They behave like mediums with a negative effective elastic constant and / or a negative effective density at the resonant frequencies.

By analogy with "double negativity" in electromagnetism [47], Jensen Li and C.T.Chan [51] have theoretically demonstrated the possibility of having both an elastic constant and a negative effective density in a PCLR (rubber spheres suspended in the water) for wavelengths far exceeding the periodicity of the crystal, that is to say an Acoustic "double negativity" of their structure. This is physically explained by the fact that the medium can manifest an abnormal elastic behavior, as for example a response to a compressive force by expansion or displacement in the opposite direction to the effort exerted. This physical behavior is obviously impossible and cannot be naturally intrinsic to a medium, unlike the electromagnetic case where the permittivity and permeability may well be negative. However, in PCLR, composed of very soft resonators, compared to the very hard material of the matrix, the reasoning adopted to describe its dynamic behavior changes in the presence of local resonance phenomenon. Indeed, Milton and Willis [52] show that the behavior of a composite material, that is to say PCLR in our case, must be defined in the frame work of a new law which replaces that describing the Newtonian movement. They thus places a new and more generalized formulation of elastodynamic equations, which allow us to analyze certain extreme cases, where the environment studied manifests a negative effective density at local resonant frequencies. By taking this approach, the effect of "Double negativity" of effective

density and elastic constant has been highlighted on several PCLRs designed by researchers interested in acoustic metamaterials [44].

Finally, and to better understand the vibrational behaviors of acoustic metamaterials, in particular at resonance frequencies, some analytic studies have conducted on simple models. These have composed of a well-defined arrangement and grouping of masses and springs modeling a local resonance system [53]. With the latter, the researchers were easily able to reproduce a negative effective mass effect at resonant frequencies where the elastic energy of the wave is essentially confined, leading to the wave's attenuation throughout the system.

All the studies carried out on PC's and acoustic metamaterials are essentially theoretical, but the researchers did not miss the opportunity to start a set of experimental realizations making it possible to complete the observations and highlight most of the phononic systems properties. The third part of this chapter will be devoted to the main experimental studies carried out on PC's, in order to develop their use in the daily life of humans.

1.5. Experimental studies and applications

The first studies on PC between the end of the 80s and the beginning of the 90s were purely theoretical. They allowed to explore the dispersive properties for the acoustic waves and to predict the possibility of the prohibited bands existence. It was necessary to initiate experimental studies in order to establish the acoustic "barrier" behavior. It was not very obvious at the time, taking into account the difficulties linked not to the design of the PC's, but also and mostly to the reliable characterization means that had designed and implanted.

Despite this, the race to experimental studies had already started since the first theoretical work on PC's.

1.5.1. Examples of experimental achievements

When we talk about experimental measurement in phononic network without mentioning the cells made by Martinez Sala *et al* in 1995 on sculpture by Eusebio Sempere exhibited in the garden of the Juan March Foundation in Madrid. This sculpture made up of steel cylinders of 2.9cm in diameter distributed in a simple square network with a pitch of 10cm, has marked attenuation (Figure 1.11) [54].

Figure 1.11: This modern work of art by E.Sempere represents a two-dimensional phononic crystal of steel rods with a diameter of 2.9cm arranged in a square network with a period equal to 10cm [54].

This structure only admits partial forbidden bands, i.e. prohibited frequencies only in certain directions of space. However, the phononic crystals have considered being structures having the possibility of presenting absolute forbidden bands, therefore in any direction of the incident wave.

Other experimental measurements followed, in the goal to confirm the presence of the absolute prohibited bands in phononic structures; and it was the work of several researchers among whom we can cite Sanchez Perez and all, in 1998 they worked on solid/fluid structures by considering a 2D square or hexagonal system of steel cylinders arranged in the air [55]. In the other hand, Montero and Espinosa have experimented the fluid / solid structures for longitudinal wave modes, composed by cylinders of mercury and aluminum matrix; no propagation in the frequency range between 1000

and 1120KHz, no matter what the direction we measure in [56,57]. Simultaneously, Vasseur *et al* studied solid/solid structures by periodically placing aluminum cylinders in an epoxy resin. The results demonstrated the possibility of attenuating the waves in wide frequency ranges, and for all incident direction, with phononic crystals therefore having total forbidden bands [58].

1.5.2. Guidance in Phononic structures

If initially, the artificial materials designed for their properties of the prohibited band preventing the propagation of elastic/acoustic waves, recent and current researches have devoted to a real engineering of the waves dispersion by structuring the material at various scales relative to the target wavelength. It is no longer only a question today of blocking the propagation of waves but also of "controlling" these latter at will; this is the purpose of the waveguide design.

Any study of guidance realization in phononic, requires the presence of the prohibited bands; thereby, the phononic crystals with total bang-gaps are elements well indicated for making waveguides. Acoustic wave guidance can be obtained by pre-forming a structural linear "imperfection" in the Phononic crystal or by arranging crystals to change the direction of propagation [59]. Some researchers have been able to change the direction of a sound beam using L-shaped guides [60].

Khelif *et al* [59] in their theoretical and experimental work have shown the possibility of confirming and guiding elastic waves in a phononic crystal with cylindrical inclusion having a linear or angled defect (Figure 1.12.(a)). The frequencies of the transmission waves in the guides are thus in the frequency range of the forbidden band defined by the flawless phononic crystal. In addition, by removing in the perpendicular direction to this hollow guide one or more cylinders, we can give birth to a finite size resonator (Figure 1.12.(b)) which has the effect of preventing the transmission of some of these frequencies. For example, we can remove the two cylinders in the perpendicular directions, and we create an angled guide with "L" form (Figure 1.12.(c)). We than see that the wave of well-defined frequency can propagate by following the best shape of the guide [61].
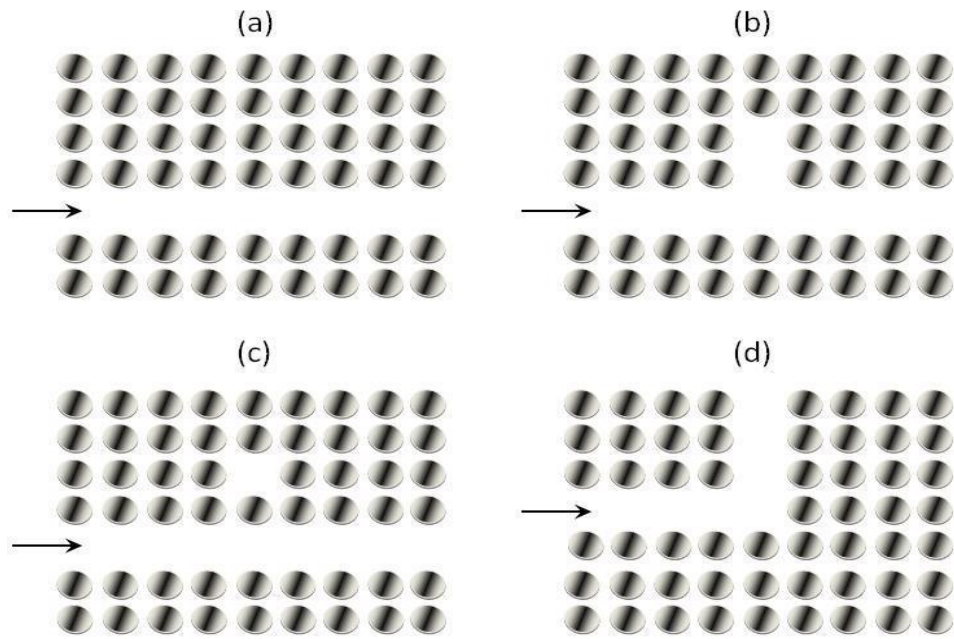
Figure 1.12: Different geometries of waveguides and filters obtained from a two-dimensional Phononic crystal: (a) linear guide, (b) resonator, (c) cavity created near the linear guide, (d) bent guide. The arrow indicates the direction of propagation of the incident wave beam [61].

Most of the wave guiding and confinement work carried out so far has focused on the Phononic prohibited band created by the Bragg mechanism. As these appear for waves having wavelengths of the order of the structure periodicity, the waveguides generally have width of the same order. On the other hand, few studies have therefore concerned PCLRs [62] because these latter have forbidden bands at low frequencies; the associated wavelengths are very wide compared to the periodicity of the structure [31].

Oudich [31], as part of his doctoral thesis was interested in the confinement and guidance of Lamb waves in a PCLR in the sonic and hypersonic regimes, considering an epoxy plate on which cylinders of elastomer are periodically arranged in a square symmetry. After, he created a waveguide by making a linear "imperfection", after removing a row of items from the PC. His interest was focusing on the propagation of Lamb waves in the direction defined by this guide.
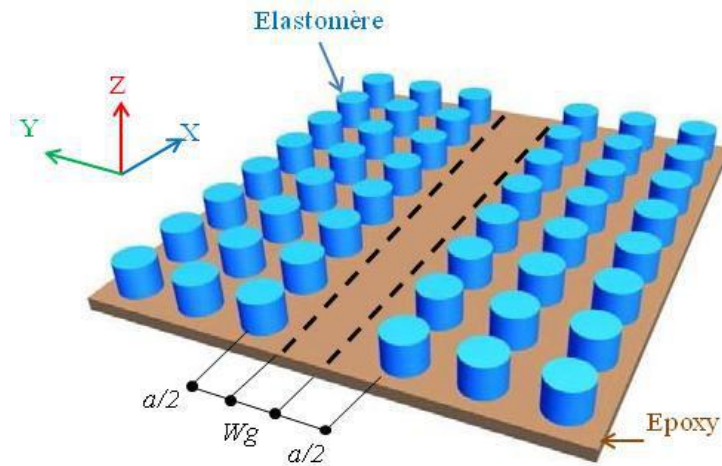
Figure 1.13: Linear guide structure studied. The width of the guide is noted Wg and is in the direction X of the Cartesian coordinate system [31].

He showed the possibility of confinement, guidance and transmission of a single defect mode, and this, compared to the Bragg mechanism, where several defect modes appear in the band-gap. He concluded that guidance using band-gaps based on local resonance could open up application possibilities for the manufacture of devices for filtering or demultiplexing.

We can also design guides, filtering and demultiplexers by local resonances in order to obtain a selective filter with an easily adjustable frequency. As a reminder, multiplexing is the operation that allows us to inject into a single guide incoming frequencies of two or more waveguides [63]. Demultiplexing is the reverse operation allowing us to extract frequencies from one waveguide and send them to another waveguide. This type of phononic crystal can find applications in the field of sensors [64].

1.5.3. Potential applications of PCs

Controlling the waves propagation in a complex medium is a major challenge, with this important challenge are associated objectives that are just as important. The development of PC's has contributed to extend their potential applications as it ranges from the control of seismic waves in the earth's crust at a frequency of a few tens of Hz

or as barriers for sound waves in buildings, highways, airports, etc. To the control of phonons in quantum systems around the Terahertz. Researches in this domain (based on forbidden bands and the possibility of guidance in phononic structures) has pushed forward with a big step the uses of phononic crystals not only in the information, communication and technology field, but also the potential use of PC's that could be used in sensors or filters for various detection and measurement applications. In general, filtering is a method that allows us to separate and select elements with the help of a filter from a stream. This is why in our case, the PC's serves as a filter that separates the acoustic waves having frequencies determined from the initial frequencies. The PC's serves as a waveguide to isolate some information among several carried by the wave by allowing certain frequencies to pass in the frequency range of the band-gap. Therefore, it is possible to eliminate undesirable waves (such as parasitic waves) on well-defined frequency intervals, while acting on the band-gap.

Since the field of use of PC's is very vast, we mention some possible potential applications : the potential use of PC's in energy recovery and harvesting especially in the field of clean and renewable energies, the development of high-frequency signal processing devices for wireless communications, bio-detection applications in gaseous and liquid environments, design of hybrid waveguides (simultaneous confinement of photons and phonons) to obtain acousto-optical and opto-mechanical devices used in communication, etc [32,56,65-66].

CHAPTER 2: NUMERICAL METHODS FOR THE STUDY OF PHONONIC CRYSTALS

2. Theoretical formulation

2.1. Wave equation

In the context of linear elasticity, the propagation of an elastic wave in a composite and isotropic medium given by the following equations [64,67]:

$$\rho(\vec{r})\,\frac{\partial^2 u_i(\vec{r},t)}{\partial t^2} = \sum_j \frac{\partial \sigma_{ij}(\vec{r},t)}{\partial x_j} \qquad (2.1)$$

$$\sigma_{ij}(\vec{r},t) = c_{ijkl}.\,\varepsilon_{ij} \qquad (2.2)$$

$$\varepsilon_{ij} = \frac{1}{2}\left(\frac{\partial u_i(\vec{r},t)}{\partial x_j} + \frac{\partial u_j(\vec{r},t)}{\partial x_i}\right) \qquad (2.3)$$

In which $\rho(\vec{r})$ is the density of the crystal at the point identified by the vector $\vec{r}$, u_{ij} represents the displacement in direction i, at point $\vec{r}$, ε_{ij} designates the tensor of the strains, C_{ijkl} the tensor of the elastic constants and $\sigma_{ij}(\vec{r},t)$ the tensor of the stresses perceived locally by the crystal at the point $\vec{r}$.

Many methods exist to solve these propagation equations and describe the behavior of the structure. Among them, we can cite:

- Plane waves (*PWE*);

- The finite difference time domain (*FDTD*) method;

- The finite element method (*FEM*);

- Transfer matrices;

- Green's functions.

2.2. Bloch-Floquet's theorem and Fourier series of a periodic function [68]

The theory of Bloch-Floquet is a transformation function that intervenes as a tool for analyzing differential equation to periodic coefficients. It mainly used for the modeling of the propagation of waves passing through periodic is one or several directions.

In addition, the method of Bloch-Floquet used for determination of the dispersion diagrams of the periodic structures. The constitutive low of material assumed to be linear, elastic and isotropic.

Stated in 1928, Bloch's theorem initially used to describe the function of electronic waves in a periodic potential. Indeed, in semiconductor physics, the band structure obtained by solving the problem with a one body (an electron) of the equation of Schrödinger in the reciprocal network. The periodicity of the potential energy in a crystal allows the use of the Bloch-Floquet. This establishes that if the potential energy $E(r)$ is periodic with the period of the structure, then wave function $\phi_k(r)$ solution of the Schrödinger equation is of the form [69]: $\vec{k} = \boldsymbol{k} , \vec{r} = \boldsymbol{r}$

$$\phi_k(r) = u_k(r)e^{jkr} \tag{2.4}$$

K obviously represents the wave vector. This theorem transposed to periodic photonic and Phononic structures then, for which the periodicity of the potential have been replaced by that of the refraction for the former and by the elastic constants for the latter. The Bloch-Floquet function is periodic, in direct space, this allows therefore to decompose them into Fourier series: $\vec{G} = \boldsymbol{G}$

$$\phi(r) = \sum_G \phi(G)e^{j\boldsymbol{G}.r} \tag{2.5}$$

The periodicity of the Bloch-Floquet function leads to redundancy of values of the wave's vectors determined by solving the equation over all space. Indeed to be limited very relevant of this vector, we can solve only in the irreducible Brillouin zone, in the direct network as in the reciprocal network.

The density and the elastic parameters are periodical functions of the position. The means that ρ and c_{ij} are functions of x and y coordinates and where the z-axis of the cylinders as in our case. Considering the double periodicity in the xOy plan, ρ and c_{ij} can be written as Fourier series.

$$\rho(r) = \rho(x, y) = \sum_G \rho(G) \, e^{jGr} \qquad (2.6)$$

And

$$c_{ij}(r) = c_{ij}(x, y) = \sum_G c_{ij}(G) e^{jGr} \qquad (2.7)$$

2.3. Direct network, reciprocal network

We use the tool of crystallography and solid-state physics in order to represent in a precise and complete way the properties of periodic media. A crystalline structure 1D, 2D or 3D combine the direct network of Bravais. This is the repetition of an elementary pattern according to a vector a_i with i= [1, 2, 3]. We associates with this direct network reciprocal network whose primitive vectors b_j, with j = [1, 2, 3] are defined such that $b_{-i}, a_j = 2\pi\delta_{ij}$ (δ_{ij} the symbol of kronecker).

The Brillouin zone obtained from the reciprocal lattice that has the same symmetry properties are the Bravais lattice. For the same reasons of symmetry, we can reduce this area to the irreducible zone of Brillouin while contains the points of high symmetry or critical points of the network.

2.4. Brillouin zone

With his many contributions to quantum mechanics and condensed matter physics, Brillouin was at the origin of the development of concept of the zones which bear its name:"Brillouin zones". This discovery has laid the foundations for a rigorous mathematical treatment of propagation movements of waves is the space of the reciprocal network; he has been applied to all problems involving wave's propagation in a medium periodic. Its formalism gives direct access to the dispersion curves of a periodic structure, i.e. the frequency depending on the number or wave vector.

The first Brillouin zone is the elementary cell of space reciprocal where the points are close to the origin than to all the others nodes of the periodic network; it therefore has the symmetry of the Bravais lattice. This area uniquely defined by the method for constructing the Wigner-Seitz (Figure 2.1).
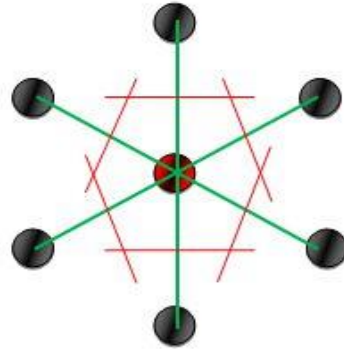
Figure 2.1: Method of construction of the Wigner-Seitz cell.

Figures 2.2 and 2.3 show different examples of periodic networks as well as the corresponding irreducible Brillouin zones.
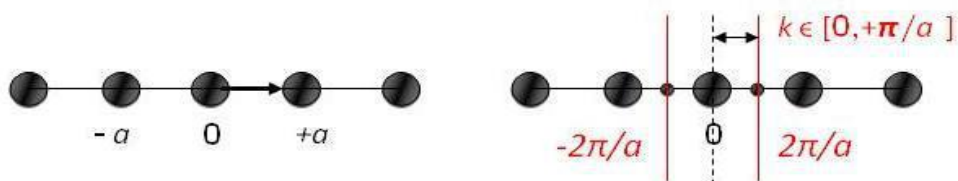
Figure 2.2: Example of a one-dimensional periodic lattice (left) and corresponding Brillouin zone (right). The interval [-π / a; +π / a] is the first Brillouin zone and [0; +π / a] the irreducible Brillouin zone.
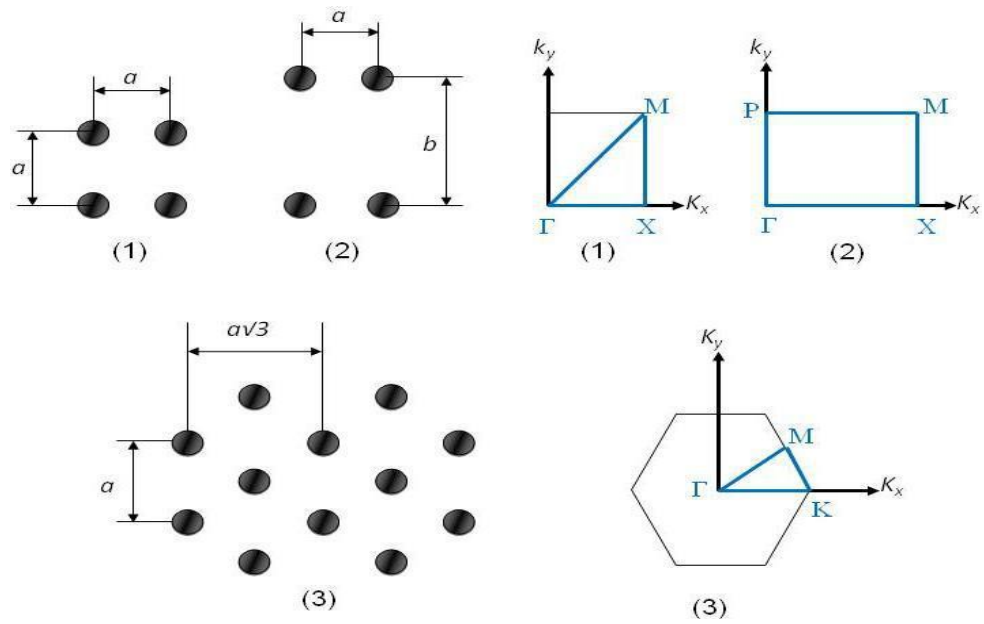
Figure 2.3: Example of a one-dimensional periodic lattice (left) and corresponding Brillouin zone (right). The interval [-**π** / a; +**π** / a] is the first Brillouin zone and [0; +**π** / a] the irreducible Brillouin zone.

In the 1D and 2D cases, the first Brillouin zone obtained by drawing the perpendicular bisectors of the segments joining the origin to the nodes closet to the reciprocal network (Figures 2.1 and 2.2). From the domain thus delimited, we can cover the entire reciprocal space. It the words, it suffices to change k in this domain to reciprocal all the crystal dispersion curves. This domain of evolution of k can be further reduced by taking advantage of the symmetry of the crystal. In the 1D, the symmetry of the crystal with respect to the origin has the consequence that, if a wave of vector k and frequency ω is the solution of the problem, then the wave propagation in the opposite direction, of the vector –k and of same frequency, is also. We can thus restrict the study interval to [0;+π/a] instead of [-π/a; +π/a] where is the pitch of the network (Figure 2.1). Now consider the two-dimensional crystal with square symmetry. This supposedly infinite periodic structure has 4 axes of symmetry which are deduce from each other by symmetries of $\pi/4$. The reciprocal lattice is also a square lattice and the first Brillouin zone (Figure2.3.(1)) defined by:

$$-\frac{\pi}{4} \leq k_x \leq +\frac{\pi}{4} \quad \text{And} \quad -\frac{\pi}{4} \leq k_y \leq +\frac{\pi}{4}$$

It has been shown that the study interval of k can be further reduced by using the different symmetry of the structures. Finally, the study interval of the values of k reduced to a right isosceles triangle whose two equal sides have length π/a. the point Γ(0,0), X(π,0) and M(π,π) denote the three vertices of the triangle which constitutes the irreducible Brillouin zone of the square lattice (Figure 2.3.(1)). In the study of scatter plots, we generally limit ourselves to the three sides of the triangle.

In the case of a two-dimensional crystal with rectangular symmetry of the length a and width b, the reciprocal lattice is also a rectangular lattice and the first Brillouin zone is a rectangle (Figure 2.3.(2)) whose length is π/a and width π/b [70]. Again, in the study of scatter plots, we limit ourselves to the four sides of the rectangle [71].

In the case of a two-Dimensional crystal with hexagonal symmetry, the reciprocal lattice is also a hexagonal lattice and first Brillouin zone is a hexagon (Figure 2.3.(3)). In this case, we have axes of symmetry, which are deduced from each other by rotation of $\pi/6$ with invariance by rotation $\pi/3$. It show that the irreducible Brillouin zone is an usually denote by Γ(0,0), k($4\pi/3a$,0) and M(π/a, π/b). As for the first case, note that in the study of scatter diagrams, we limit ourselves to the three sides of the triangle.

2.5. Propagation of elastic waves in solids

The study of vibration solids is attracting growing interest among mechanics and physicists. From the point of view of the propagation of elastic waves, the diversity of the different polarization likely to propagate within a continuous medium enriches day by day the physics of solids, particularly that which relates to periodic structures.

2.5.1. Basic concepts of the elastic waves

The equation describing the linear propagation of elastic waves is solids, called Navies' equation, obtained from three fundamental relations:

- The motion equation, from the fundamental relation (2.8), with ρ the density, F the resultant of the υ volumetric force, μ the displacement field, and σ the stress tensor.

$$\rho \frac{\partial^2 \mu}{\partial t^2} = div(\sigma) + \rho f \qquad (2.8)$$

- Hooke's law or Stress-strain relation (2.9) written in convention of Einstein, with ε the strain tensor and C_{ijkl} the elastic tensor.

$$\sigma_{ij} = C_{ijkl} \cdot \varepsilon_{kl} \tag{2.9}$$

- The Cauchy relation or displacement-strain (2.10) with μ_i the components of the displacement field and x_i the directions of space. $\vec{u} = \boldsymbol{u}$

$$\varepsilon_{ij} = \frac{1}{2}\left(\frac{\partial \boldsymbol{u}_i}{\partial x_j} + \frac{\partial \boldsymbol{u}_j}{\partial x_i}\right) \tag{2.10}$$

2.5.2. Simplification of the elasticity tensor

The elastic nature of a materials contain in expression of C_{ijkl} tensor. This tensor of order 4 initially has 81 elements. By symmetry arguments concerning the stress tensor, we know that the elements of the elasticity tensor obtained by relation (2.9) will be redundant.

We can simplify the elasticity tensor to $C_{ijkl} = C_{\alpha\beta}$ with α and β can take the values from 1 to 6 with convention $(11) \Leftrightarrow 1, (22) \Leftrightarrow 2, (33) \Leftrightarrow 3, (23) = (32) \Leftrightarrow 4, (13) = (31) \Leftrightarrow 5, (12) = (21) \Leftrightarrow 6$.

In the elastic strain, where the solid returns to its initial state in the absence of external action, we can show that this 6*6 matrix is also symmetrical with respect to the main diagonal. So there so there are 21 elements to be determined to fully characterize the elastic response of a solid medium. In the case of a homogeneous isotropic medium, it can show that only a pair of coefficients c_{11} and c_{12} can describe the 6*6 matrix.U

$$C_{\alpha\beta} = \begin{bmatrix} C_{11} & C_{12} & C_{13} & 0 & 0 & 0 \\ C_{21} & C_{22} & C_{23} & 0 & 0 & 0 \\ C_{31} & C_{32} & C_{33} & 0 & 0 & 0 \\ 0 & 0 & 0 & C_{44} & 0 & 0 \\ 0 & 0 & 0 & 0 & C_{44} & 0 \\ 0 & 0 & 0 & 0 & 0 & C_{44} \end{bmatrix} \tag{2.11}$$

It should be noted that the coefficients C_{11}, C_{12} and C_{44} can be express as a function of the Young modulus E and Poisson ratio ν or as function of lame coefficients μ and λ.

$$C_{11} = \frac{E(1-\nu)}{(1+\nu)(1-\nu)} = \lambda + 2\mu \tag{2.12}$$

$$C_{12} = \frac{E\nu}{(1+\nu)(1-\nu)} = \lambda \tag{2.13}$$

$$C_{44} = \frac{E}{2(1+\nu)} = \mu = \frac{C_{11}-C_{12}}{2} \tag{2.14}$$

For an isotropic elastic material, the elasticity tensor is equal to:

$$C_{ijkl} = \lambda\delta_{ij}.\delta_{kl} + \mu(\delta_{jk}.\delta_{il} + \delta_{jl}.\delta_{ik}) \tag{2.15}$$

2.5.3. Navies' equation for a homogenous isotropic solid

In the case of a homogenous isotropic solid, Hooke's relation is simplified (2.16) with the δ_{ij} the symbol of kronecker and ε_{kk} the sum of the diagonal elements of ε.

$$\sigma_{ij} = \lambda\varepsilon_{kk}.\delta_{ij} + 2\mu\varepsilon_{ij} \tag{2.16}$$

Or

$$\varepsilon_{ij} = \frac{1}{2\mu}\sigma_{ij} - \frac{\lambda}{2\mu(3\lambda+2\mu)}\sigma_{kk}\delta_{ij} \tag{2.17}$$

By replacing this expression in Cauchy's formula (2.10) then in the motion equation (2.8), we find the formula of the elastic of Navies' (2.18) defined for each displacement component u_i.

$$\rho\frac{\partial^2 u_i}{\partial t^2} = \mu\Delta\mathbf{u} + (\lambda + \mu)\nabla(\nabla.\boldsymbol{u}) = (\lambda + 2\mu)\nabla(\nabla.\mathbf{u}) - \mu\nabla \wedge (\nabla \wedge \mathbf{u}) \tag{2.18}$$

2.6. The finite element method

The finite element method, called FEM (*Finite Element Method*), is widely used in numerical simulation for solving equations with partial derivatives, describing physical phenomena. Historically, its first and wide uses concern the problems related to mechanical structures requiring the search for solutions of stresses and strains in elastic media. This is also the case for the study of the propagation of elastic acoustic waves in Phononic media. Indeed, the method is easily prepared for the application in the elaboration of the Eigen value problems allowing the computation of the band structures. Among its applications in Phononics, we can cite the work of Khelif *et al* [21] who used it to calculate the dispersion curves of a two-dimensional PC made up of cylindrical inclusions in a plate. The opening of forbidden bands as well as the guiding of elastic waves in these Phononic structures with inclusions [72] were also studied by using the finite element method. T.Chen and T-T.Wu were also interested in band structures and in the guiding of elastic waves, but in a new type of PC made up of cylinders periodically deposited on an aluminum plate. In all these studies, FEM has shown its efficiency in terms of convergence and computation time, compared to PWE, especially in the case of finished plates.

2.6.1. General principle

The finite element method is suitable for solving almost all types of partial differential equations (PDEs) governing any physical problem, in particular the equations relating to the propagation of elastic waves.

For an acoustic or elastic wave propagating in a cubic or isotropic medium, the propagation equations are written as follows:

$$
\begin{cases}
\rho\omega^2 \boldsymbol{u}_x = \frac{\partial}{\partial x}\left(C_{11}\frac{\partial \boldsymbol{u}_x}{\partial x} + C_{12}\frac{\partial \boldsymbol{u}_y}{\partial y} + C_{12}\frac{\partial \boldsymbol{u}_z}{\partial z}\right) + \frac{\partial}{\partial y}\left(C_{44}\frac{\partial \boldsymbol{u}_x}{\partial y} + C_{44}\frac{\partial \boldsymbol{u}_y}{\partial x}\right) + \frac{\partial}{\partial z}\left(C_{44}\frac{\partial \boldsymbol{u}_x}{\partial z} + C_{44}\frac{\partial \boldsymbol{u}_z}{\partial x}\right) \\[3mm]
\rho\omega^2 \boldsymbol{u}_y = \frac{\partial}{\partial y}\left(C_{12}\frac{\partial \boldsymbol{u}_x}{\partial x} + C_{11}\frac{\partial \boldsymbol{u}_y}{\partial y} + C_{12}\frac{\partial \boldsymbol{u}_z}{\partial z}\right) + \frac{\partial}{\partial z}\left(C_{44}\frac{\partial \boldsymbol{u}_y}{\partial z} + C_{44}\frac{\partial \boldsymbol{u}_w}{\partial y}\right) + \frac{\partial}{\partial x}\left(C_{44}\frac{\partial \boldsymbol{u}_x}{\partial y} + C_{44}\frac{\partial \boldsymbol{u}_y}{\partial x}\right) \\[3mm]
\rho\omega^2 \boldsymbol{u}_z = \frac{\partial}{\partial z}\left(C_{12}\frac{\partial \boldsymbol{u}_x}{\partial x} + C_{12}\frac{\partial \boldsymbol{u}_y}{\partial y} + C_{11}\frac{\partial \boldsymbol{u}_z}{\partial x}\right) + \frac{\partial}{\partial x}\left(C_{44}\frac{\partial \boldsymbol{u}_x}{\partial z} + C_{44}\frac{\partial \boldsymbol{u}_z}{\partial x}\right) + \frac{\partial}{\partial y}\left(C_{44}\frac{\partial \boldsymbol{u}_y}{\partial z} + C_{44}\frac{\partial \boldsymbol{u}_z}{\partial y}\right)
\end{cases}
$$

$$(2.19)$$

Where the unknown functions are the components of the field of displacement $(\boldsymbol{u}_i)_{i\in\{x,y,z\}}$. To this system of equations are added the boundary conditions which constrain the sought solutions.

In order to describe the finite element method more easily, we will start from a more general formulation by writing the system (2.19) rather in the following form:

$$-\nabla.(C\nabla\boldsymbol{u}) = \omega^2\boldsymbol{u} \qquad\qquad (2.20)$$

This equation is to be solved on a domain $\boldsymbol{\Omega}$ of $\mathbf{IR}^3$. With the boundary conditions on the $\delta\boldsymbol{\Omega}$ boundary of the domain $\boldsymbol{\Omega}$.

It specify that the adhesion of $\boldsymbol{\Omega}$, noted $\overline{\boldsymbol{\Omega}} = \boldsymbol{\Omega} \cup \partial\boldsymbol{\Omega}$, is a compact set.

The principle of the finite element method can be summarized as follows:

- Writing in the variational form: the partial differential equations written in a verified variational form for test functions belonging to a well-defined vector space V. This form is called the weak form of the problem;
- And discretization: the solution of the variational problem is decomposed in the base of a finite dimensional vector space $V_N \epsilon V$. The elements of this base called the shape functions.

The variational formulation of the problem is then expressed as a function of the shape functions of the space V_N, and the system is finally written in matrix form. The resolution of the matrix system makes it possible to obtain the solution function of the problem.

CHAPTER 3: UNIT-CELL AND SUPERCELL PC's MODELING FOR DISPERSION CALCULATION

3.1. Comsol Multiphysics

3.1.1. History

Mr. Svante Littmarck and Mr. Farhad [73] in Sweden founded the COMSOL Group in 1986. It has now grown to United Kingdom, U.S.A, and Finland and so on. Nowadays, The COMSOL Multiphysics software has been widespread used in various domains of science research and engineering calculation, for example, it was used in global numerical simulation [73,74]. COMSOL Multiphysics is a finite element analysis, solver and Simulation software package for solving various physics and engineering applications. COMSOL group published the first version of COMSOL Multiphysics software in 1998 and it was 33 named as Toolbox. At the beginning time, this software is only applied in the field of Structural Mechanics. The COMSOL Multiphysics simulation environment facilitates all steps in the modeling process: defining your geometry, specifying your physics, meshing, solving and then post-processing your results [75,76].

3.1.2. Introduction

COMSOL Multiphysics is an integrated environment for solving system of time-dependent or stationary second order in space partial differential equations in one, two, and three dimensions. Moreover, such equations may be coupled in an almost arbitrary way. COMSOL Multiphysics provide sophisticated (and convenient) tools for geometric modeling. Therefore, for many standard problems, there exist predefined so-called application modes, which act like templates in order to hide much of the complex details of modeling by equations. The application modes make use of the language used in the respective engineering discipline [77].
COMSOL (formerly known as FEMLAB) is a finite element analysis and solver software package for various physics and engineering applications, especially coupled phenomena, or Multiphysics. It includes a complete environment for modeling any physical phenomenon that can be described using ordinary or PDEs. It has become the industry standard for Multiphysics modeling, research, design, and development

(COMSOL 2008b; Zimmerman 2006). The software package supports nearly all platforms (e.g., Windows, Mac, Linux, and UNIX). COMSOL allows for building coupled systems of PDEs. The PDEs can be entered directly or using the so-called weak form. COMSOL also offers an extensive and well-managed interface to Math Works MATLAB and its toolboxes for a large variety of programming, preprocessing, and post processing possibilities [78].

COMSOL Multiphysics is a powerful interactive environment for modeling and solving all kinds of scientific and engineering problems based on partial differential equations (PDEs). With this product, you can easily extend conventional models for one type of physics into Multiphysics models that solve coupled physics phenomena— and do so simultaneously. Accessing this power does not require an in-depth knowledge of mathematics or numerical analysis. Thanks to the built-in physics modes, it is possible to build models by defining the relevant physical quantities—such as material properties, loads, constraints, sources, and fluxes rather than by defining the underlying equations.

3.1.3. PDE Modes

COMSOL Multiphysics compiles internally a set of PDEs representing the entire model. Access to the power of COMSOL Multiphysics as a stand-alone product is achieved through a flexible graphical user interface, or by programming scripts in MATLAB language. As noted, the underlying mathematical structure in COMSOL Multiphysics is a system of partial differential equations. In addition to the physics mode and the modules, these provide three ways of describing PDEs through the following PDE modes:

• Coefficient form, suitable for linear or nearly linear models.

• General form, suitable for nonlinear models.

• Weak form, for models with PDEs on boundaries, edges, or points, or for models using terms with mixed space and time derivatives.

Using the application modes in COMSOL Multiphysics, that can perform various types of analysis including:

• Stationary and time-dependent analysis.

• Linear and nonlinear analysis.

•Eigen frequency and modal analysis.

To solve the PDEs, COMSOL Multiphysics uses the proven finite element method (*FEM*). The software runs the finite element analysis together with adaptive meshing and error control using a variety of numerical solvers [79].

3.1.4. Work flow

To Set Up and Run a Simulation with COMSOL Multiphysics the next work flow must done as shown in (Figure 3.1):
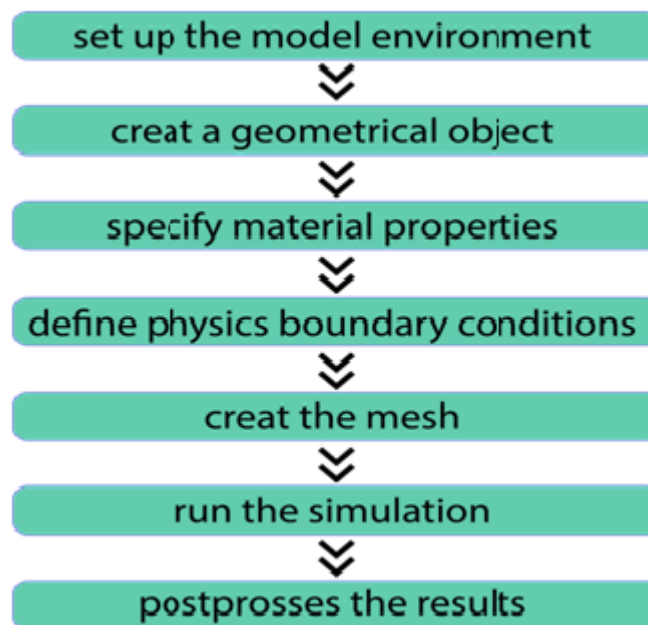

Figure 3.1: Flow chart of COMSOL Multiphysics.

3.1.5. Application areas

There are several application-specific modules in COMSOL Multiphysics. The most common applications are [73]:

AC/DC Module, Acoustics Module, CAD Import Module, Chemical Engineering Module, Earth Science Module, Heat Transfer Module, Material Library.

3.1.6. Characteristics

The spread usage of COMSOL Multiphysics in various domains largely depends on its marked characteristics. These characteristics are [73]:

● It can be used to solve multi-physics problem.

● The user can specify their own Partial Differential Equations.

● Professional predefined modeling interfaces.

● CAD models can be made directly.

● CAD package can be added.

● Exuberance of simulation capability [74].

One unique feature in COMSOL Multiphysics is something we refer to as extended Multiphysics, the use of coupling variables to connect PDE models in different geometries. This represents a step toward system-level modeling.

Another unique feature is the ability of COMSOL Multiphysics to mix domains of different space dimensions in the same problem. This flexibility not only simplifies modeling, it also can decrease execution time. In its base configuration, COMSOL Multiphysics offers modeling and analysis power for many application areas. For several of the key application areas we also provide optional modules. These application-specific modules use terminology and solution methods specific to the particular discipline, which simplifies creating and analyzing models [79].

3.1.7. Application modes in Comsol Multiphysics

- **Physics mode**

Use the physics modes to instantly access convenient templates for specific application areas. Here can specify physical properties for models in fields such as acoustics, diffusion, or electromagnetic.

- **Deformed mesh application modes**

These application modes provide support for applications with moving boundaries using the Moving Mesh (*ALE*) application mode and for parameterized geometries in 2D.

- **The optimization and sensitivity analysis application modes**

The Sensitivity Analysis application mode adds sensitivity analysis to any type of Multiphysics model. The Optimization application mode provides functionality for

combining Multiphysics modeling with optimization (for example, topology optimization and inverse modeling).

- **The PDE modes**

Turn to these modes to model directly with PDEs when there cannot find a suitable physics mode. With these modes when define the problem in terms of mathematical expressions and coefficients. COMSOL Multiphysics includes three PDE modes:

• The Coefficient form allowed solving linear or almost linear problems using PDEs and coefficients that often correspond directly to various physical properties.

• The General form provides a computational framework specialized for highly nonlinear problems. Consider using a weak form for these problems, too.

• The Weak form makes it possible to model a wider class of problems, for example, models with mixed time and space derivatives, or models with phenomena on boundaries, edges, or points as described with PDEs. In terms of convergence rate, these modes also set a computational framework suited for all types of nonlinear problems.

3.1.8. Selecting an application mode

- **Modeling using a single application mode**

Most of the physics application modes contain stationary, Eigen value, and dynamic (time-dependent) analysis types. As already mentioned, these modes provide a modeling interface that lets performed modeling using material properties, boundary conditions, and initial conditions. Each of these modes comes with a template that automatically supplies the appropriate underlying PDE. If cannot found a physics mode that matches a given problem, try one of the PDE modes, which allowed to define a custom model in general mathematical terms. Indeed, COMSOL Multiphysics can model virtually any scientific phenomena or engineering problem that originates from the laws of science.

- **Modeling Multiphysics or systems with several dependent variables**

When modeling a real-world system, you often need to include the interaction between different kinds of physics. For instance, the properties of an electronic component such as an inductor vary with temperature [79].

3.2. Modeling of Phononic crystals

3.2.1. Mathematical modeling

A mathematical model of a physical law is a description of that law in the language of mathematics. Such models make it possible to use mathematical methods to deduce results about the physical world that are not evident or have never been observed. Mathematical modeling is a technique, which builds on a firm understanding of the basic terminology, notation, and methodology of mathematics. It involves the following steps. First, the problem or objective of the study must be stated in a way that reflects accurately the needs of the organization. The second step includes finding data relevant to the problem, which can be applied to the model, and often includes the scaling of these measurements. This process often yields a more realistic model, the results of which are more easily comprehended. The third step in the modeling process is the development of a mathematical model that addresses the concerns of the organization. In developing the mathematical model, the primary goal is to provide a quantitative structure for analyzing a large group of possible situations. Model formulation frequently includes the selection of the appropriate mathematical functions to explain the phenomenon. In the fourth step, the data collected at the second step are applied to the mathematical model to obtain quantitative results. Step five involves the interpretation of the analysis completed in the previous step. It is very important that the results be interpreted in a clear and comprehensible way. Next, the results of the analysis are verified as to their applicability to a wide range of possibilities for the organization. The ability of a model to predict accurately is fundamental to verification. If the model is verified as useful to the organization, then it will be implemented. After implementation, use of the model may lead to additional applications for similar models, adjustments and refinements of the model, or eventual rejection of the model if it is found inapplicable to function. Mathematical models and the modeling process serve as learning aids by emphasizing the applied aspects of mathematical analysis [80].

3.2.2. Computation modeling

The computational modeling is applied in various scientific areas, including more theoretical ones (alternating direction method for solving Poisson) [81]. and parabolic equations [82-83] as well as for solving applied problems when modeling blood glucose dynamics , anisotropic media , moisture diffusion in wood [84], piezoelectric and ultrasound actuators , protein spot detection and others. Computational modeling is the only way to solve the problems presented by the mathematical models of the biosensors since the analytical solutions exist only at extreme set of parameter values [85].

3.3. Modeling of our Phononic crystal under Comsol Multiphysics 5.4

3.3.1. Model definition

Most of the studies on periodic structures were interested in band-gaps and the properties of these bands, and how to use a periodic structure in different domains.

In our work we are interested in studying and simulating different periodic structures starting from a unit-cell going to a simple supercell and finishing with a multi-supercell.

First we are going to study the dispersion curves and it properties, and in the second part the transmission curves and compare the results, and see the effect of the corridor on the properties of our structures.

3.3.2. Model parameters

For the simulation under Comsol, we have chosen Parameters in the table below:

Name	Value	Description
aa[m]	0.004	quote
K_{xx}[rad]	0	k_x
K_{yy}[rad]	0	k_y
K_{zz}[rad]	0	k_z
rr	0.4*aa	Pillar radius
hpillar	1.1*aa	Pillar height
tt	0.25*aa	Plate thickness
ww	0.3*aa	Width
U_{x0}[m]	0	
V_{y0}[m]	0	
W_{z0z}[m]	1e-10	

Table 3.1: Parameters of the Phononic crystal.

Note: we'll use the same parameters in all models for both dispersion / transmission.

3.3.3. The physics entering in our model

- **Solid Mechanics (sld)**

The Solid Mechanics interfaces [available in 3D, 2D (plane stress, plane strain, and generalized plane strain) and 2D axial symmetry] provide the most general approach to analyzing solid structures. By using a geometrically nonlinear formulation, we can analyze situations with arbitrarily large rotations and strains.

The COMSOL Multiphysics implementation of the equations in the Solid Mechanics interface is based on the principle of virtual work.

The principle of virtual work states that the sum of virtual work from internal strains is equal to work from external loads.

The total stored energy, *W*, for a linear material from external and internal strains and loads equals: $\vec{u} = \boldsymbol{u}$

$$W = \int_V (-\varepsilon : s + \boldsymbol{u}.F_V)dv + \int_S (\boldsymbol{u}.F_S)ds + \int_L (\boldsymbol{u}.F_L)dl + \sum_P (\boldsymbol{U}^t.F_P)$$

(3.1)

The principle of virtual work states that $\delta W = 0$ which leads to:

$$\int\limits_V (-\varepsilon_{test} : s + \boldsymbol{u}_{test}.F_V - \rho\boldsymbol{u}_{test}.\boldsymbol{u}_{tt})dv + \int\limits_S (\boldsymbol{u}_{test}.F_s)ds + \int\limits_L (\boldsymbol{u}_{test}.F_L)dl + \sum_P (\boldsymbol{U}_{test}^t.F_P)$$

(3.2)

The Solid Mechanics interface supports stationary (static), eigenfrequency, time-dependent (transient), frequency domain…etc. In our model its stationary study type, which means that COMSOL Multiphysics uses an implementation based on the stress and strain variables. The normal and shear strain variables depend on the displacement derivatives [86].

Using the tensor strain, stress, and displacement variables, the principle of virtual work is expressed as:

$$\delta W = \int\limits_V (-\varepsilon_{test} : s + \boldsymbol{u}_{test}.F_V)dv + \int\limits_S (\boldsymbol{u}_{test}.F_S)ds + \int\limits_L (\boldsymbol{u}_{test}.F_L)dl + \sum_P (\boldsymbol{U}_{test}^t.F_P)$$

(3.3)

3.4. Unit-cell

3.4.1. Definition

It's the smallest element building block of a crystal, whose geometric arrangement defines a crystal's characteristic symmetry and whose repetition in space produces a crystal lattice. In our model's case, it's a pillar in the form of a cylinder with **rr** and **hpillar** as dimensions deposited on a cubic plate with **tt** and **aa** as dimensions.

3.4.2. Simulation steps

3.4.2.1. Geometry description

- For the first simulation, we'll use a **3D** geometry and add the **Solid mechanics** as well as the **Eigenfrequency** study type.
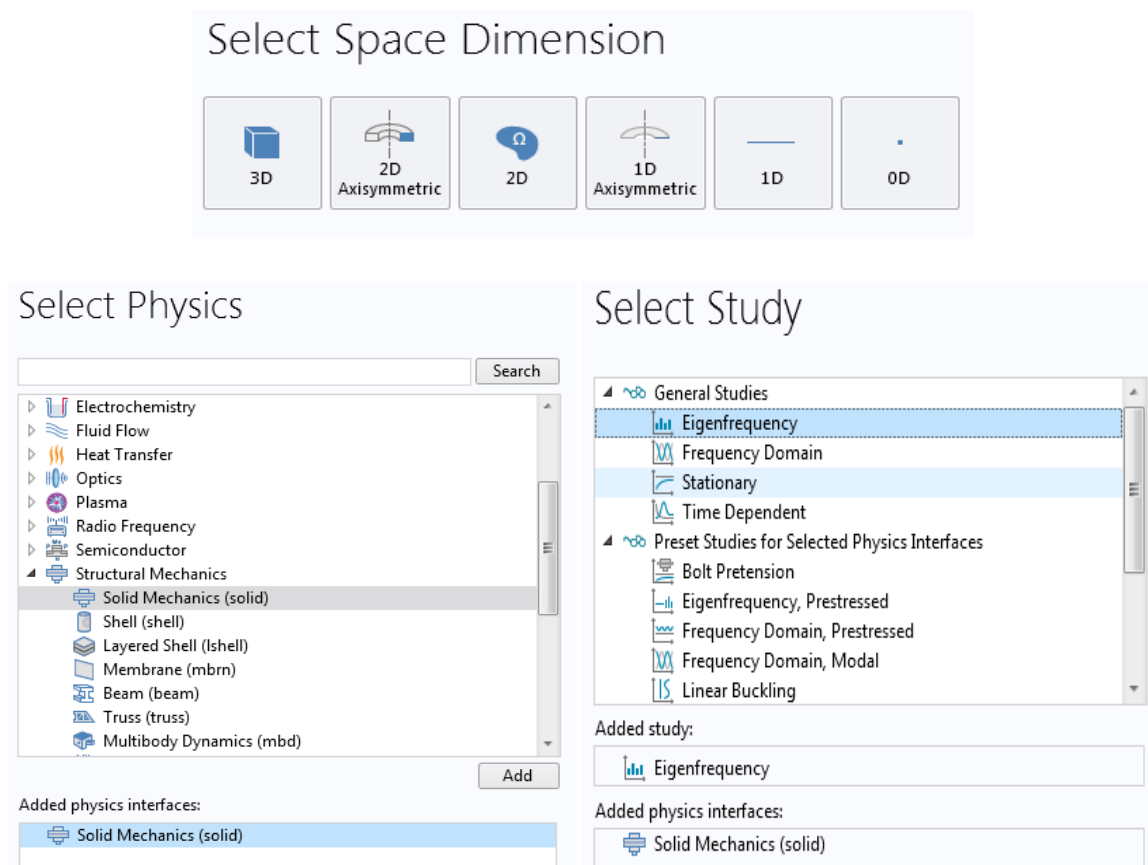
Figure 3.2: Dimension, physics and study selection in COMSOL Multiphysics 5.4.

- After that, we enter the following parameters for both plate (block) and pillar (cylinder):
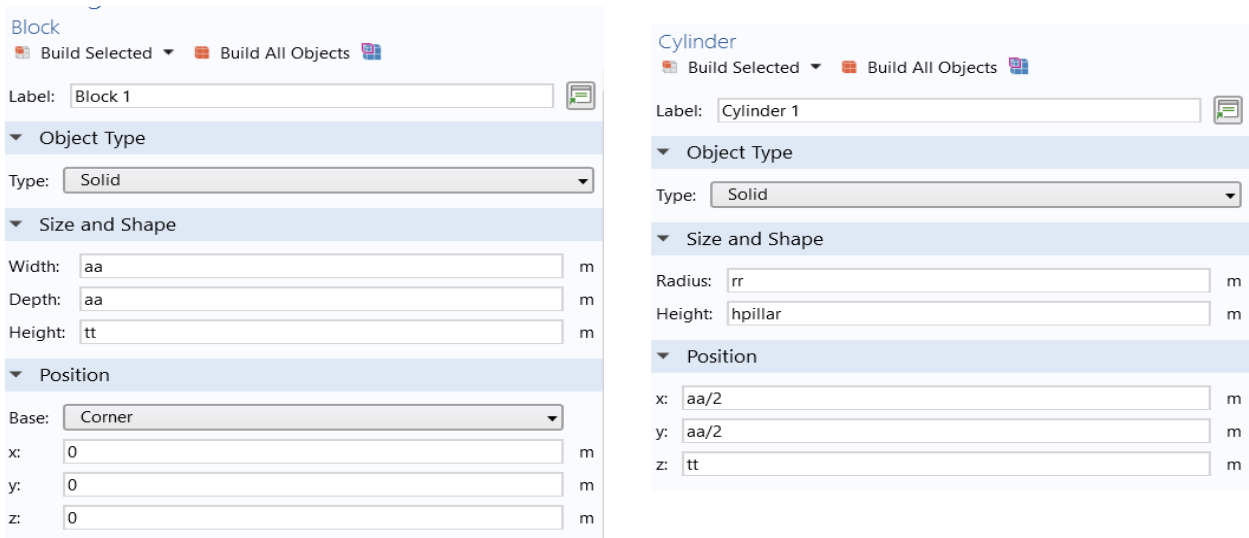
Figure 3.3: Unit cell geometry parameters.

- We will have the following model:
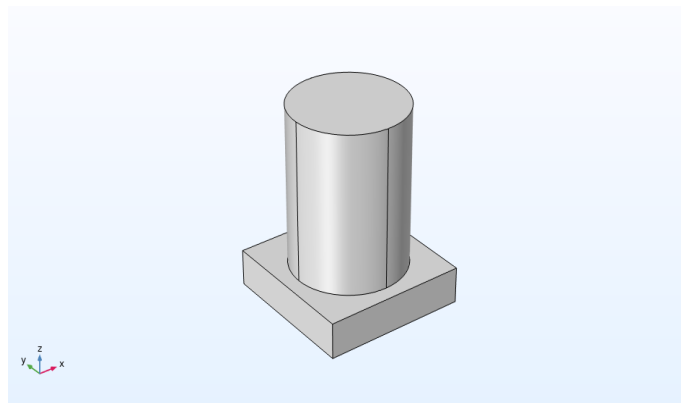
Figure 3.4: Geometry of the Unit cell 1.

- We add **Bolefortal** (aluminum-based composite) as material, with the following properties:

Figure 3.5: The model's material and its properties.

3.4.2.2. Solid mechanics

- To run this simulation we need to set the best solutions, so we go first to **solid mechanics** and choose **periodic condition** for the periodicity in the **x** direction and we add second one in the **y** direction to make a simulation as infinite crystal.

Figure 3.6: Periodic condition along x and y.

- In **periodic condition** we go to **periodicity settings** and select **Floquet periodicity** and setup the wave vector. And after that, we click right on **periodic condition** and choose **destination selection** and we set this in both directions.
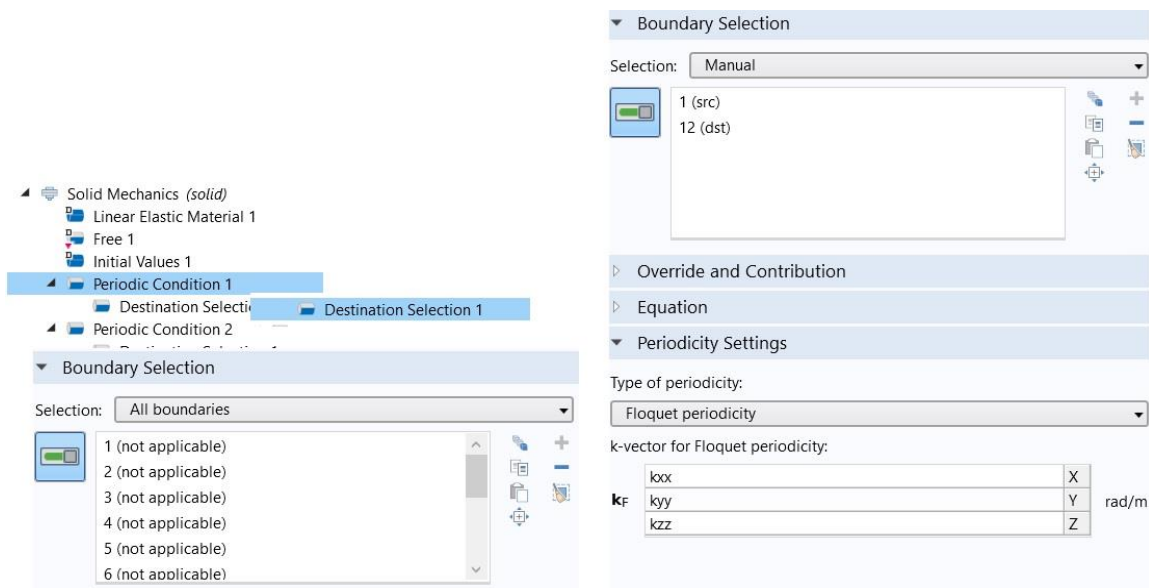
Figure 3.7a: Floquet periodicity and destination selection for periodic condition 1.
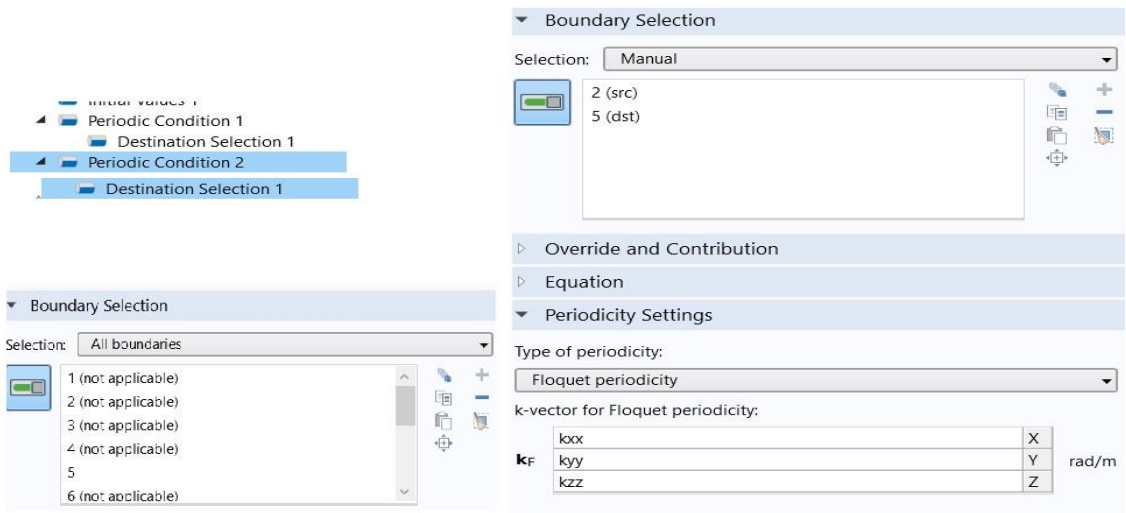
Figure 3.7b: Floquet periodicity and destination selection for periodic condition 2.

### 3.4.2.3. Mesh and study

- We choose a **mesh** for our model.
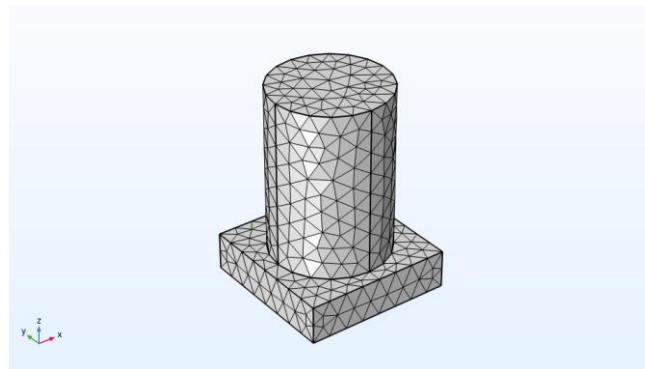
Figure 3.8: Meshing of the model.

- We still need one more step to run this simulation. We click right on **study** and select **parametric sweep** and on **study settings** we add a parameter **kxx** and add a range for this parameter.

- After that, we click on **step1: eigenfrequency** from the **desire number of eigenfrequencies** we choose **20** and the unity is **Hz**.

- Then we press **compute**.
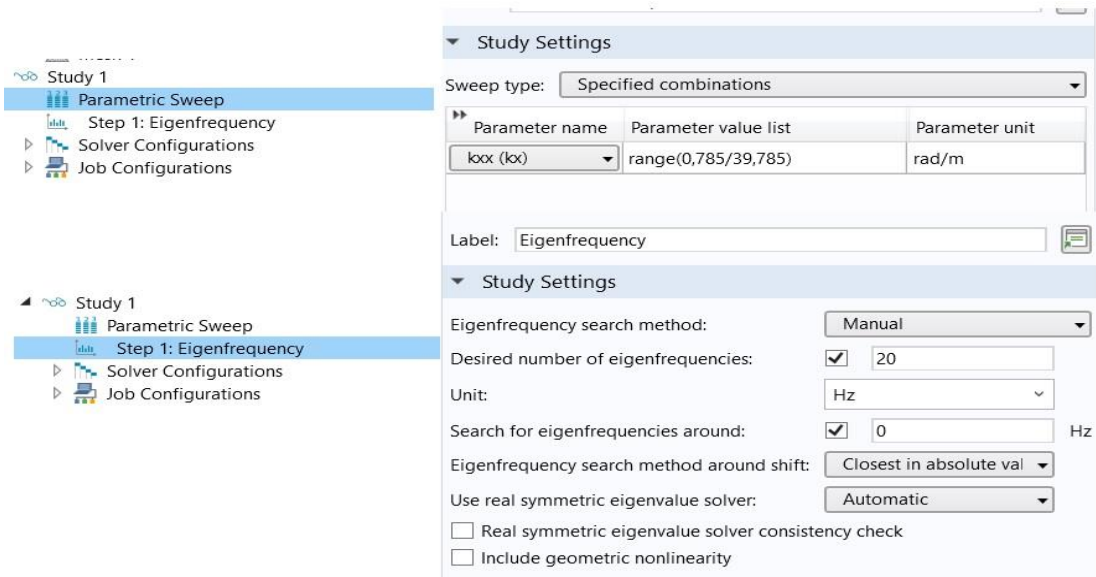
Figure 3.9: Range for both parametric sweep and step1: eigenfrequency.

3.5. Supercell without corridor

Note: in this study we'll be using **Bolefortal** as material for all the remaining models (supercell with / without corridor), with the following parameters:
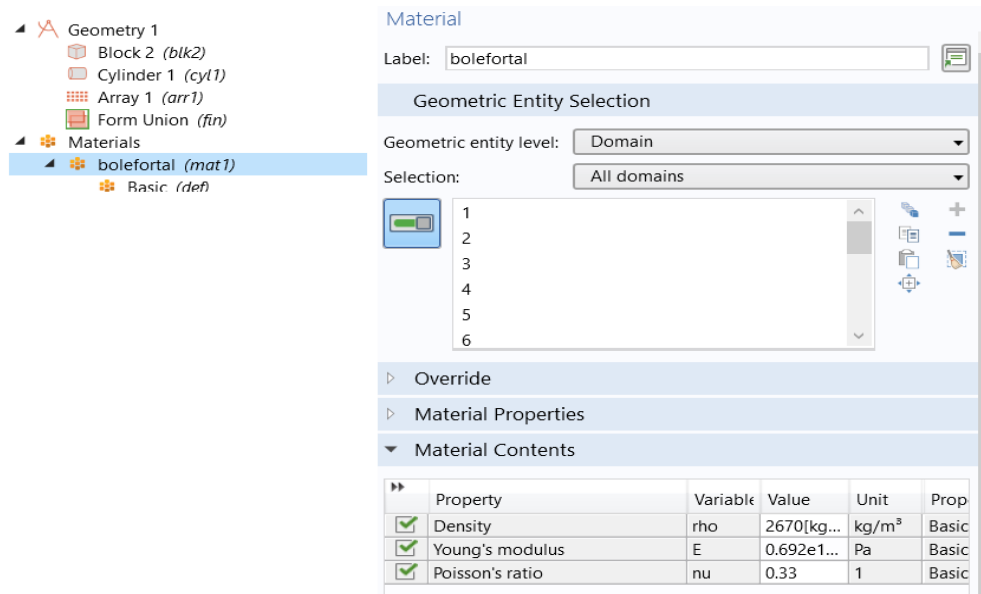
Figure 3.10: The models material and its properties.

3.5.1. Definition of a supercell

We know that a crystal structure is described by a unit-cell. When these unit-cells repeat themselves along a certain direction in the crystal, they form what we call a supercell, which describes the same crystal, but has a larger volume than the unit-cell.

3.5.2. Simulation steps

3.5.2.1. Geometry description

- For the second simulation we'll the use the same parameters as the unit-cell (**3D** geometry, **Solid mechanics**, **stationary**).

- Then we enter our model's parameters:
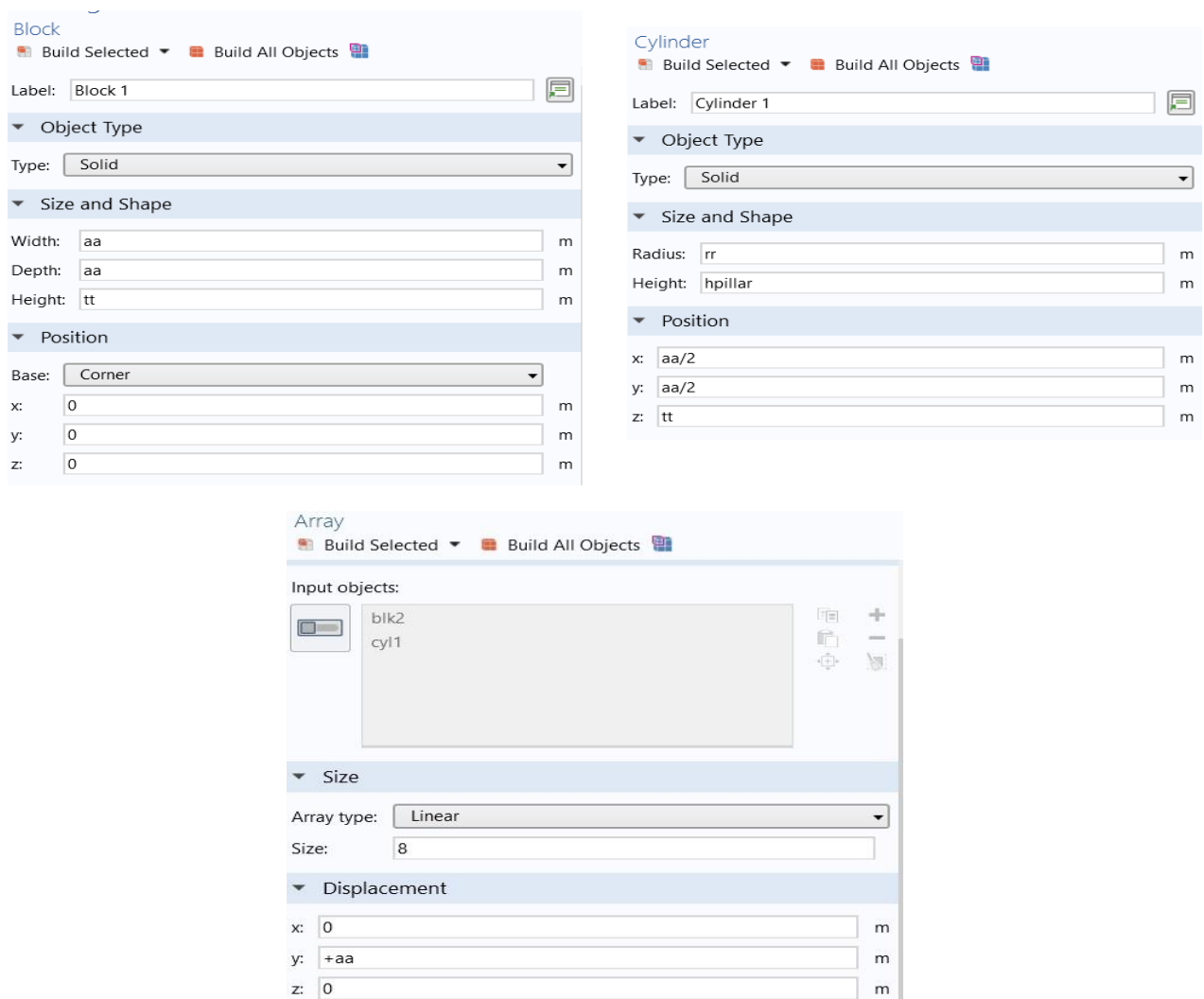
Figure 3.11: Supercell geometry parameters.

- Our model this time will be:
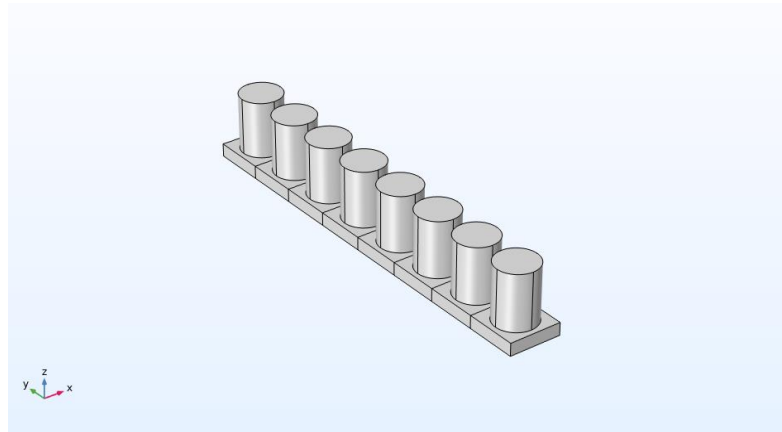
Figure 3.12: Geometry of the supercell.

3.5.2.2. Solid mechanics

- For run this simulation with success we need to set the best solutions, so we go first for **Solid mechanics** and choose **periodic condition** for the periodicity in the **x** direction and we add second one in the **y** direction to make a simulation as infinite crystal.
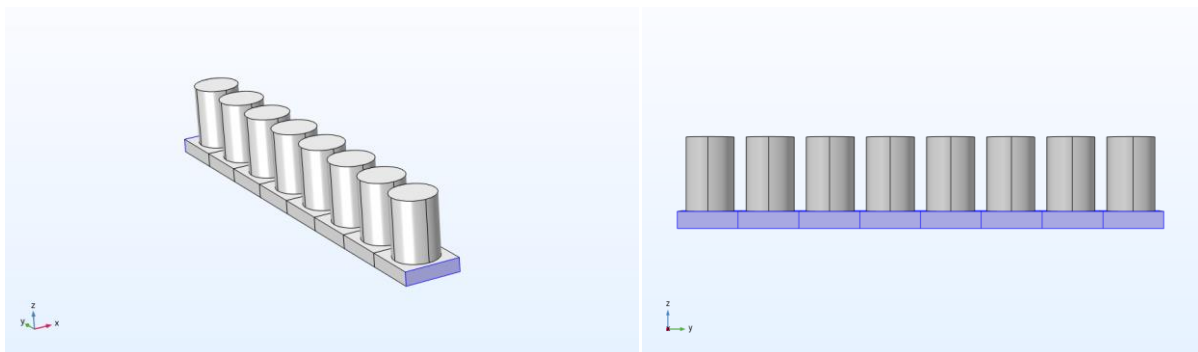
Figure 3.13: Periodic condition along x and y.

- In **periodic condition** we go to **periodicity settings** and select **Floquet periodicity** and setup the wave vector. And after that, we click right on **periodic condition** and choose **destination selection** and we set this in both directions.
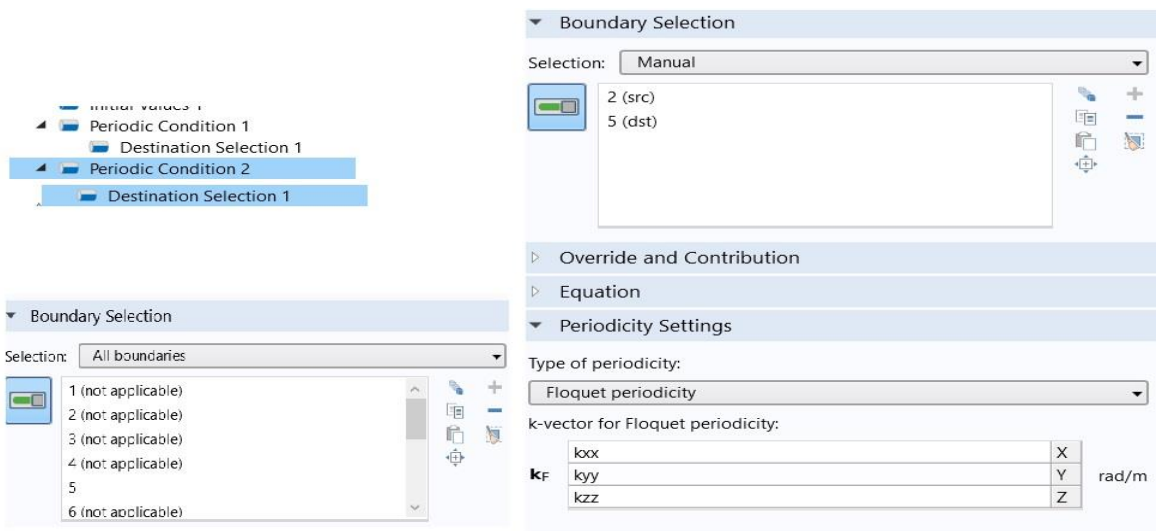
Figure 3.14a: Floquet periodicity and destination selection for periodic condition 1.
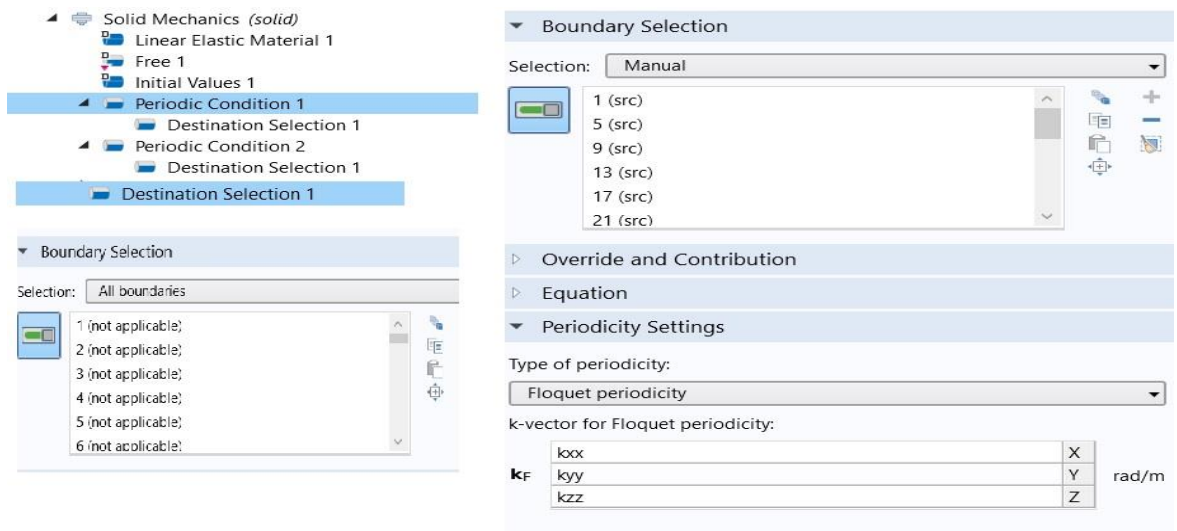
Figure 3.14b: Floquet periodicity and destination selection for periodic condition 2.

3.5.2.3. Mesh and study
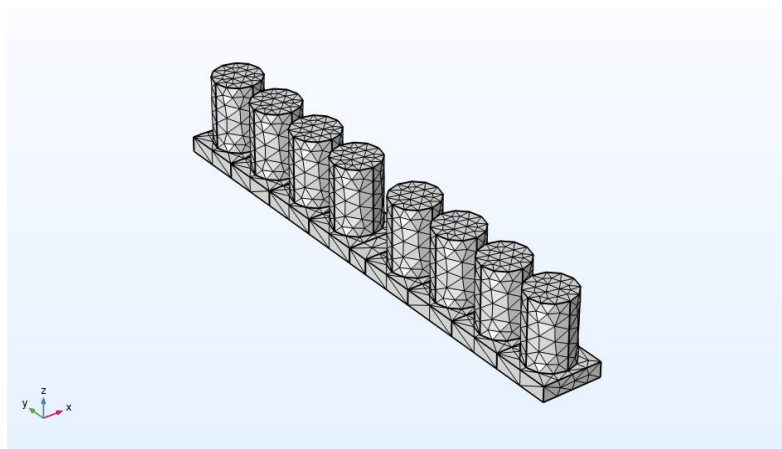
- First, we choose a **mesh** for our model.
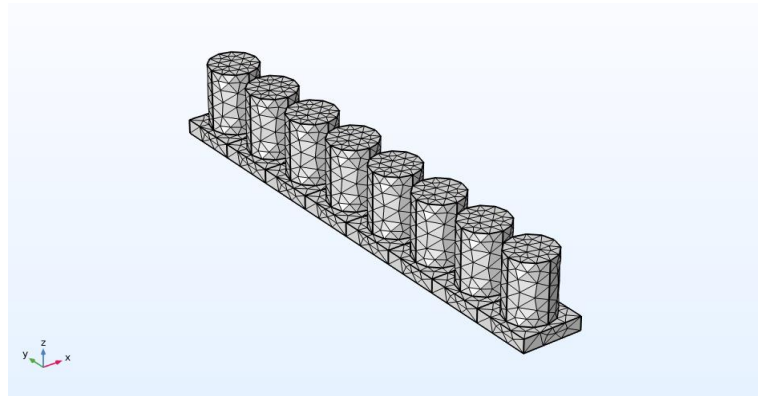
Figure 3.15: Meshing of the model.

- To run this simulation we still need one more step. We click right on **study** and select **parametric sweep** and on **study settings** we add a parameter **kxx** and add a range for this parameter.

- After that, we click on **step1: eigenfrequency** from the **desire number of eigenfrequencies** we choose **200** and the unity is **Hz**.
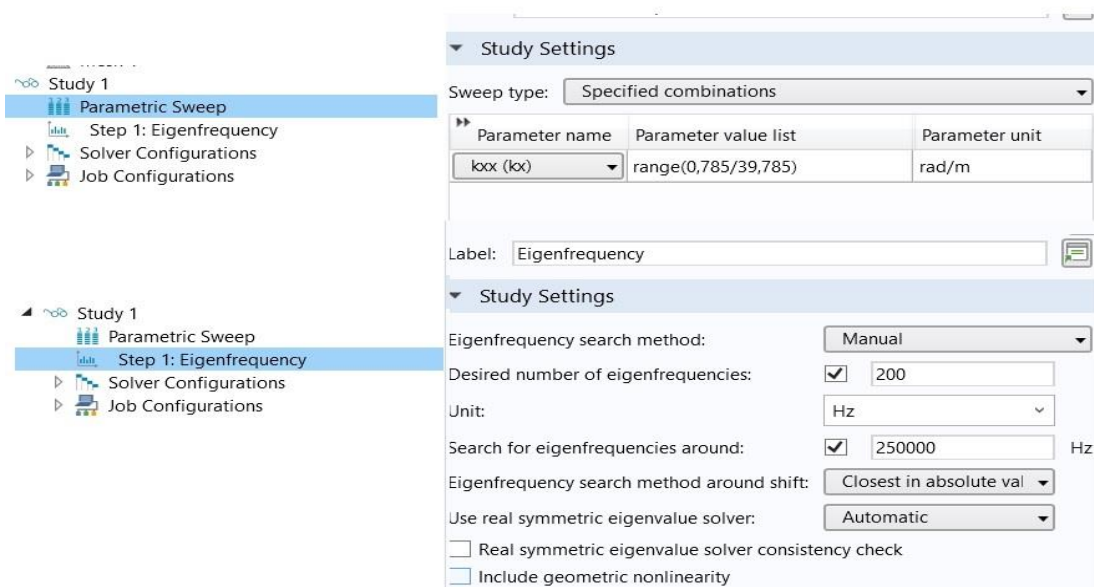
Figure 3.16: Range for both parametric sweep and step1: eigenfrequency.

- Then, we press **compute**.

3.6. Supercell with corridor

In this part we will build a same supercell as the one before with the same dimensions as well, but this time we'll cut the periodicity in half with three different **corridors**, with a distance of: 1)- **ww= 0.22*aa** / 2)- **ww= 0.30*aa** / 3)- **ww= 0.38*aa**.

3.6.1. Geometry of the models

- We'll have the following geometries:
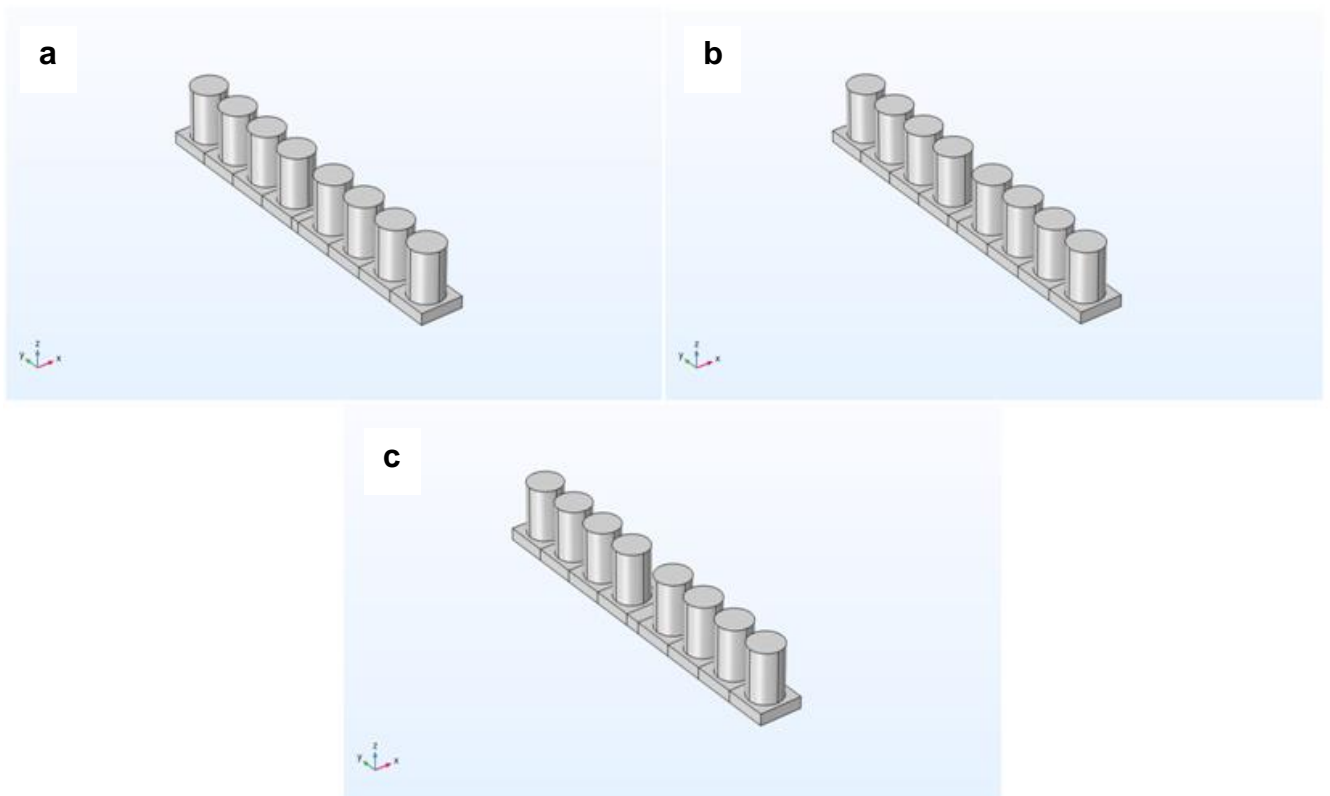
Figure 3.17: Geometry of the model for: a)- ww= 0.22*aa / b)- ww= 0.30*aa / c)- ww= 0.38*aa.

3.6.2. Simulation steps

3.6.2.1. Solid mechanics

- For us to run this simulation we need to set the best solutions, so we go first for **Solid mechanics** and choose **periodic condition** for the periodicity in the **x** direction and we add second one in the **y** direction to make a simulation as infinite crystal.
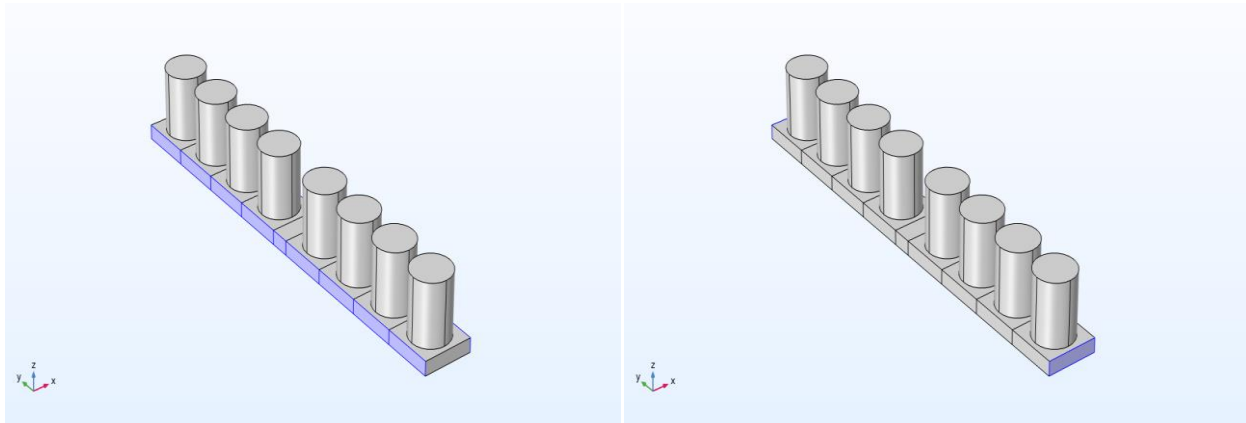
Figure 3.18: Periodic condition along x and y.

- In **periodic condition** we go to **periodicity settings** and select **Floquet periodicity** and setup the wave vector. And after that, we click right on **periodic condition** and choose **destination selection** and we set this in both directions.
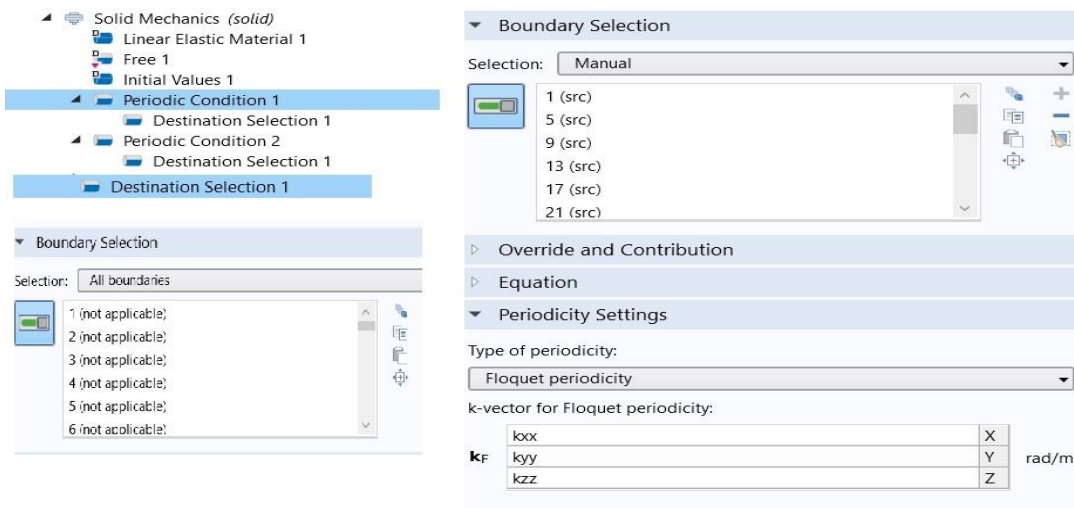
Figure 3.19a: Floquet periodicity and destination selection for periodic condition 1.
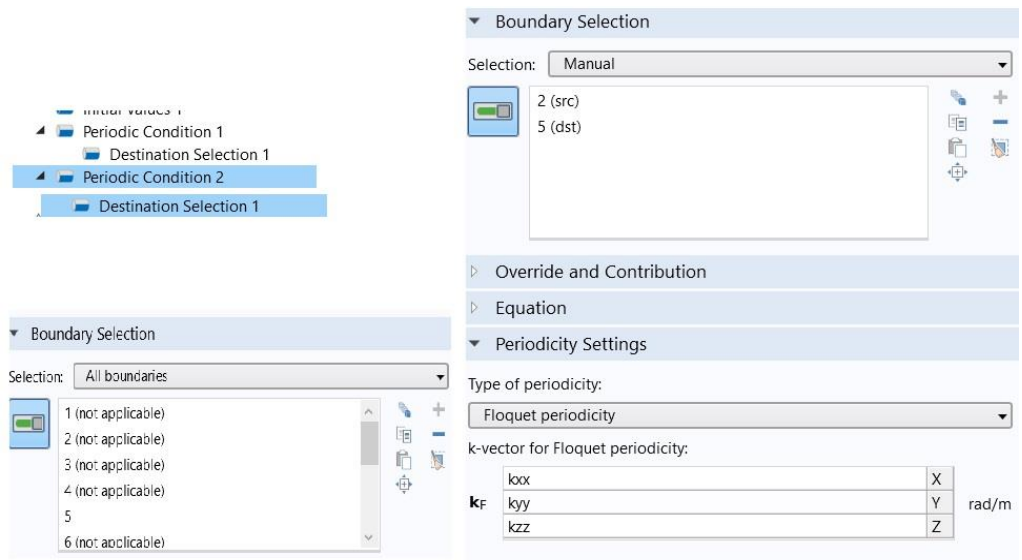
Figure 3.19b: Floquet periodicity and destination selection for periodic condition 2.

3.6.2.2. Mesh and study

- We'll set the **meshing** for our model.

Figure 3.20: Meshing of the model.

- Before we run this simulation we still need one more step. We click right on **study** and select **parametric sweep** and on **study settings** we add a parameter **kxx** and add a range for this parameter.

- After that, we click on **step1: eigenfrequency** from the **desire number of eigenfrequencies** we choose **200** and the unity is **Hz**.
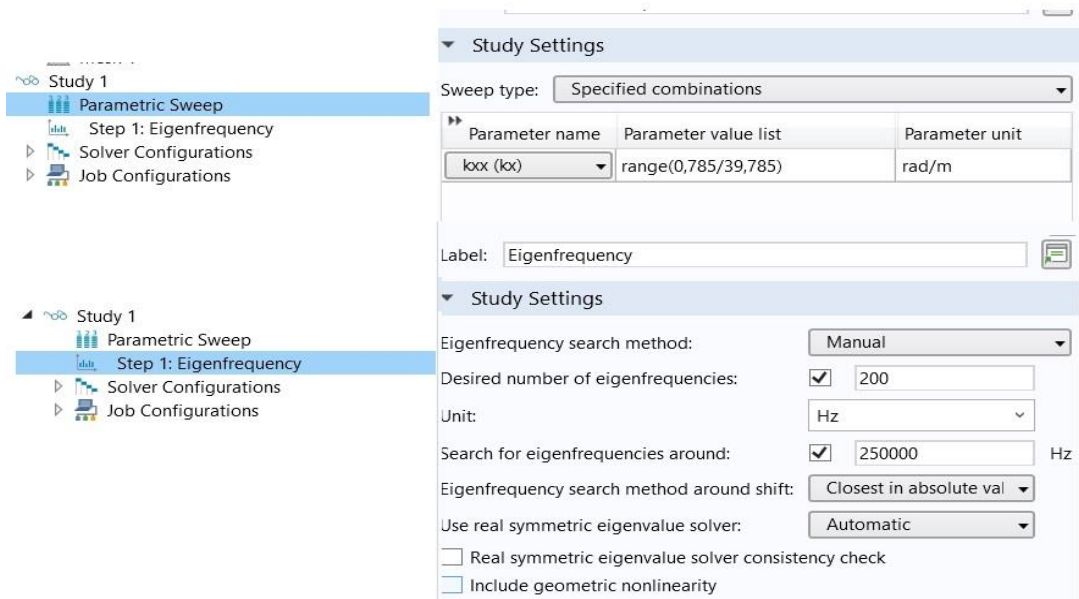
Figure 3.21: Range for both parametric sweep and step1: eigenfrequency.

- Finally, we press **compute**.

Note: we used the same simulation steps for the three models (ww= 0.22*aa / ww=0.30*aa / ww= 0.38*aa).

3.7. Gap mapping

- For this study we'll be using a unit-cell with the same **study type**, **geometry parameters**, **material**, **periodic condition** (along x and y), **wave vector**, **mesh** as the one in the precedent study.
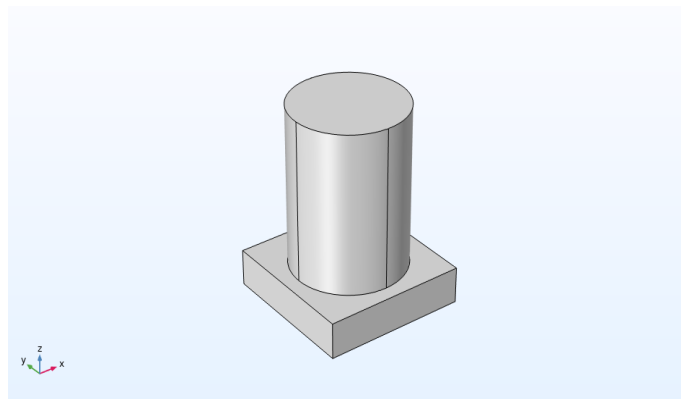
Figure 3.22: Geometry of the unit cell 2.

- We'll follow the same simulation steps, only this time before starting our simulation; we'll change the pillar's height by changing the **range** of the **hpillar** in **Study settings** in **parametric sweep**.
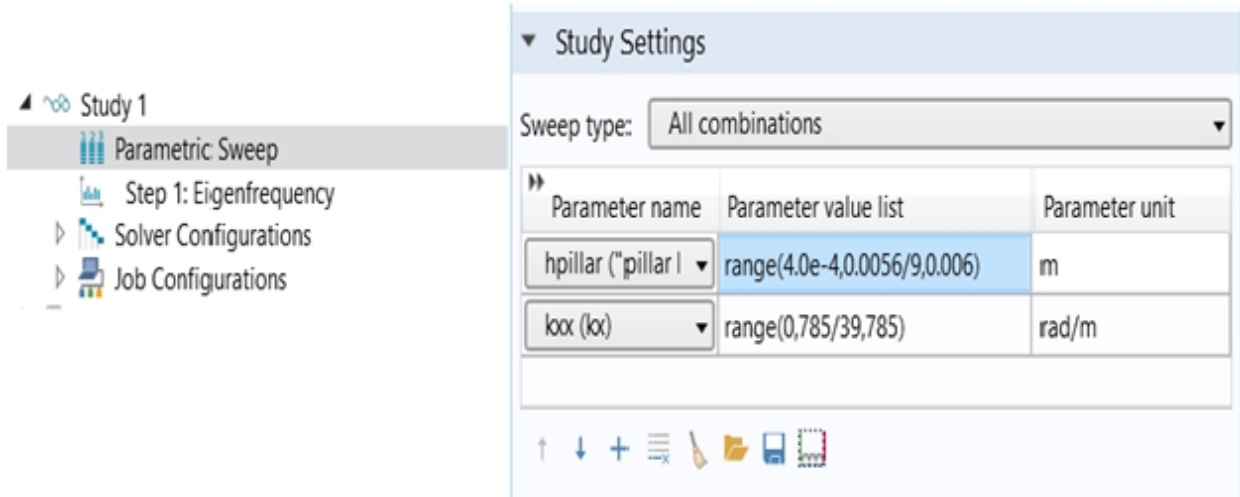
Figure 3.23: Range of hpillar in parametric sweep.

- Then, we press **compute** to begin the simulation.

CHAPTER 4: "ACTUAL" PC's WAVEGUIDE STRUCTURE MODELING FOR TRANSMISSION CALCULATION

4. Modeling under COMSOL Multiphysics 5.4

4.1. Transmission with PML

4.1.1. Definition of Perfectly Matched Layer (PML)

A perfectly matched layer (PML) is an artificial absorbing layer for waves. The essential property of a PML that distinguishes it from ordinary absorbent material is the fact that it is designed so that incident waves reaching it from a non-PML material are not reflected at the interface. This property allows PMLs to strongly absorb all the waves leaving a computational domain without returning them to this domain.

4.1.2. Geometry parameters

- We'll study a model with three different corridors, so the geometry parameters will be:
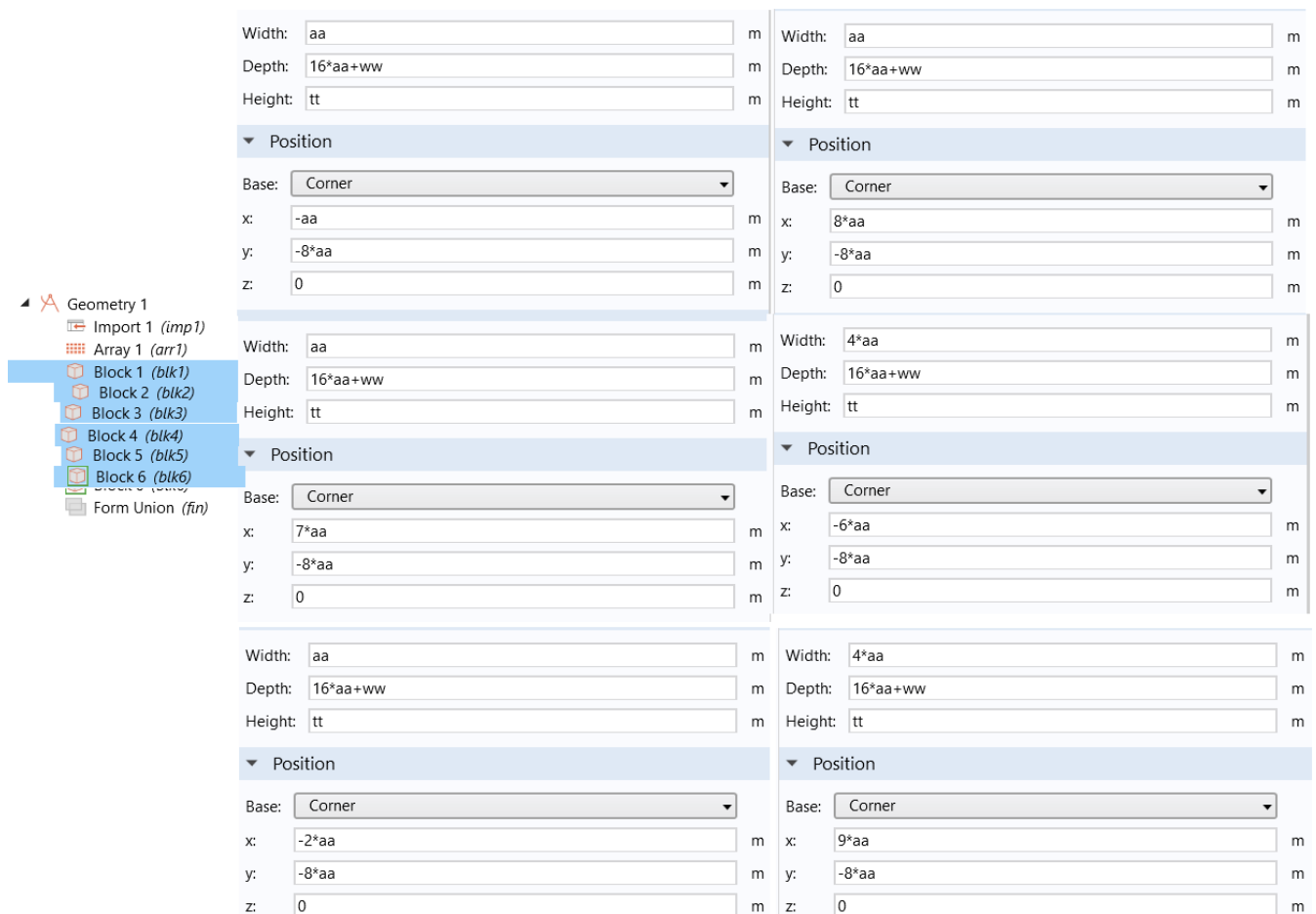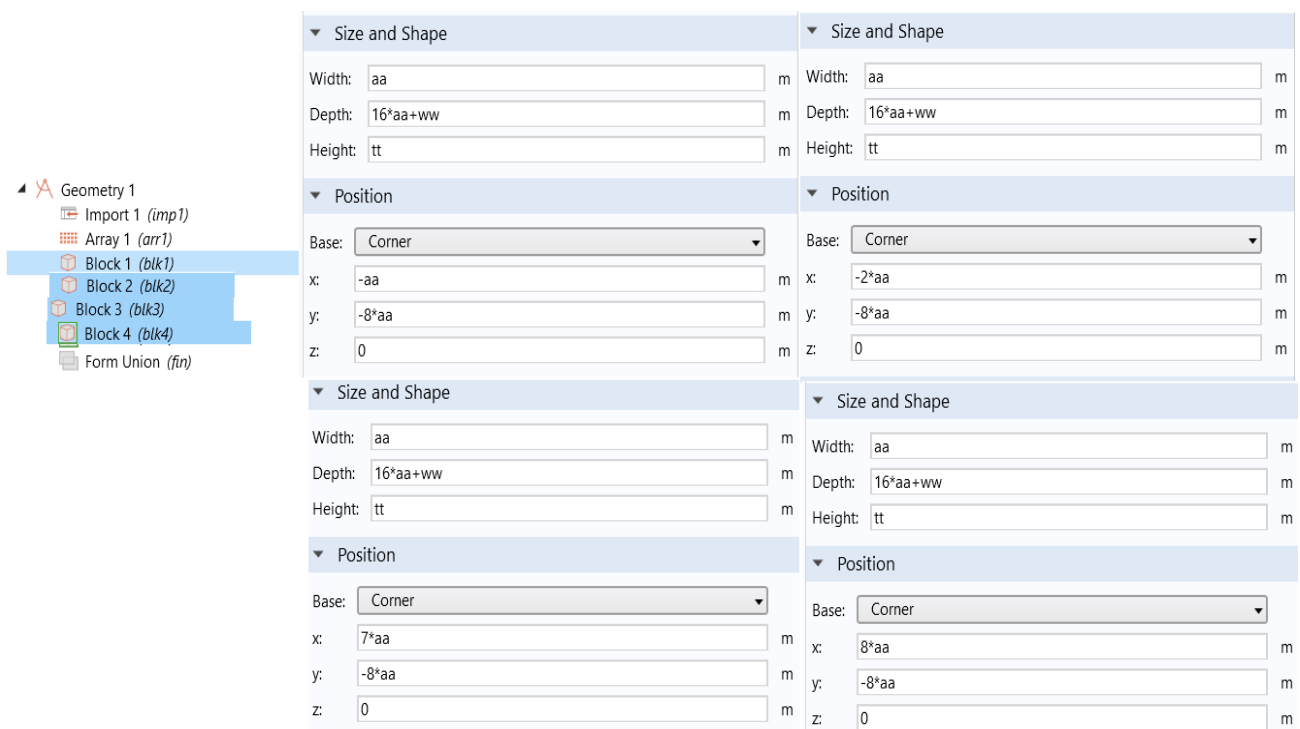

Figure 4.1: Geometry parameters.

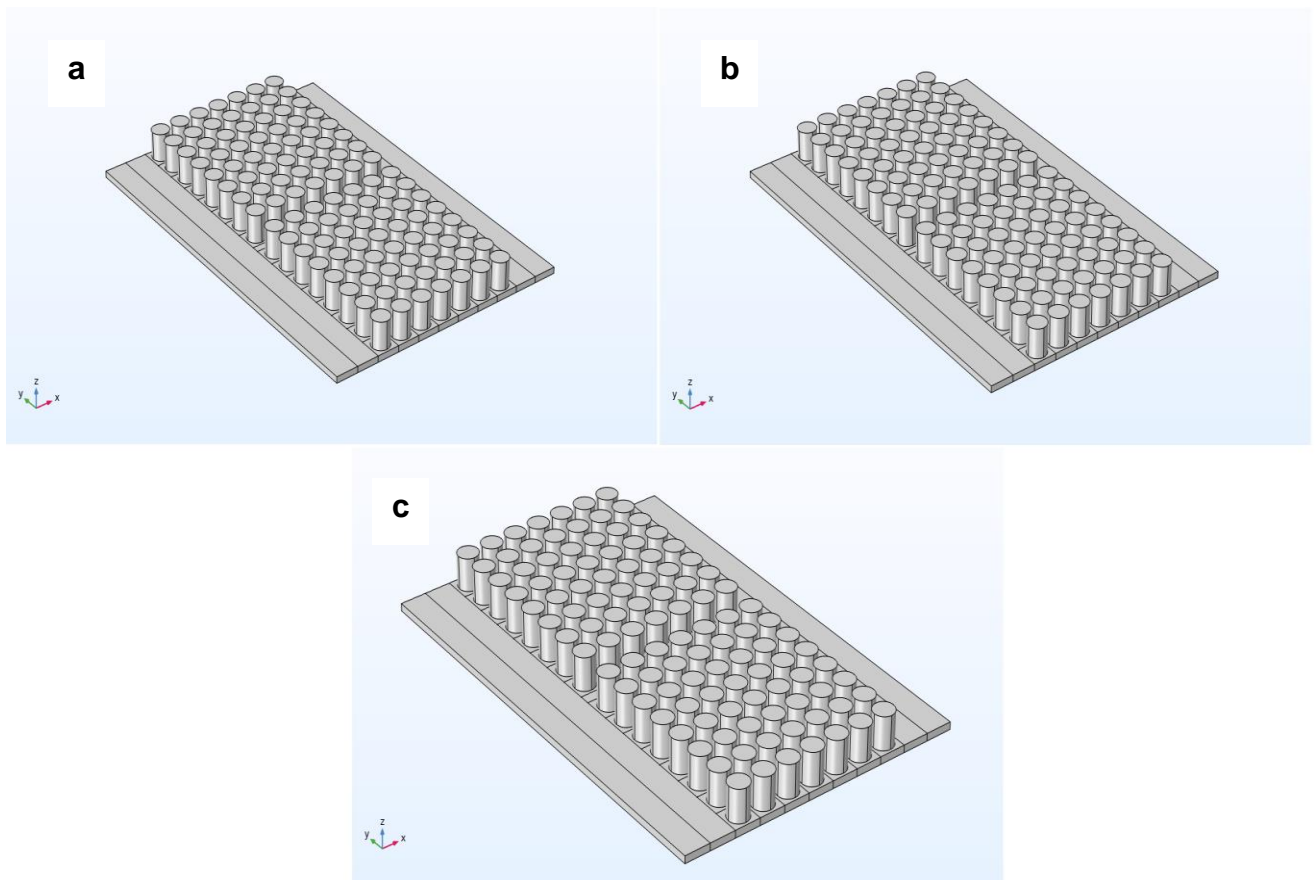### 4.1.3. Geometry of the models

- We'll have the following geometries:
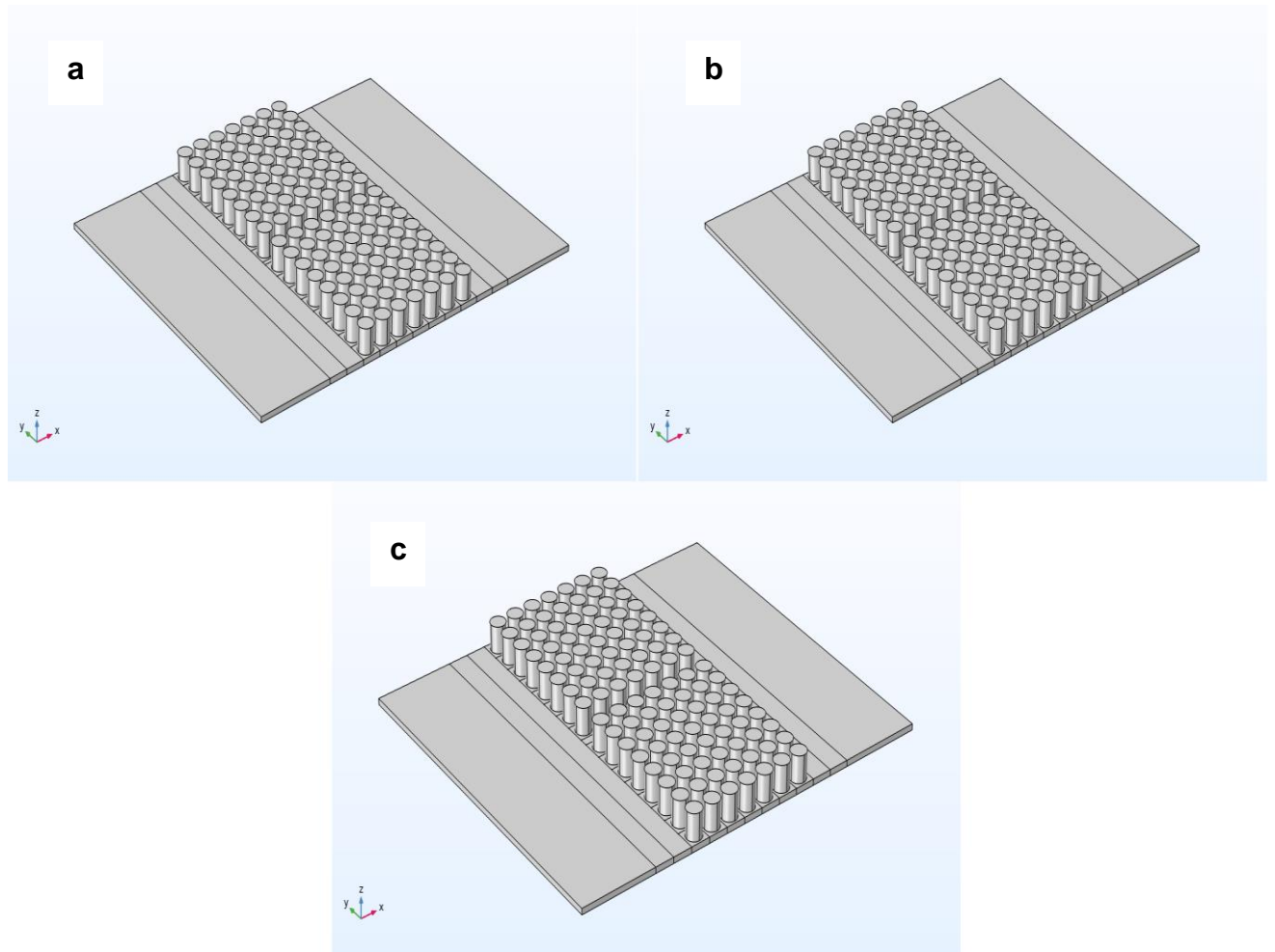
Figure 4.2: Geometry of the model for: a)- ww= 0.22*aa / b)- ww= 0.30*aa / c)- ww= 0.38*aa.

4.1.4. Material and its properties

- We'll be using the **Bolefortal**, with the following parameters:
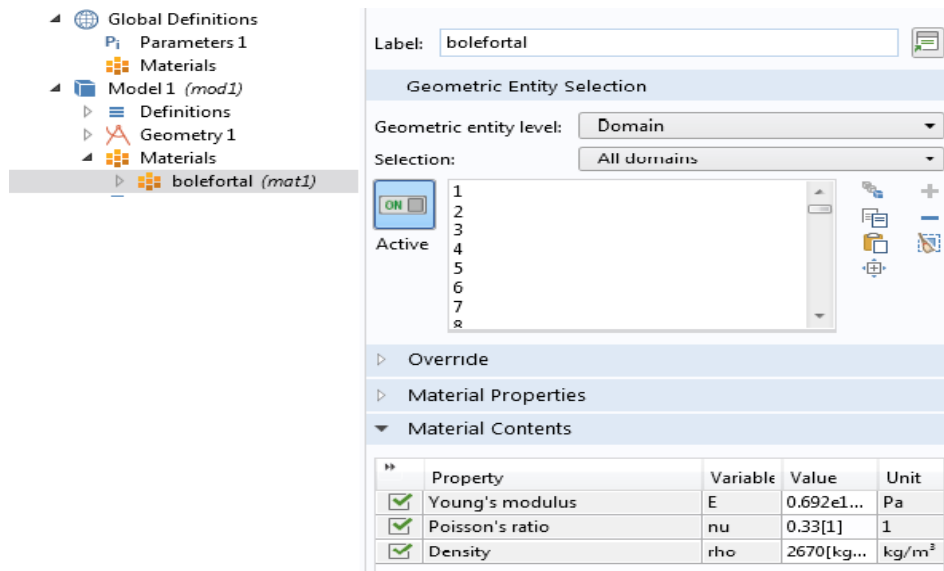
Figure 4.3: The models material and its properties.

4.1.5. Simulation steps

4.1.5.1. PML

- We'll add a **Perfectly Matched Layer (PML)** to the geometry by pressing right on **Definition**, and select the PML option:
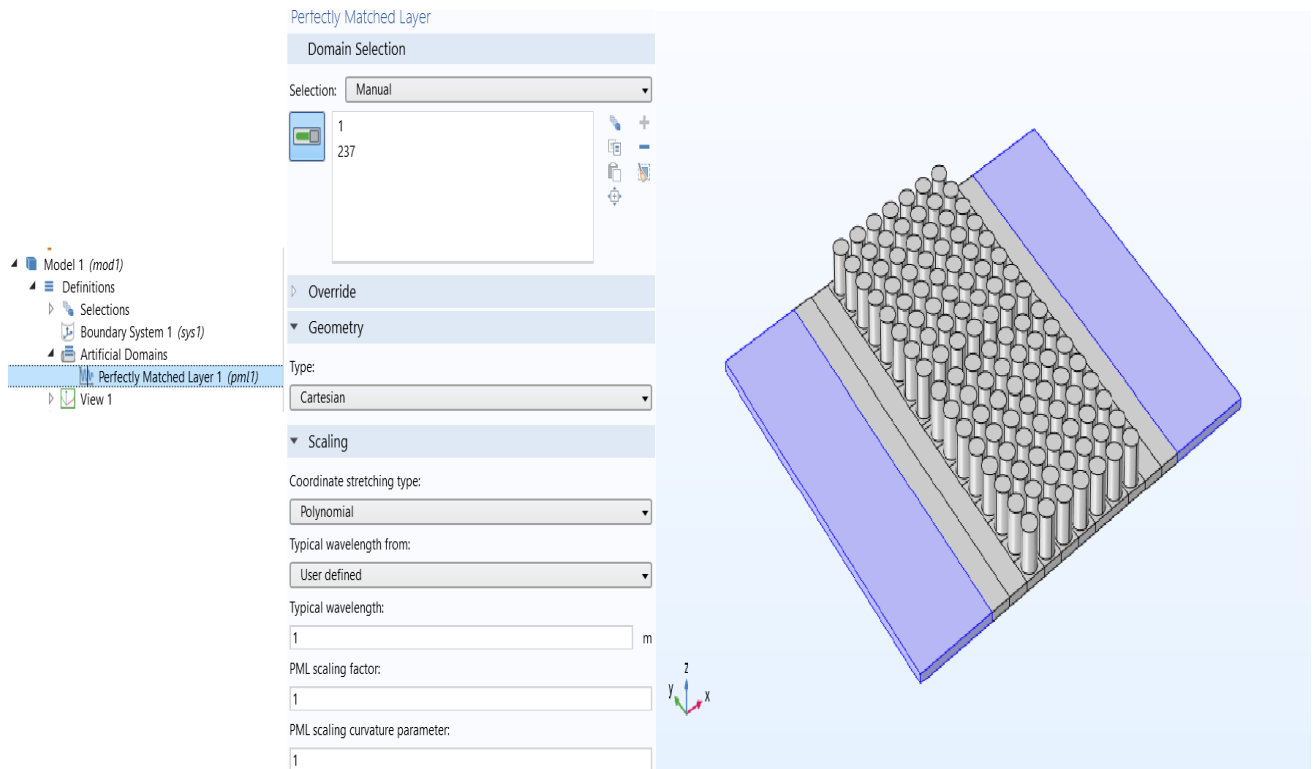
Figure 4.4: PML domains selection in our model.

4.1.5.2. Solid mechanics

- We will add a **periodic condition**, then a **Destination selection** for this latter.
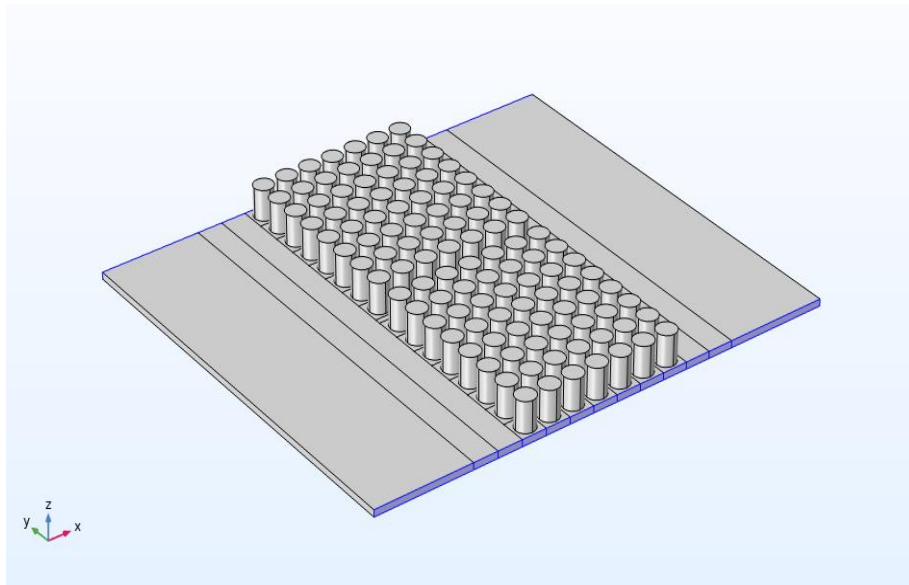
Figure 4.5: Periodic condition.

- We press right on **Solid mechanics** and choose **prescribed displacement**. After that, we press right on this latter to choose **Harmonic description**, and then setup the wave vector.
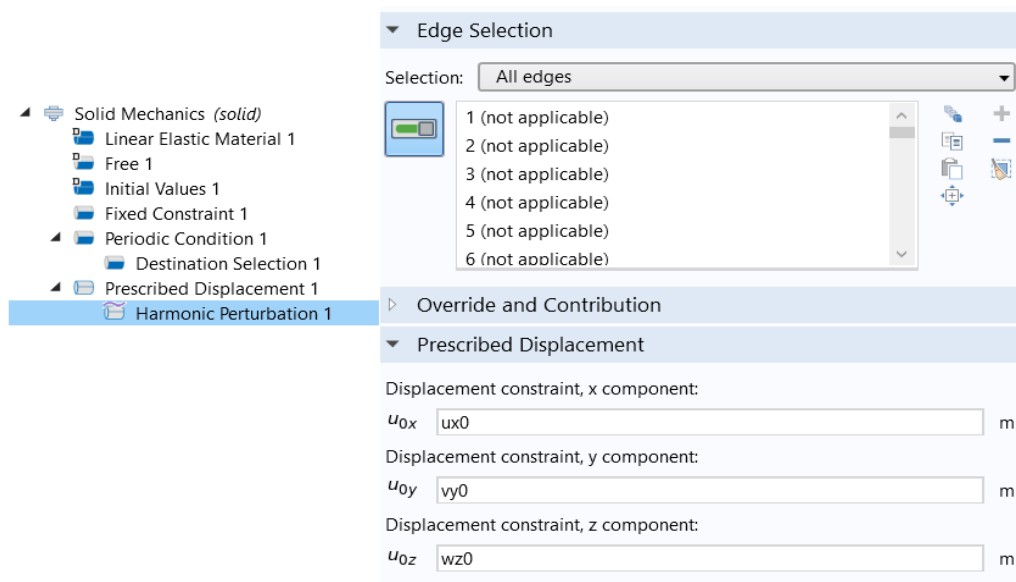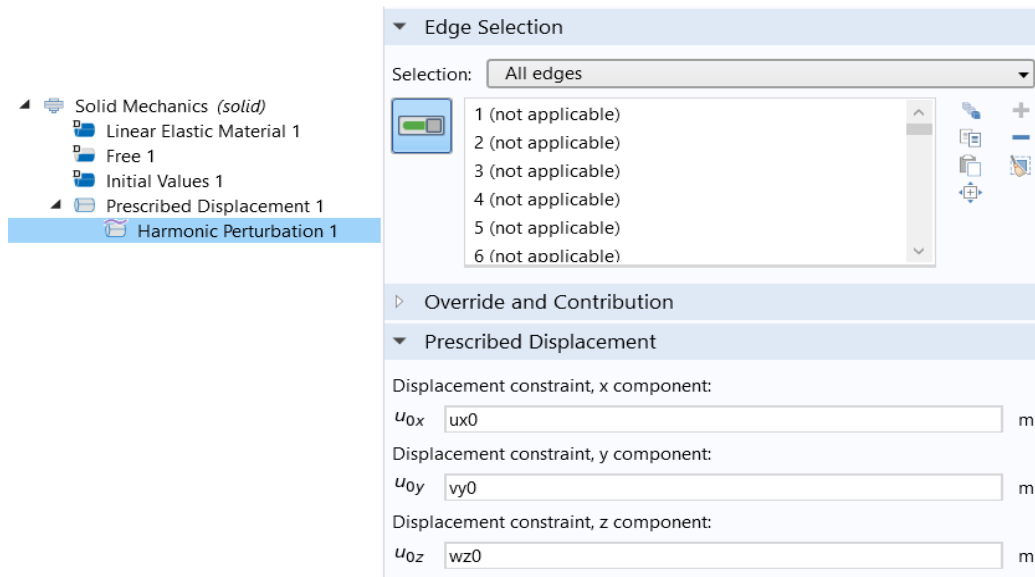

Figure 4.6: Harmonic perturbation.

- We return to **prescribed displacement** to select the edges of where we want the vibrations to start from.
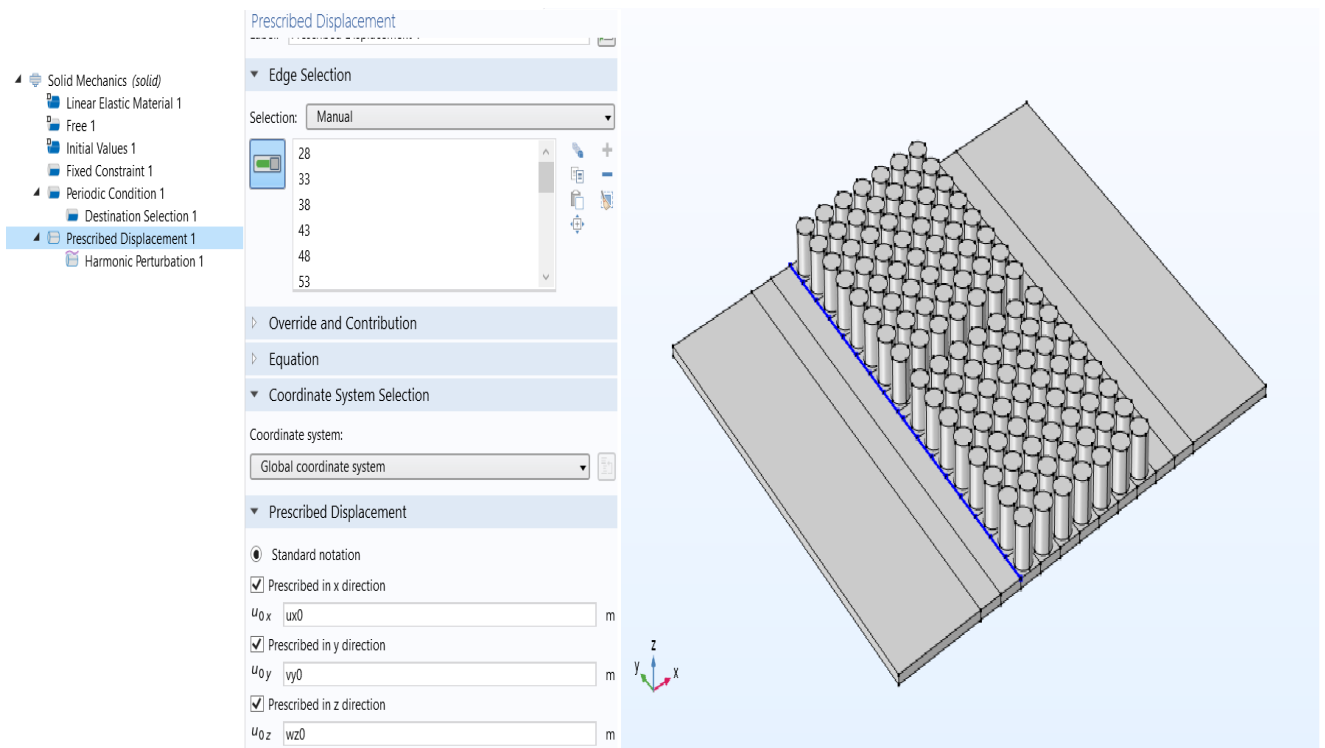
Figure 4.7: Prescribed displacement.

4.1.5.3. Mesh

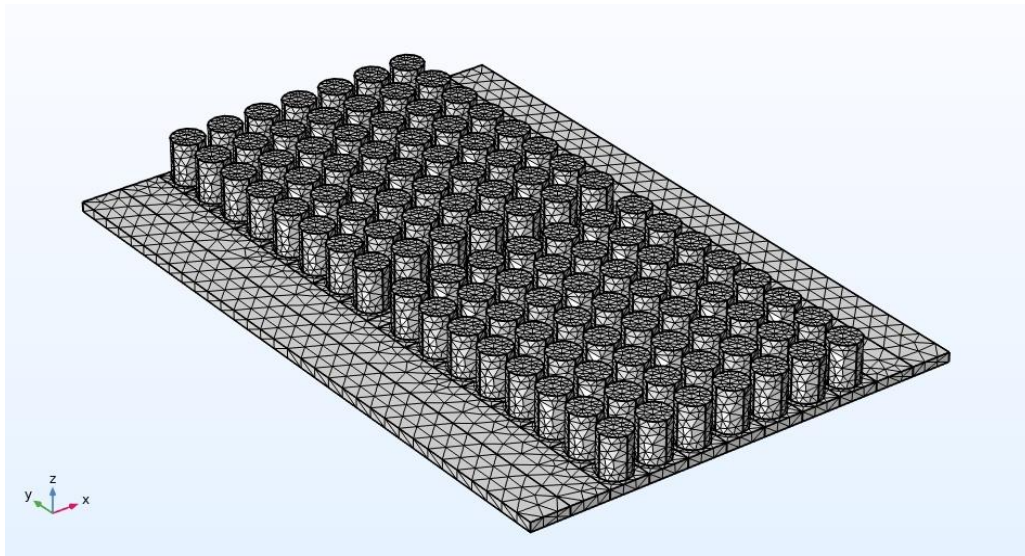- We add a **meshing** to the model.
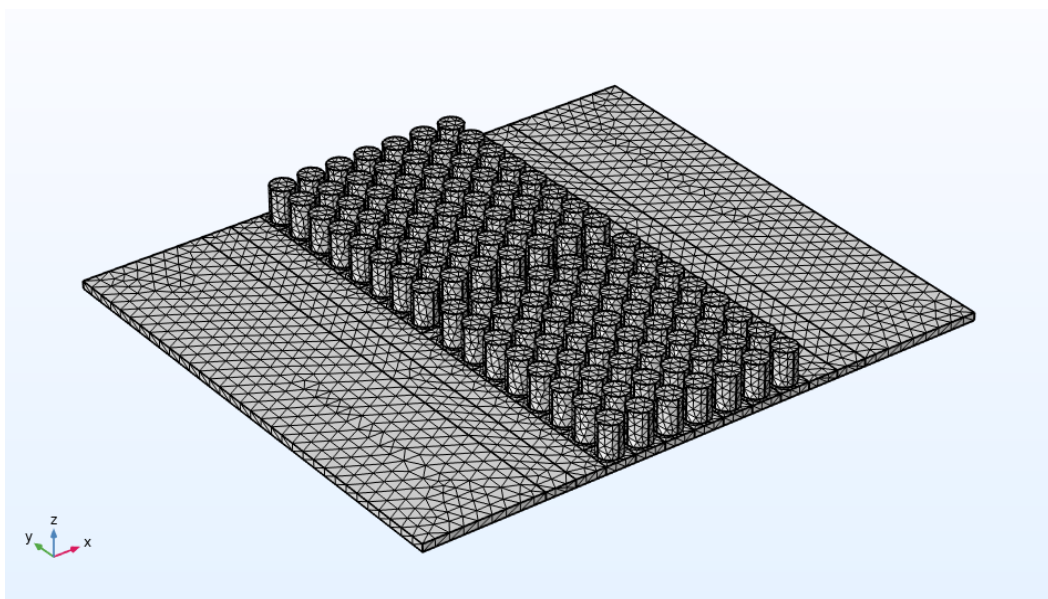
Figure 4.8: Meshing of the model.

- The last step before we start our study is to add a range to the **Frequencies** in the **study settings** of **step1: frequency domain**.
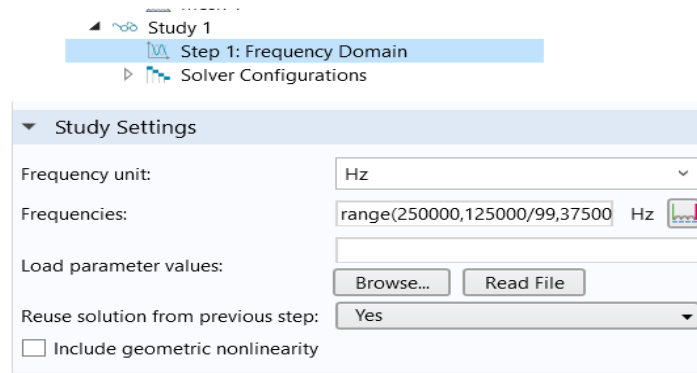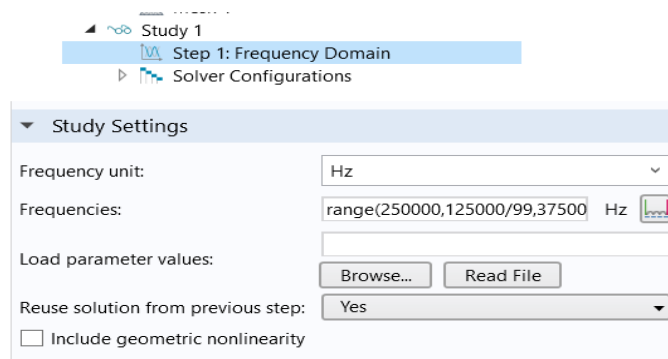

Figure 4.9: Range for Step1: Frequency domain.

- Finally, we press **compute**.

Note: we used the same simulation steps for the three models (ww= 0.22*aa / ww=0.30*aa / ww= 0.38*aa).

4.2. Transmission without PML

4.2.1. Geometry parameters

- We'll study a model with three different corridors, but this time we won't be using the Perfectly Matched Layer, so the geometry parameters will be:

Figure 4.10: Geometry parameters.

4.2.2. Geometry of the models

- We will have the following geometries:

Figure 4.11: Geometry of the model for: a)- ww= 0.22*aa / b)- ww= 0.30*aa / c)- ww= 0.38*aa.

4.2.3. Material and its properties

- We'll be using the **Bolefortal**, with the following parameters:
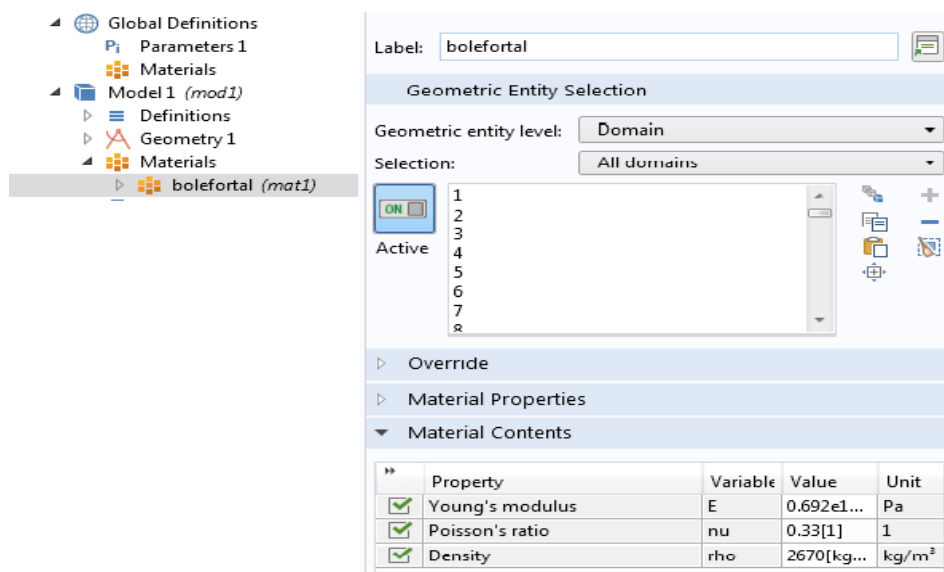
Figure 4.12: The models material and its properties.

4.2.4. Simulation steps

4.2.4.1. Solid mechanics

- We press right on **Solid mechanics** and choose **prescribed displacement**. After that, we press right on this latter to choose **Harmonic description**, and then setup the wave vector.

Figure 4.13: Harmonic perturbation.

- We return to **prescribed displacement** to select the edges of where we want the vibrations to start from.
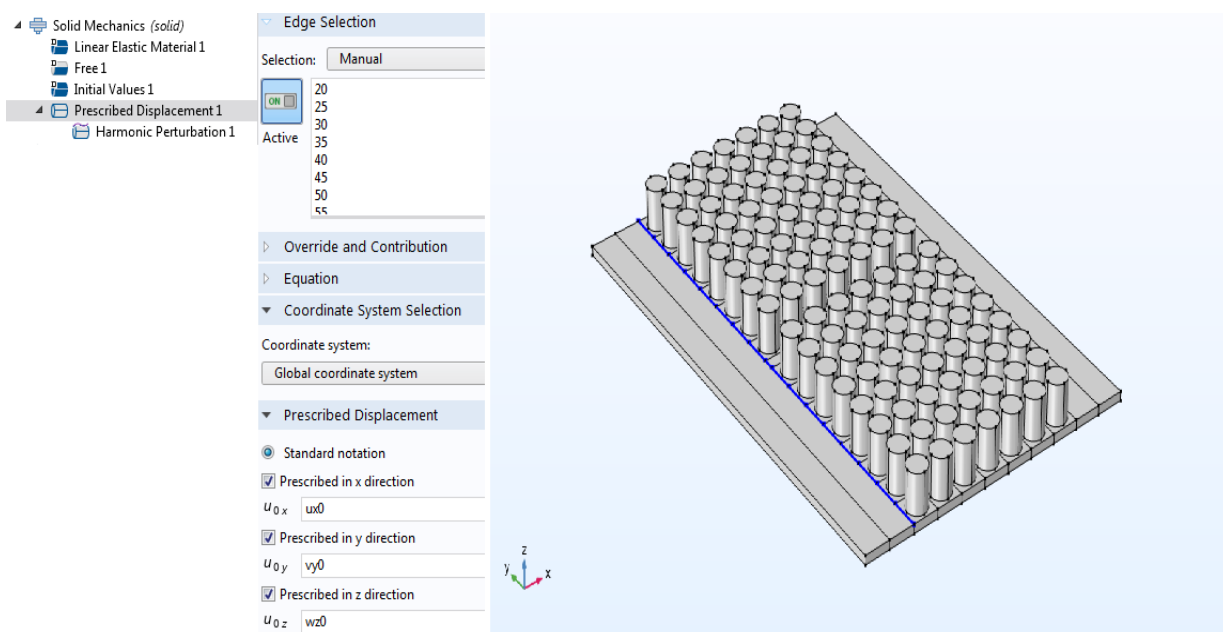
Figure 4.14: Prescribed displacement.

4.2.4.2. Mesh

- We add a **meshing** to the model.

Figure 4.15: Meshing of the model.

- The last step before we start our study is to add a range to the **Frequencies** in the **study settings** of **step1: frequency domain**.

Figure 4.16: Range for Step1: Frequency domain.

- Finally, we press **compute**.

Note: we used the same simulation steps for the three models (ww= 0.22*aa / ww=0.30*aa / ww= 0.38*aa).

4.3. Transmission with PML by removing some pillars

In this study, we will simulate the same model as the one before. Only this time, we'll be removing three pillars separately in each case of corridor.

4.3.1. Geometry parameters

- We will enter the parameters below:

Figure 4.17: Geometry parameters.

4.3.2. Material and its properties

- We'll be using the **Bolefortal**, with the following parameters:
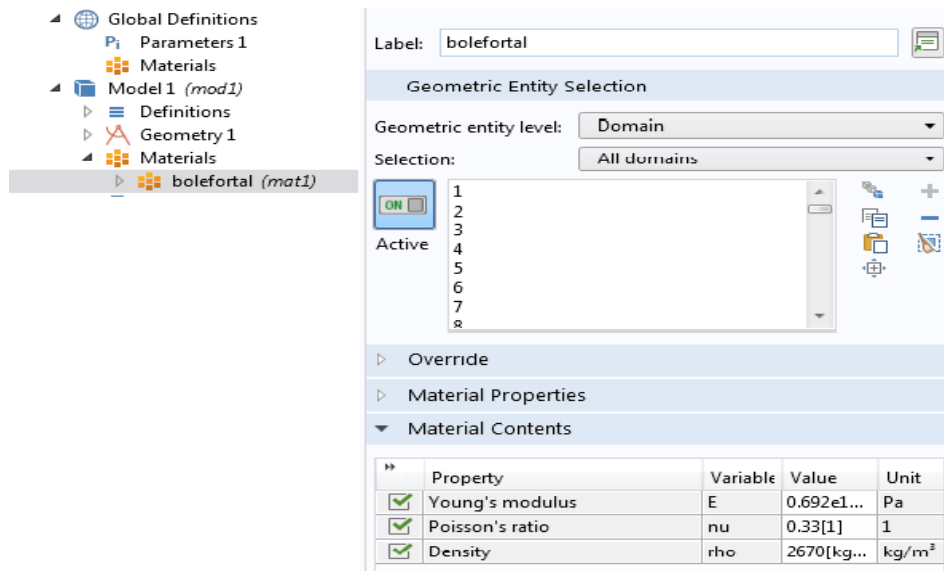
Figure 4.18: The models material and its properties.

4.3.3. The first corridor (ww= 0.22*aa)

4.3.3a. Removing the first pillar

- The geometry will become:
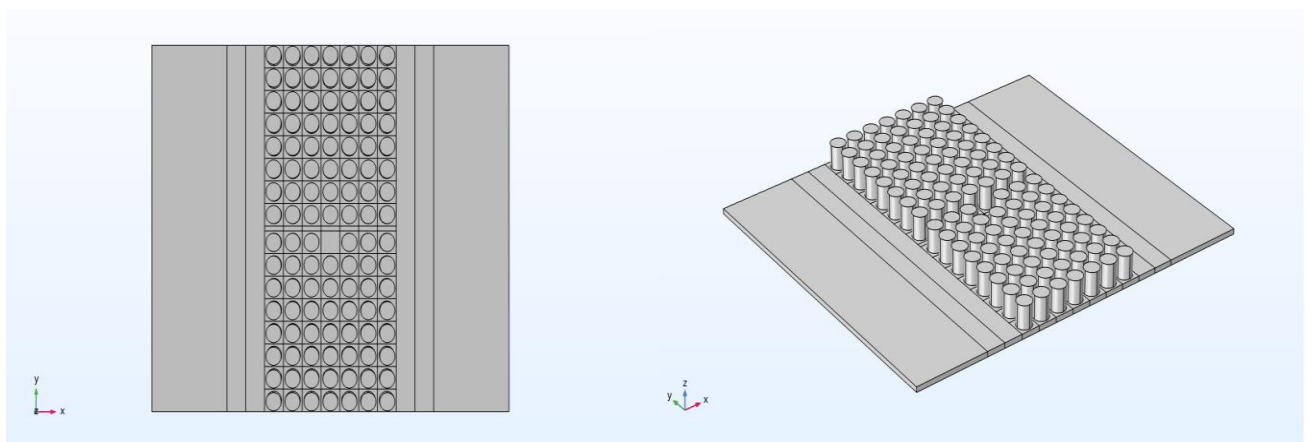
Figure 4.19a: Removing the first pillar for the first corridor (2D / 3D view).

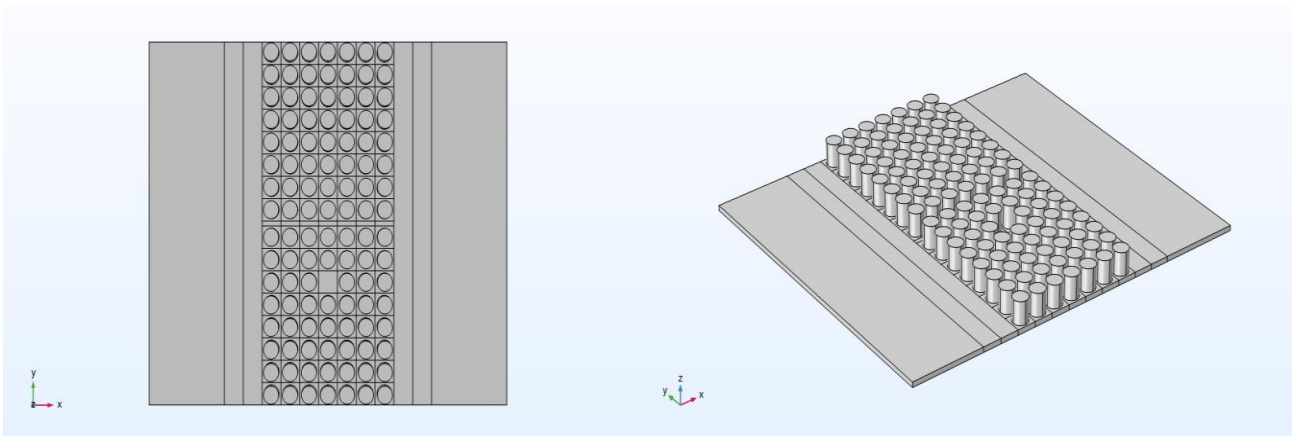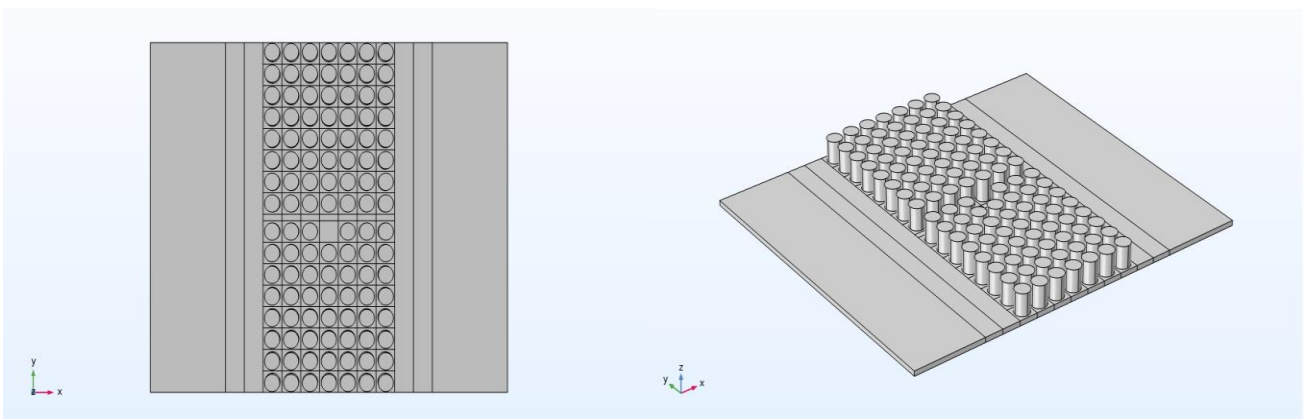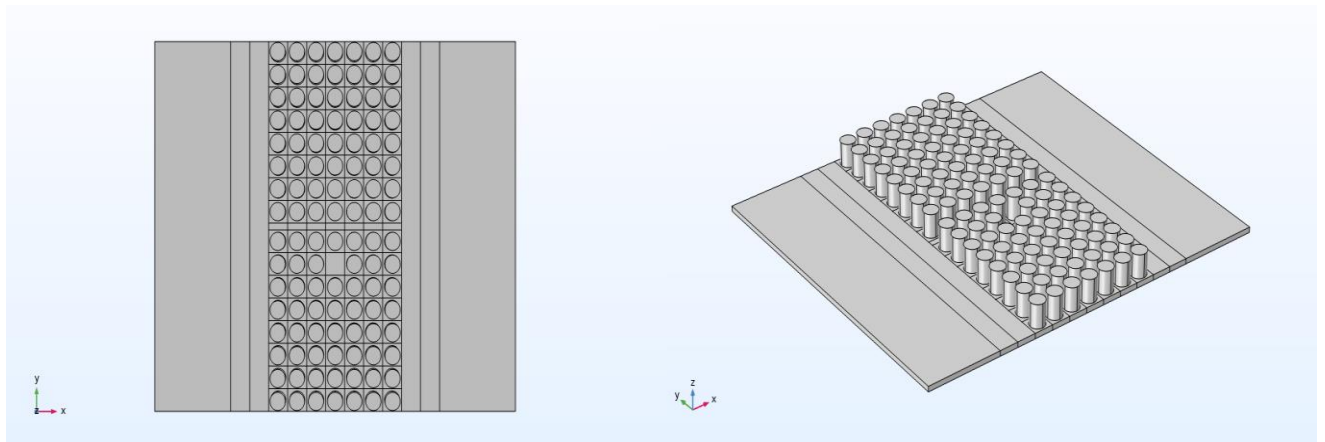## 4.3.3b. Removing the second pillar

- The geometry will be:
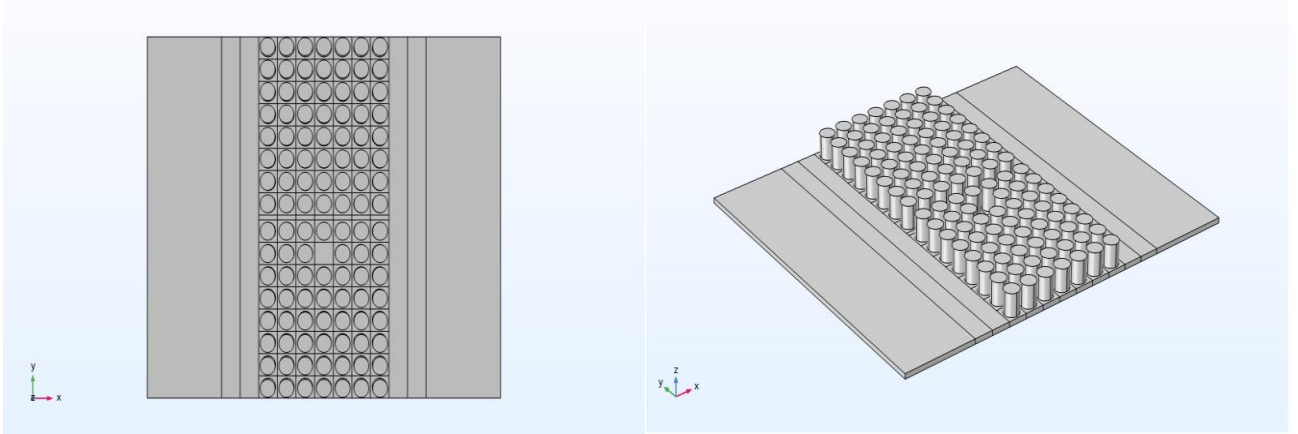
Figure 4.19b: Removing the second pillar for the first corridor (2D / 3D view).

4.3.3c. Removing the third pillar

- The geometry will become:

Figure 4.19c: Removing the third pillar for the first corridor (2D / 3D view).

4.3.4. The second corridor (ww= 0.30*aa)

4.3.4a. Removing the first pillar

- The geometry will be:

Figure 4.20a: Removing the first pillar for the second corridor (2D / 3D view).

4.3.4b. Removing the second pillar

- The geometry will become:

Figure 4.20b: Removing the second pillar for the second corridor (2D / 3D view).

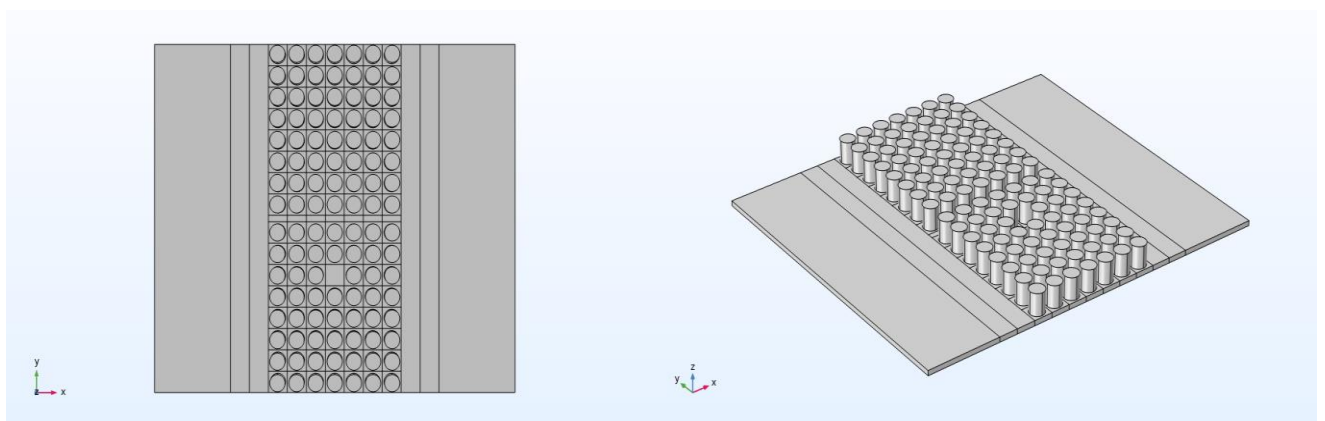## 4.3.4c. Removing the third pillar

- The geometry will be:

Figure 4.20c: Removing the third pillar for the second corridor (2D / 3D view).

4.3.5. The third corridor (ww= 0.38*aa)

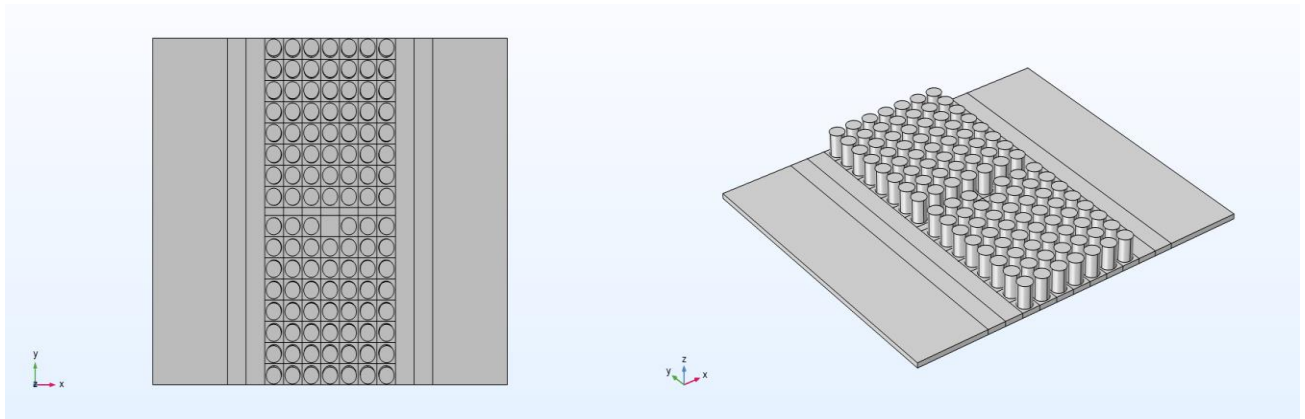## 4.3.5a. Removing the first pillar

- The geometry will become:

Figure 4.21a: Removing the first pillar for the third corridor (2D / 3D view).

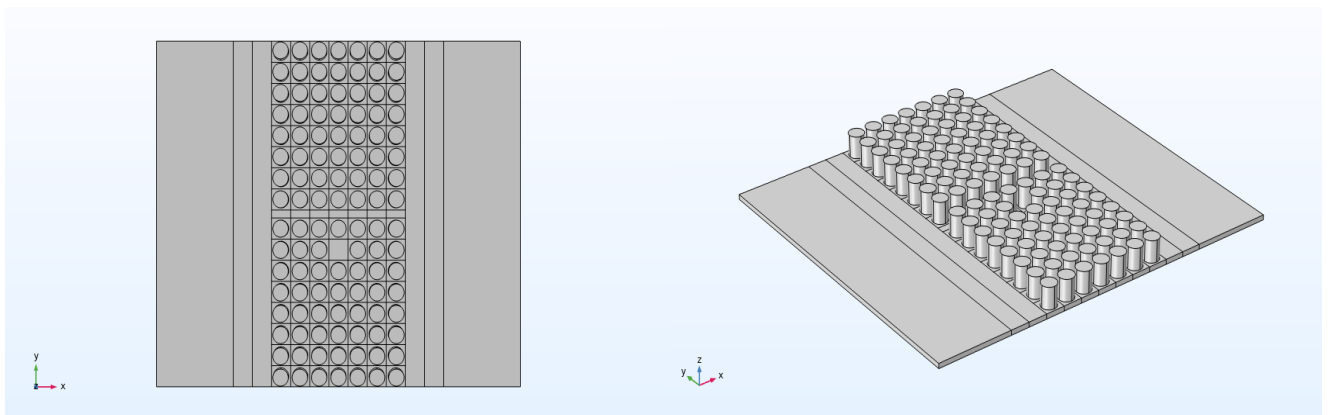### 4.3.5b. Removing the second pillar

- The geometry will be:

Figure 4.21b: Removing the second pillar for the third corridor (2D / 3D view).

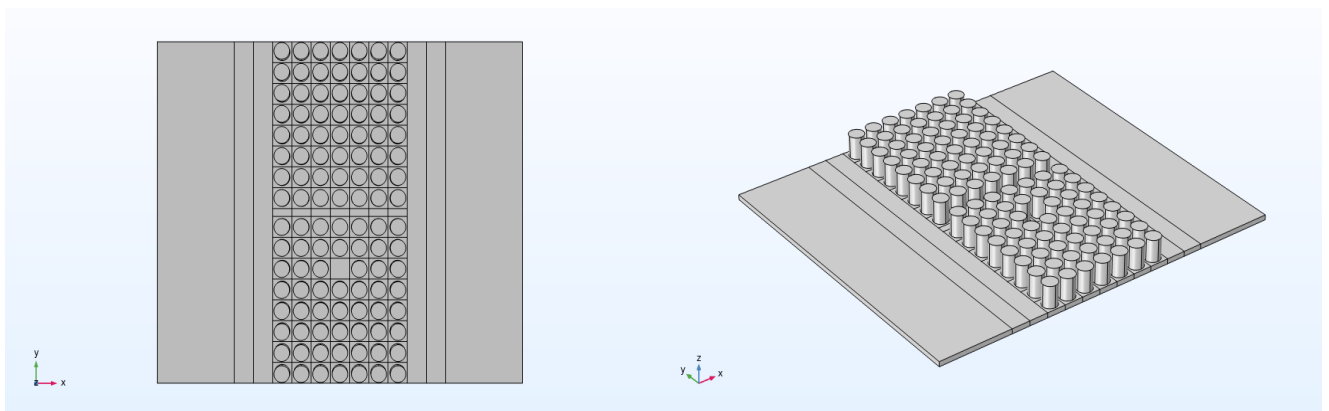### 4.3.5c. Removing the third pillar

- The geometry will become:

Figure 4.21c: Removing the third pillar for the third corridor (2D / 3D view).

4.3.6. Simulation steps

4.3.6.1. PML

- We'll add a **Perfectly Matched Layer (PML)** to the geometry by pressing right on **Definition**, and select the PML option:
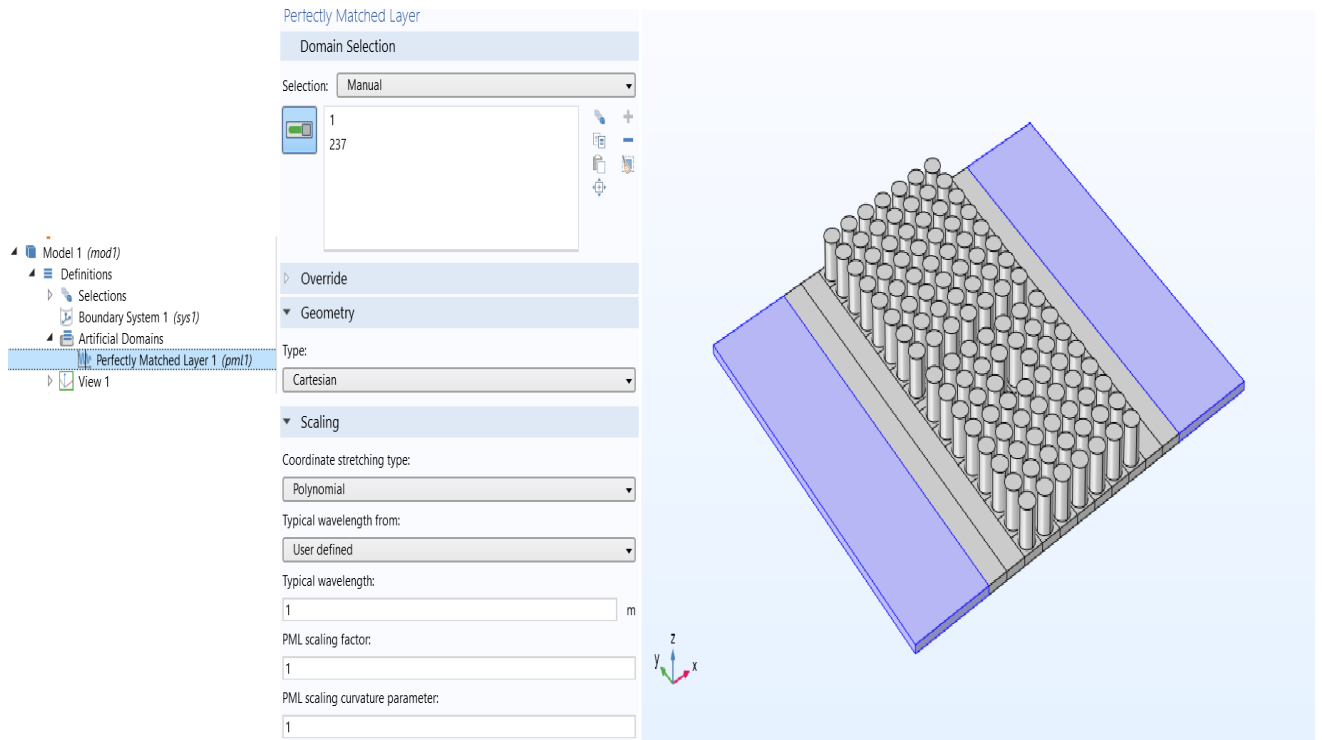

Figure 4.22: PML domains selection in our model.

4.3.6.2. Solid mechanics

- We will add a **periodic condition**, then a **Destination selection** for this latter.
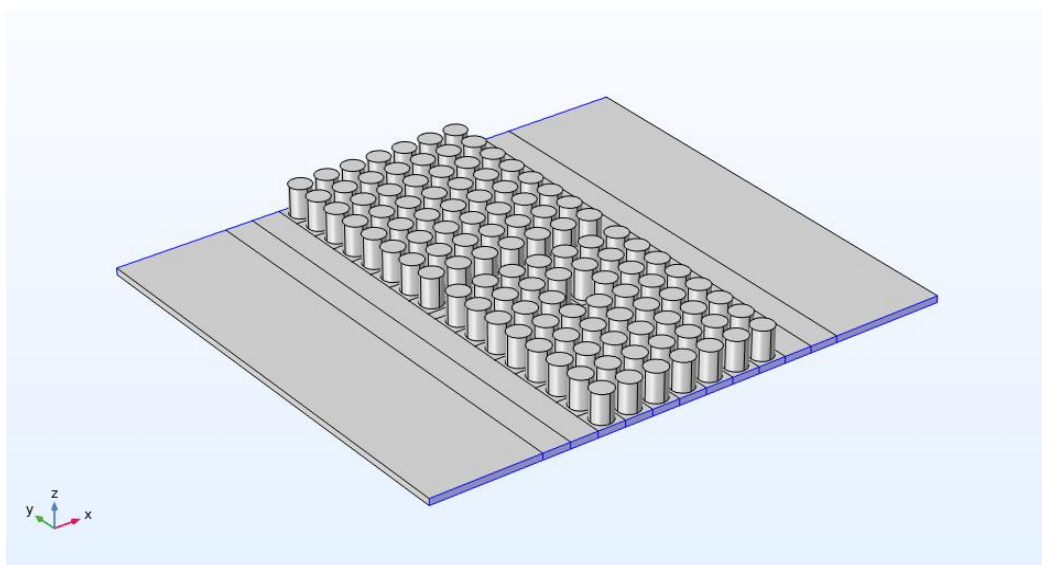

Figure 4.23: Periodic condition.

- We press right on **Solid mechanics** and choose **prescribed displacement**. After that, we press right on this latter to choose **Harmonic description**, and then setup the wave vector.
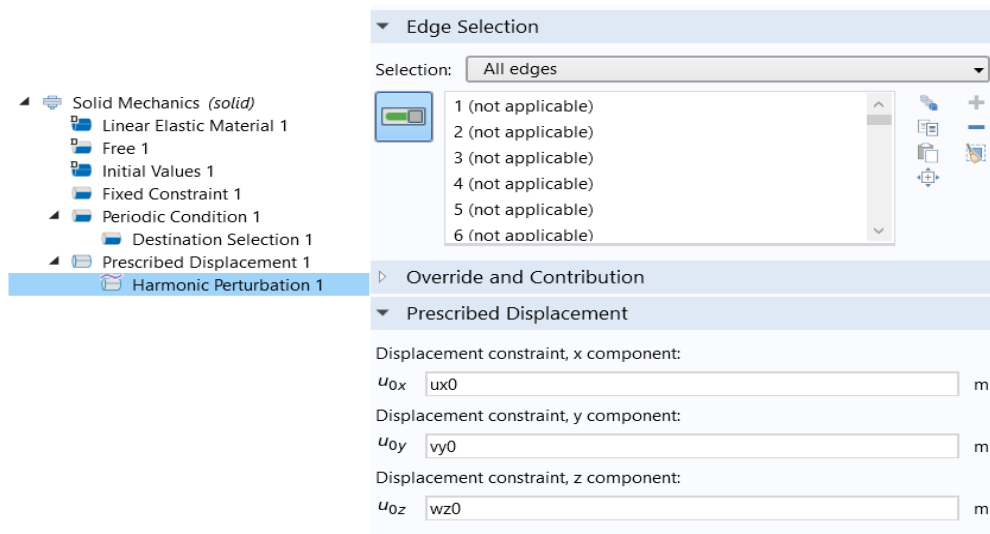

Figure 4.24: Harmonic perturbation.

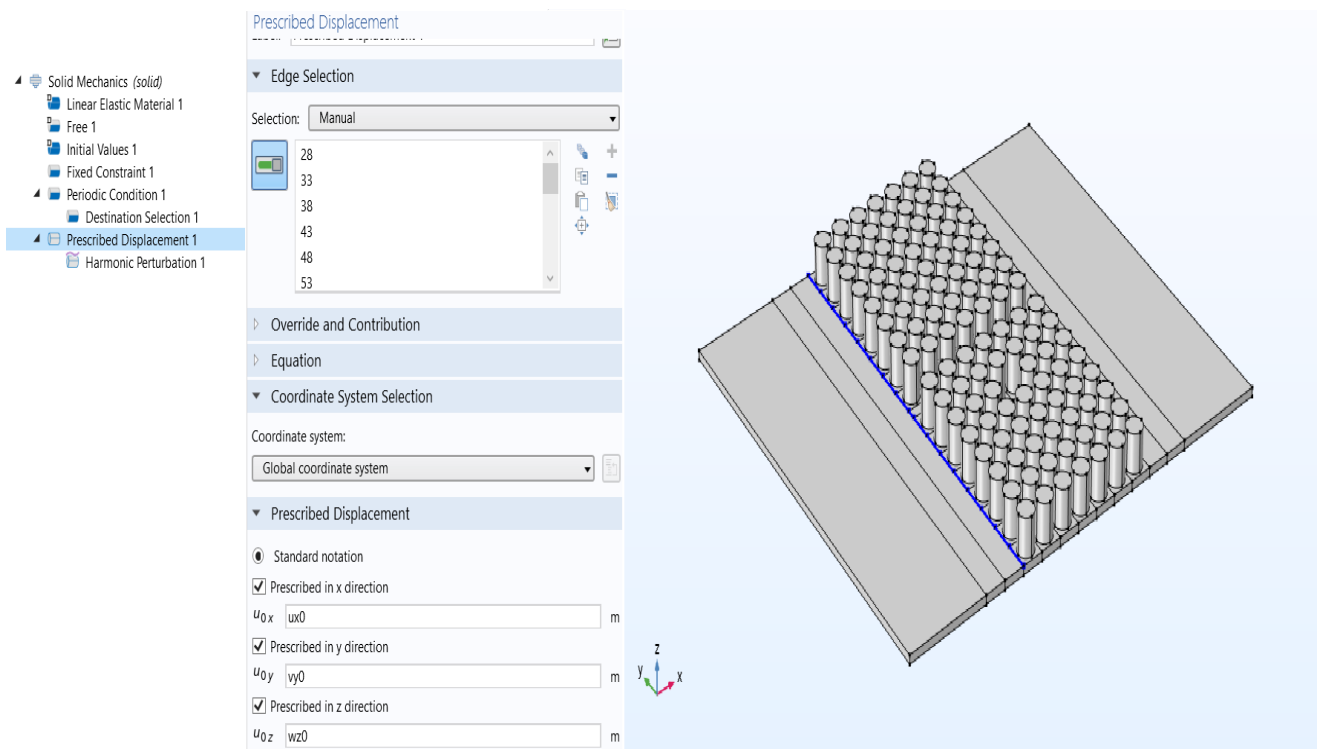- We return to **prescribed displacement** to select the edges of where we want the vibrations to start from.

Figure 4.25: Prescribed displacement.

4.3.6.3. Mesh

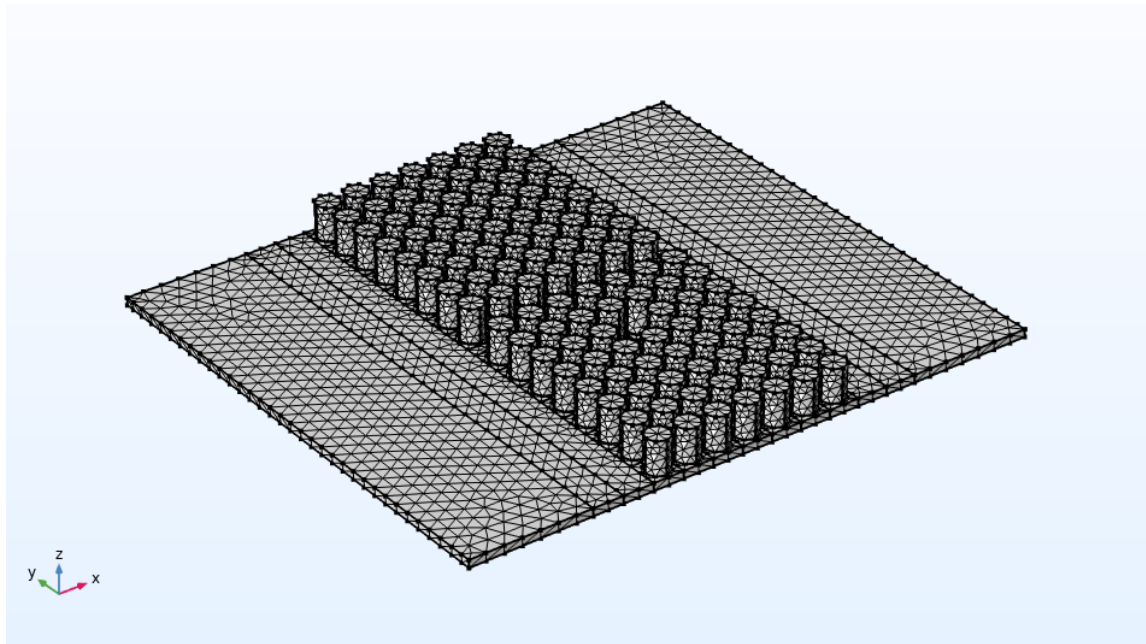- We add a **meshing** to the model.

Figure 4.26: Meshing of the model.

- The last step before we start our study is to add a range to the **Frequencies** in the **study settings** of **step1: frequency domain**.
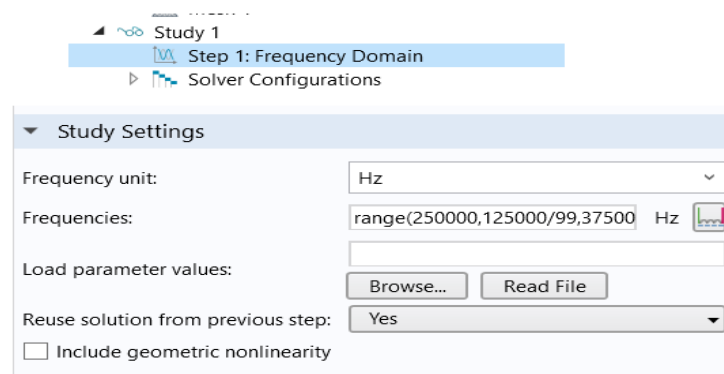

Figure 4.27: Range for Step1: Frequency domain.

- Finally, we press **compute**.

Note: we used the same simulation steps for the nine precedent models.

CHAPTER 5: RESULTS AND DISCUSSION

5.1. Dispersion curves
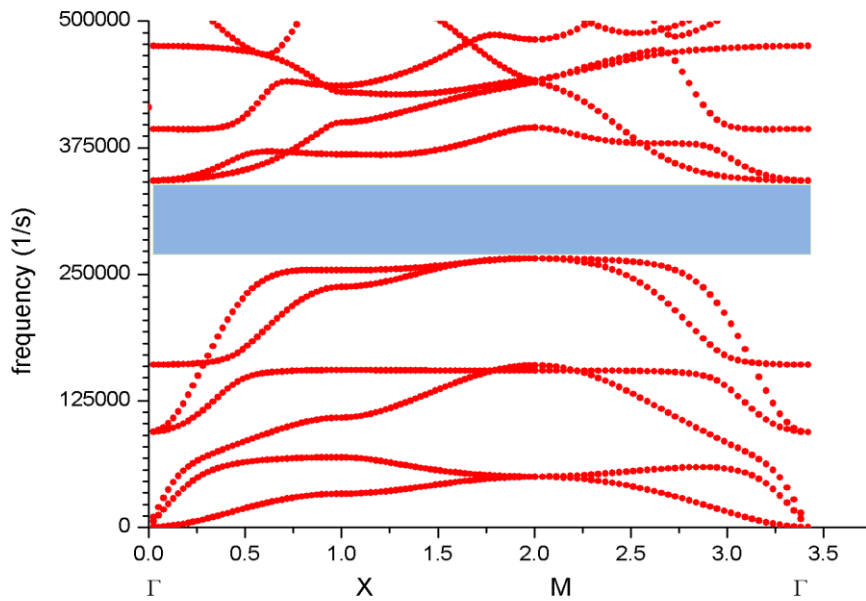
5.1.1. Unit-cell

Figure 5.1: Dispersion curve of unit-cell.

5.1.1.1. Discussion

This curve is resuming the vibration of our unit-cell. We observe a large band-gap between [262000Hz - 339000Hz] in the three directions.
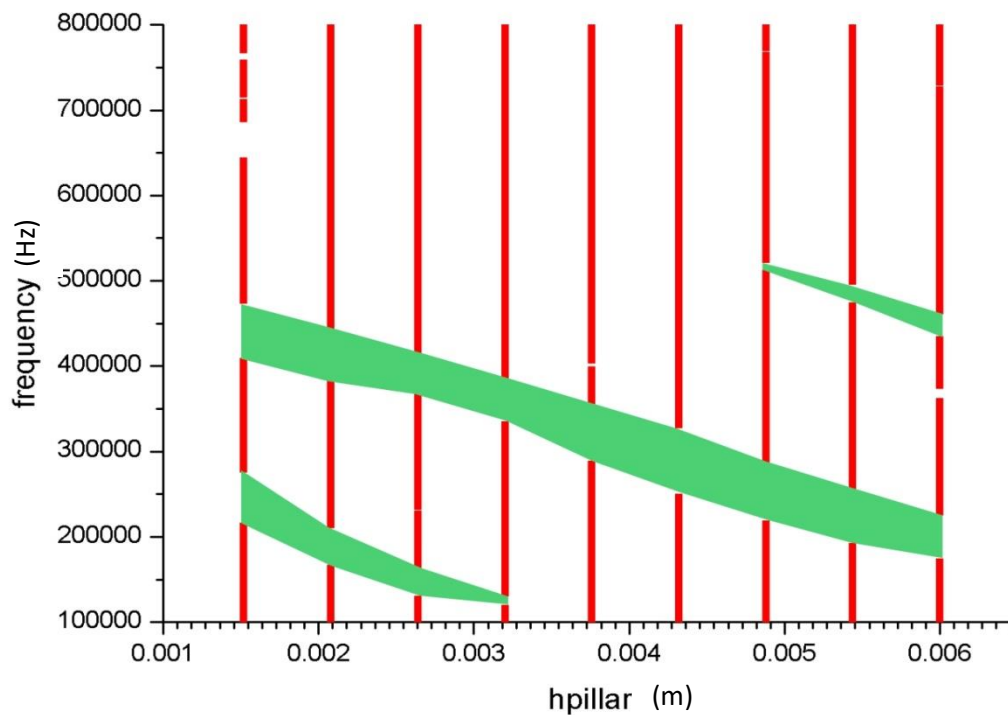
5.1.2. Gap mapping's curve

Figure 5.2: Evolution of the band-gaps according to the geometric parameter hpillar.

5.1.2.1. Discussion

The (Figure 5.2) summarize the variation in the width of the forbidden bands, their appearance and their extinction by varying the height. We can already notice that it is possible to have a first forbidden band at low frequencies for a relative height of the resonators situated between [0.0016m - 0.0033m]. We also notice the Bragg band-gap between [0.0016m – 0.006m]. And we remark that for hpillar=0.0044m the band-gap is larger than the other heights. And it depends on what range or domain of frequency we're going to work on, so we choose the best hpillar in order to get the best results we want.

5.1.3. Supercell without corridor
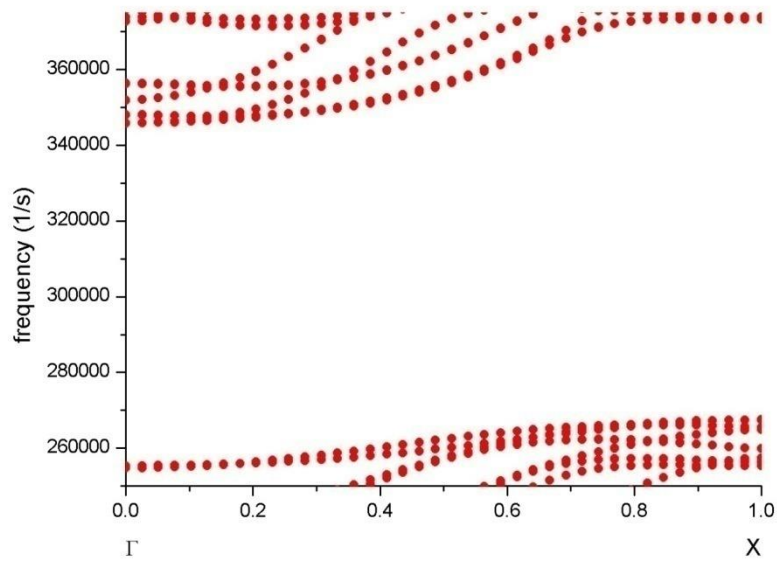

Figure 5.3: Dispersion curve of supercell without corridor.

5.1.4. Supercell with corridor
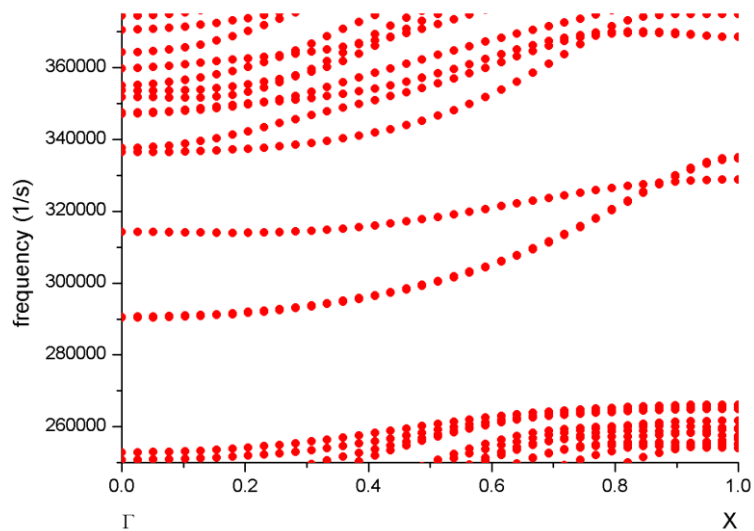
5.1.4a. The first corridor (ww= 0.22*aa)

Figure 5.4a: Dispersion curve of supercell with a corridor of ww= 0.22*aa.

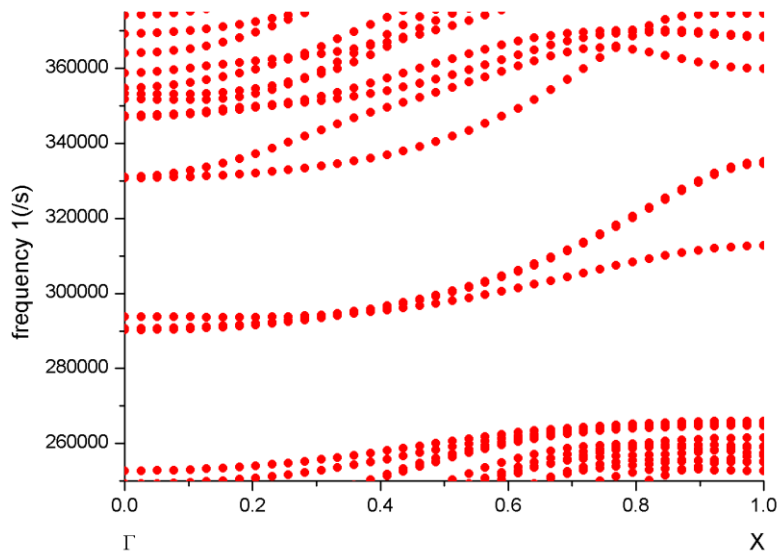## 5.1.4b. The second corridor (ww= 0.30*aa)

Figure 5.4b: Dispersion curve of supercell with a corridor of ww= 0.30*aa.

5.1.4c. The third corridor (ww= 0.38*aa)
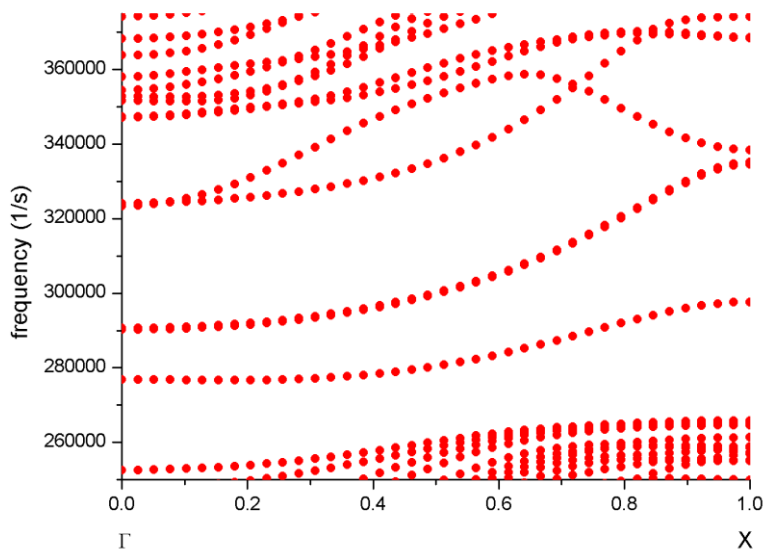
Figure 5.4c: Dispersion curve of supercell with a corridor of ww= 0.38*aa.

5.1.5. Discussion
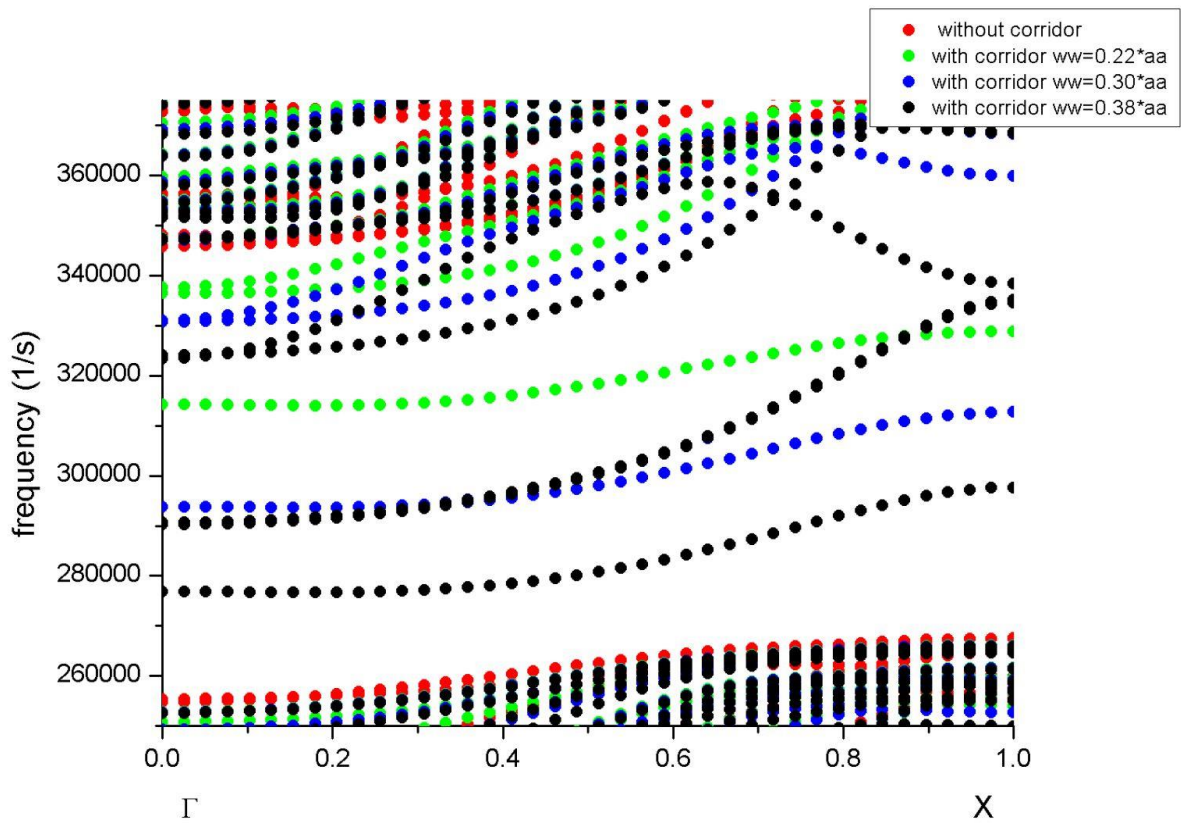
Figure 5.5: Dispersion curve of all super-cells models.

These dispersion curves show the corridor's effect in our supercell. When there is no corridor, we see that the band-gap is very large, but when we add a corridor we observe that the band-gap is divided. The more we increase the width of the corridor more the band-gap gets shorter, and when we reach a specific width of the corridor, the band-gap disappears. Also we get more vibration modes in our band-gap.

5.2. Transmission curves

5.2.1. Transmission in multi-supercell with PML

5.2.1a. The first corridor (ww= 0.22*aa)

Figure 5.6a: (a) Transmission curve of multi-supercell with a corridor of ww= 0.22*aa. (b) The geometry result on freq=2.8862 KHz.

5.2.1b. The second corridor (ww= 0.30*aa)

Figure 5.6b: (a) Transmission curve of multi-supercell with a corridor of ww= 0.30*aa. (b) The geometry result on freq=2.9123 KHz.

5.2.1c. The third corridor (ww= 0.38*aa)

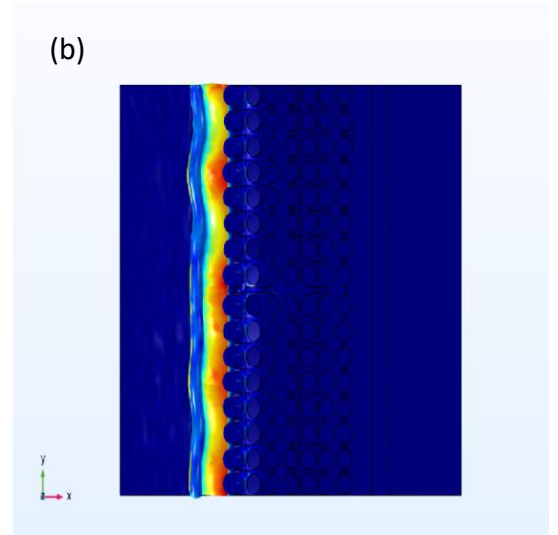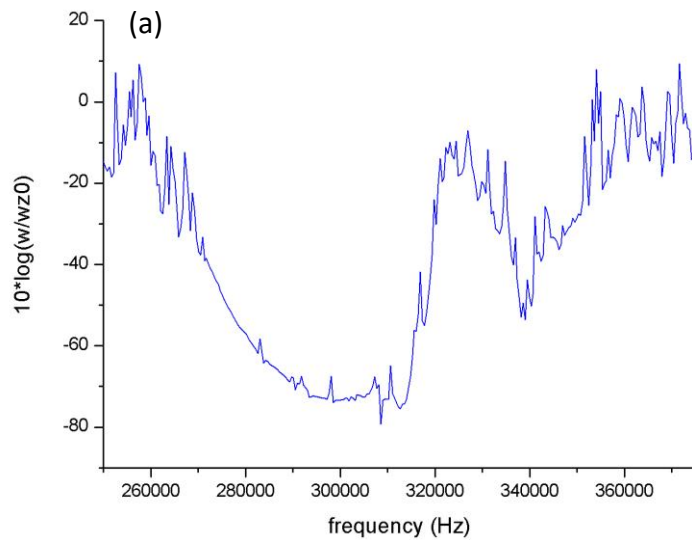**Figure 5.6c:** (a) Transmission curve of multi-supercell with a corridor of ww= 0.38*aa. (b) The geometry result on freq=2.8002 KHz.

5.2.1.1. Discussion

Figure 5.7: Transmission curve of all multi-super cells with PML with three different corridors.

Figures (5.6a, 5.6b, 5.6c) are resumed in (Figure 5.7).

These transmission curves show the attenuation peaks of the incident wave and which correspond to an absence of wave propagation (bands colored in green). These latter confirm the presence of the absolute nature of the band-gap.

Also, we notice that more the corridor is larger more the attenuation decreases. For example; for ww= 0.22*aa we get an attenuation of -75dB, and for ww= 0.30*aa the attenuation is around -70dB, for the last corridor ww= 0.38*aa the attenuation will be -50dB, that leads to a thin band-gap and a high Q factor. That leads to a more selective structure.

From these results we conclude that the corridor's width is inversely proportional to the attenuation of the incident wave.

5.2.2. Transmission in multi-supercell without PML

5.2.2a. The first corridor (ww= 0.22*aa)

Figure 5.8a: (a) Transmission curve of multi-supercell with a corridor of ww= 0.22*aa. (b) The geometry result on freq=2.6991 KHz.
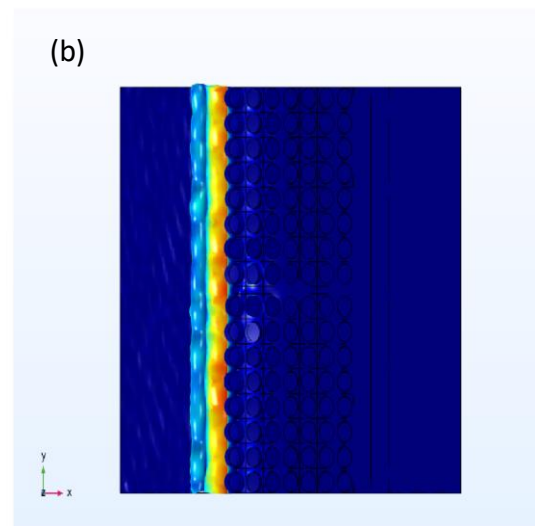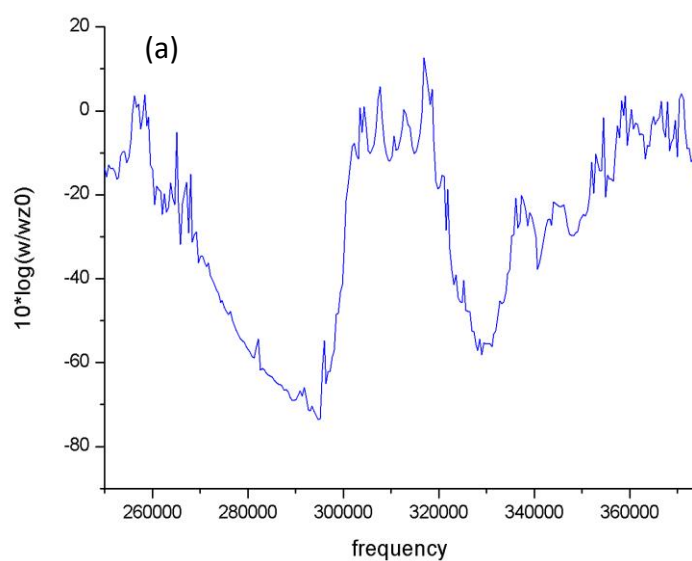
5.2.2b. The second corridor (ww= 0.30*aa)
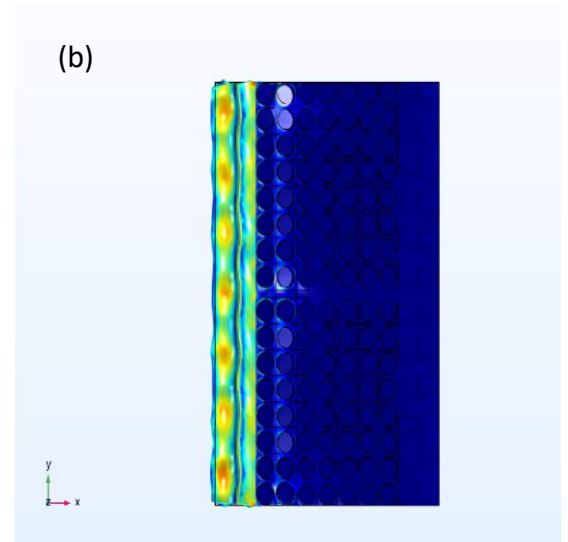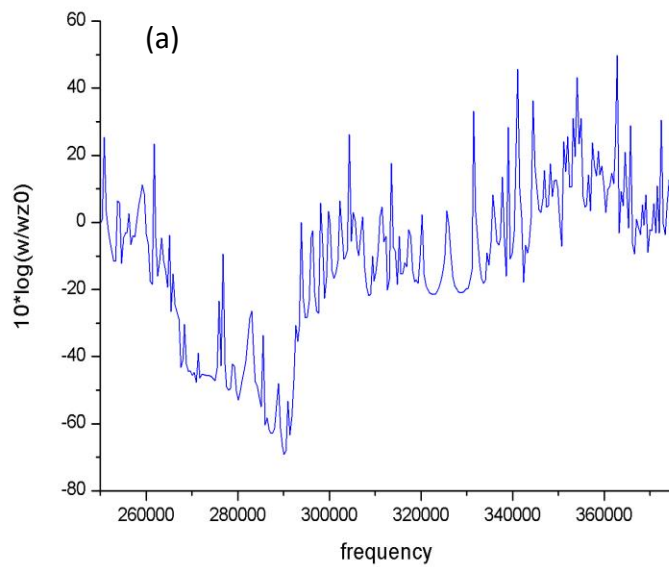
Figure 5.8b: (a) Transmission curve of multi-supercell with a corridor of ww= 0.30*aa.
(b) The geometry result on freq=2.7585 KHz.
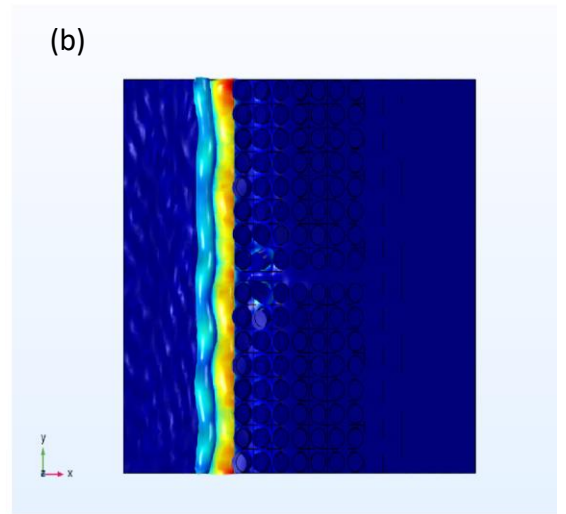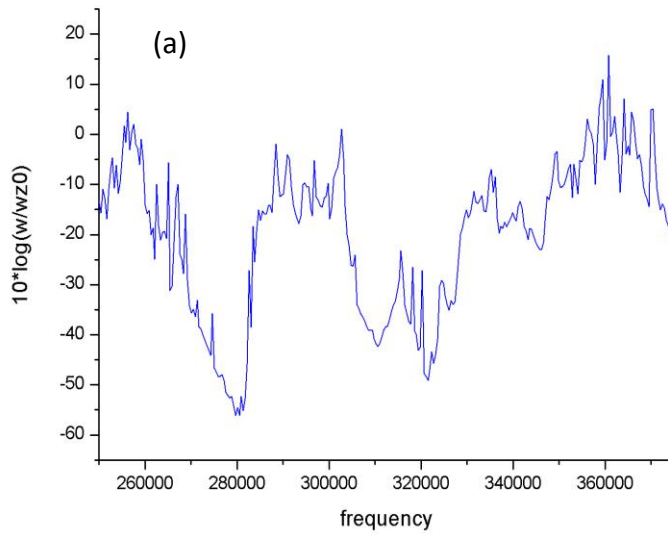

5.2.2c. The third corridor (ww= 0.38*aa)
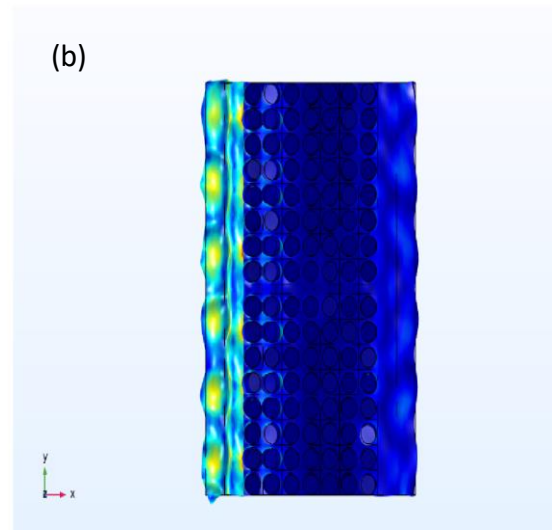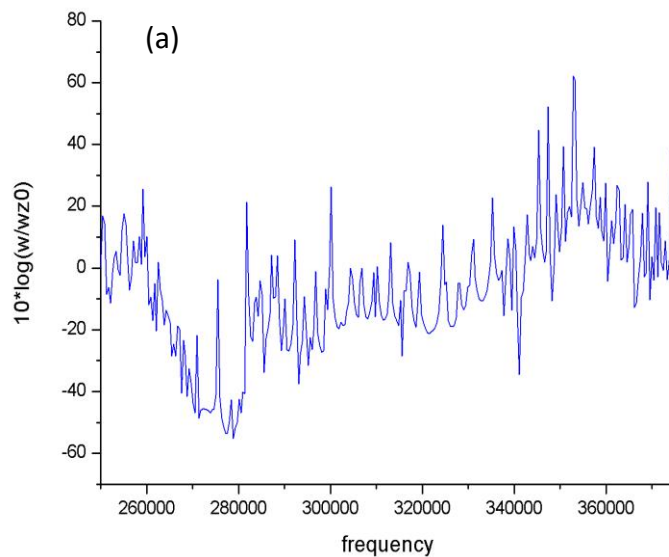
Figure 5.8c: (a) Transmission curve of multi-supercell with a corridor of ww= 0.38*aa.
(b) The geometry result on freq=2.7762 KHz.
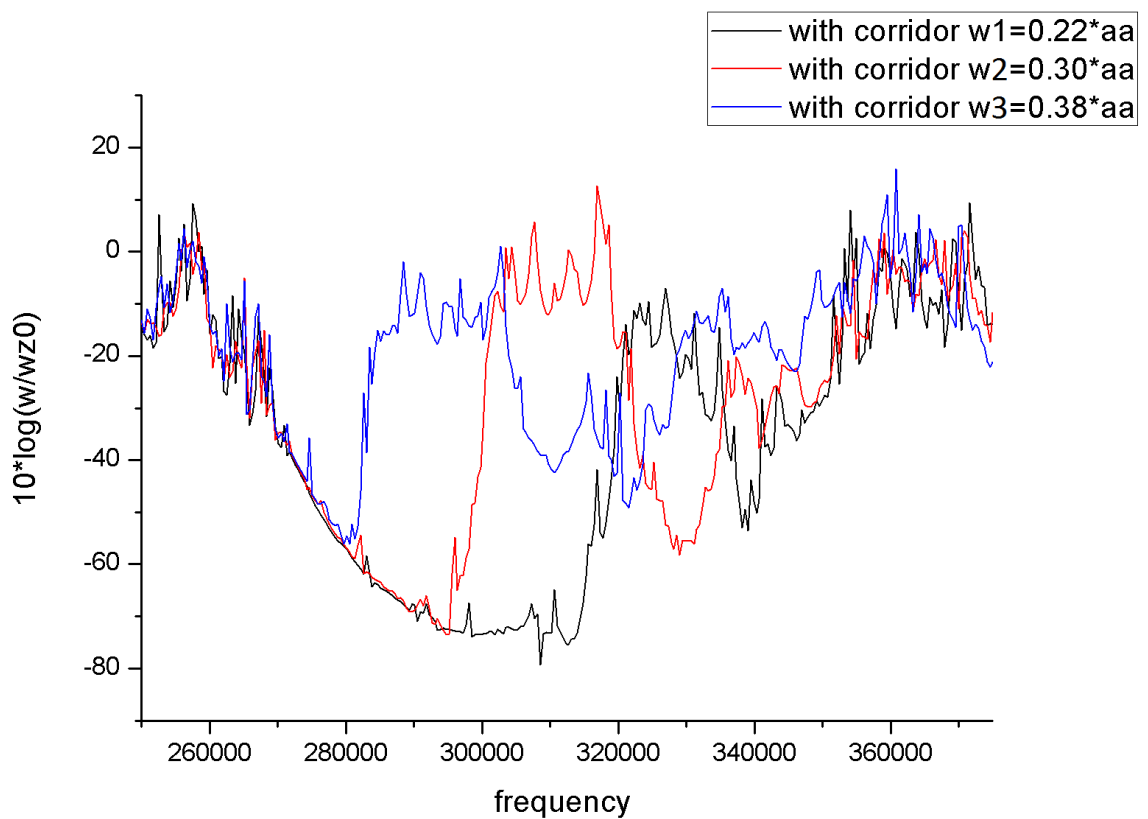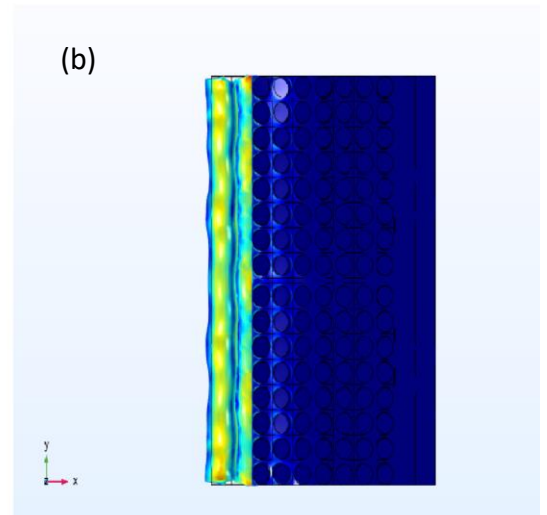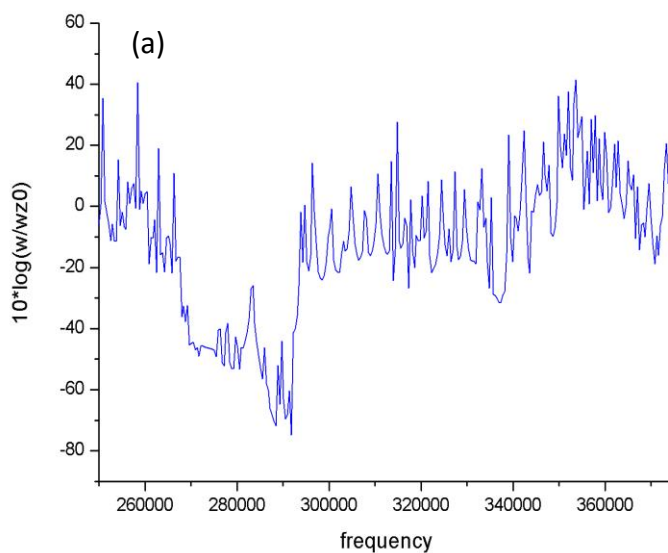
5.2.2.1. Discussion
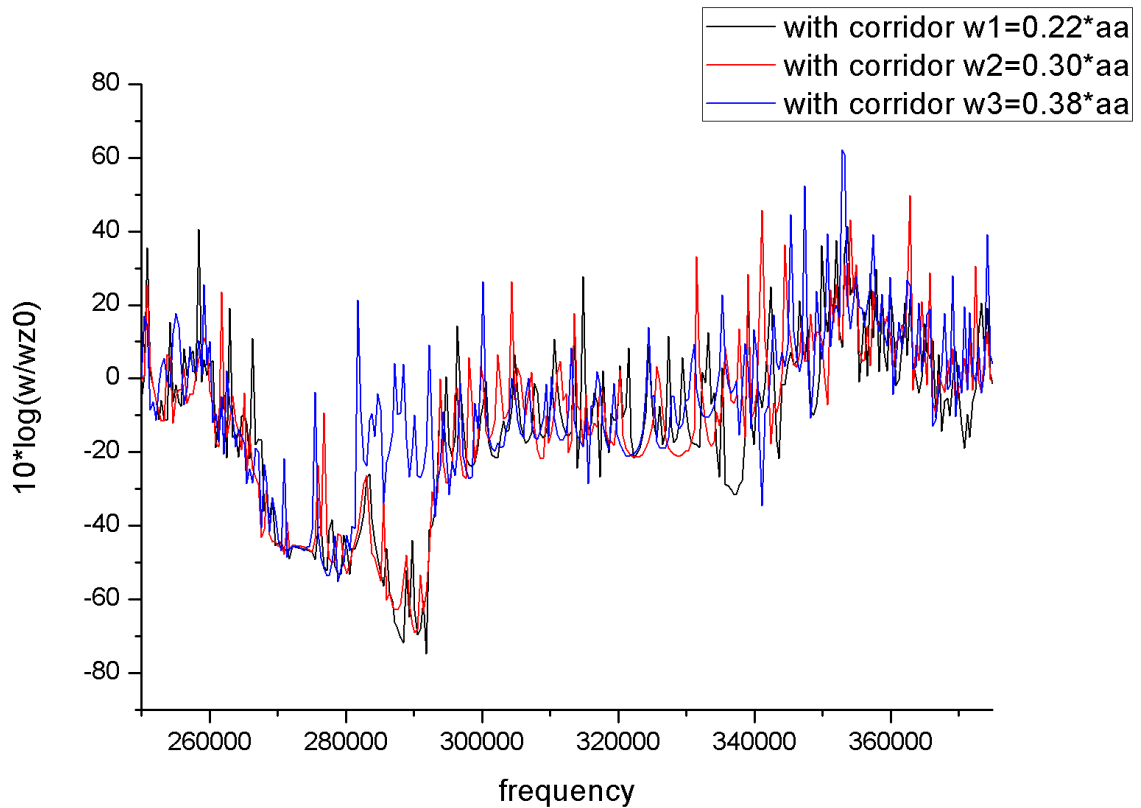
Figure 5.9: Transmission curve of all multi-super cells without PML with three different corridors.

Figures (5.8a, 5.8b, 5.8c) are resumed in (Figure 5.9).

These transmission curves show the attenuation peaks in our structure without using PML. These peaks refer to an absolute band-gap with huge attenuation. For example; for ww=0.22*aa we get an attenuation of -75dB, and for ww= 0.30*aa the attenuation is around -70dB, for the last corridor ww= 0.38*aa the attenuation will be -50dB, that leads to a thin band-gap and a high Q factor. That leads to a more selective structure.

When we compare the results of transmission curves with / without PML we see a big difference. When we used PML we got a larger band-gap which is the opposite when we didn't use PML, also the curve's form is different. And also when we didn't use PML we got more peaks then the PML structures, that's because the PML absorb all the reflected waves which create a parasite modes.

5.2.3. Transmission in multi-supercell with PML by removing one pillar

5.2.3.1. The first corridor (ww= 0.22*aa)

5.2.3.1a. Removing the first pillar

Figure 5.10a: (a) Transmission curve of multi-supercell by removing the first pillar for the first corridor. (b) The geometry result of the resonance peak on freq=2.8133 KHz.

5.2.3.1b. Removing the second pillar

Figure 5.10b: (a) Transmission curve of multi-supercell by removing the second pillar for the first corridor. (b) The geometry result of the resonance peak on freq=2.9888KHz.

5.2.3.1c. Removing the third pillar
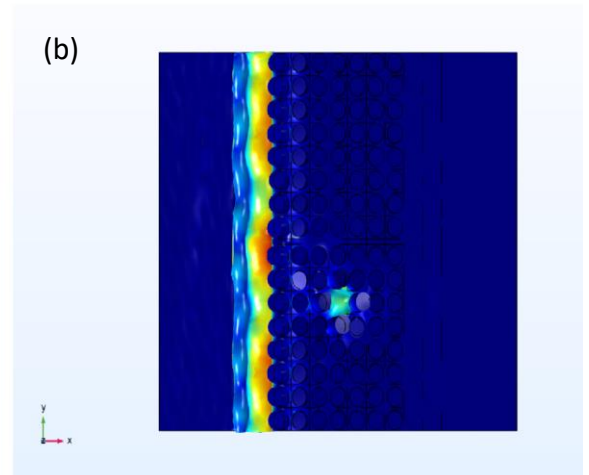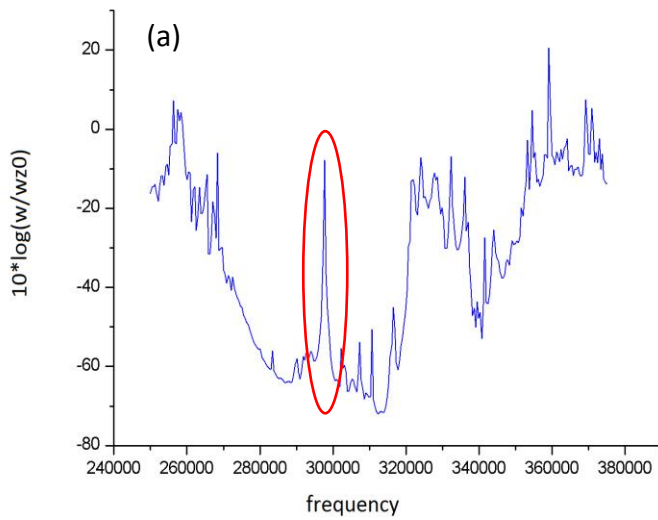
Figure 5.10c: (a) Transmission curve of multi-supercell by removing the third pillar for the first corridor. (b) The geometry result of the resonance peak on freq=2.9874 KHz.

5.2.3.2. The second corridor (ww= 0.30*aa)

5.2.3.2a. Removing the first pillar
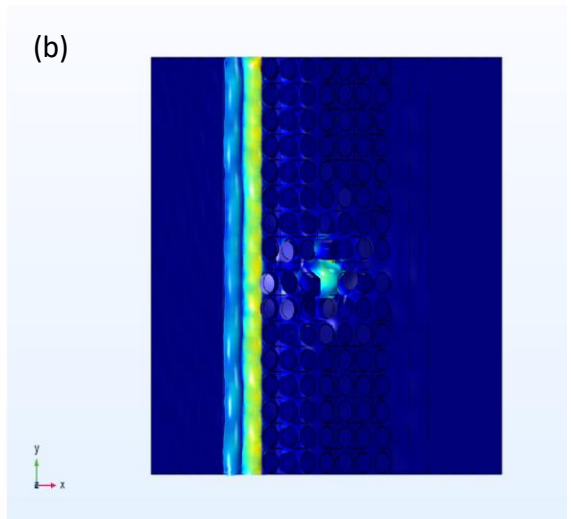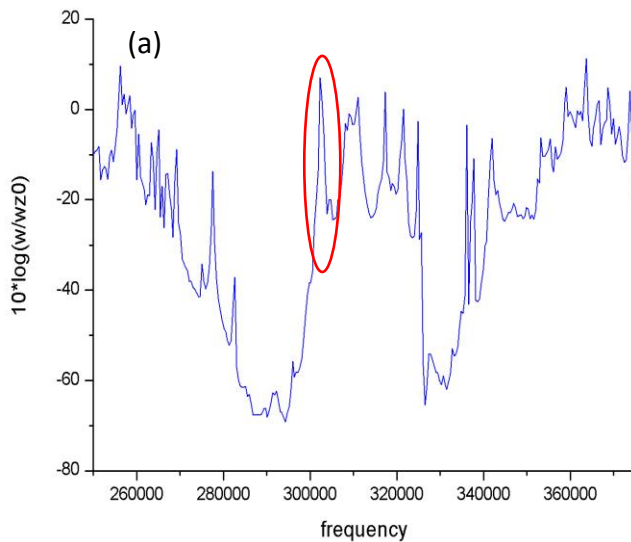
Figure 5.11a: (a) Transmission curve of multi-supercell by removing the first pillar for the second corridor. (b) The geometry result of the resonance peak on freq=3.1634KHz.

5.2.3.2b. Removing the second pillar
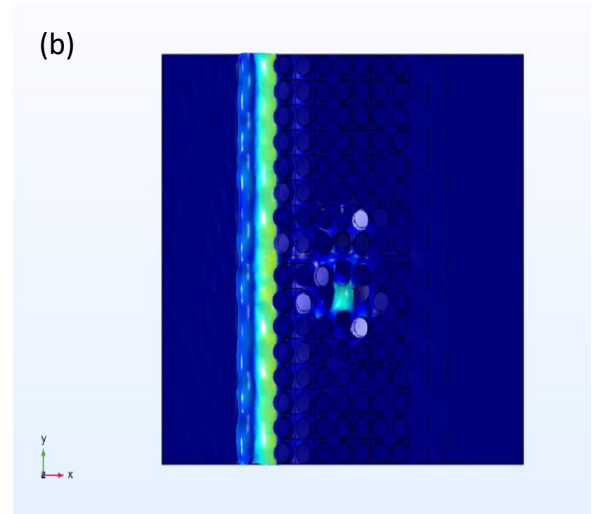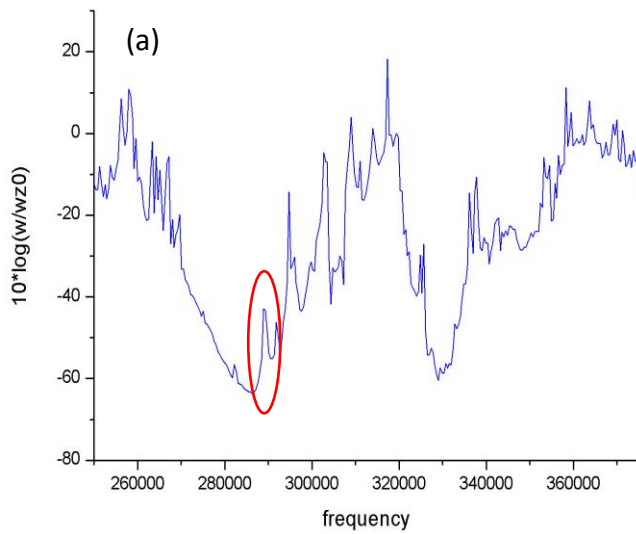
Figure 5.11b: (a) Transmission curve of multi-supercell by removing the second pillar for the second corridor. (b) The geometry result of the resonance peak on freq=2.8933KHz.

5.2.3.2c. Removing the third pillar
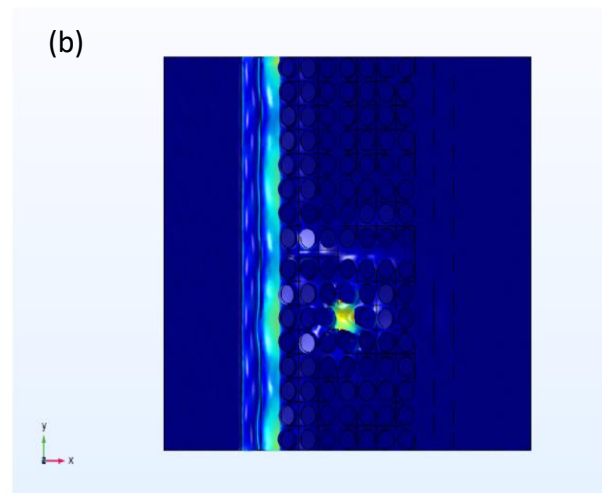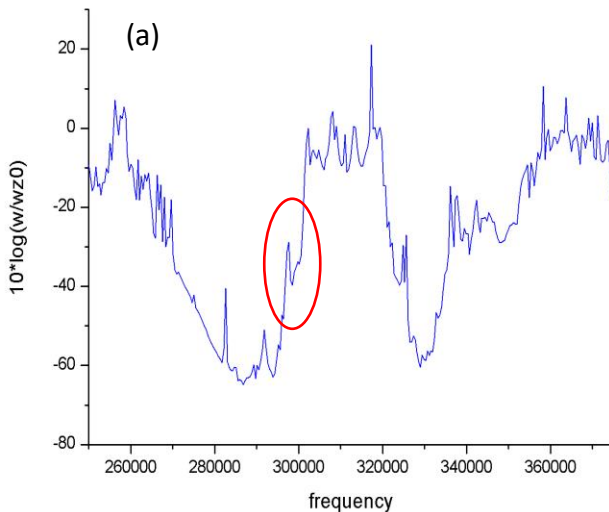
Figure 5.11c: (a) Transmission curve of multi-supercell by removing the third pillar for the second corridor. (b) The geometry result of the resonance peak on freq=2.9866KHz.

5.2.3.3. The third corridor (ww= 0.38*aa)

5.2.3.3a. Removing the first pillar
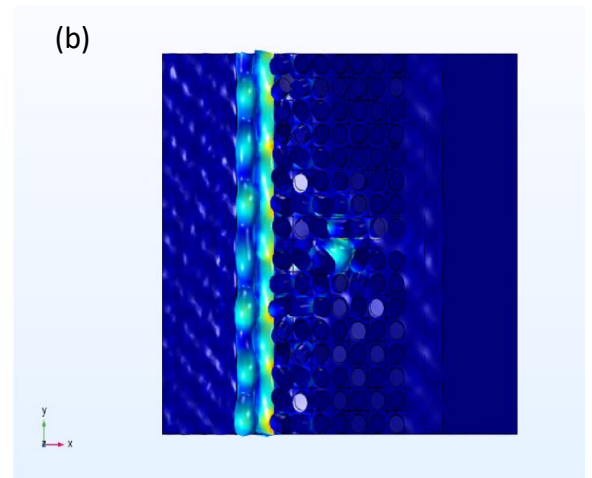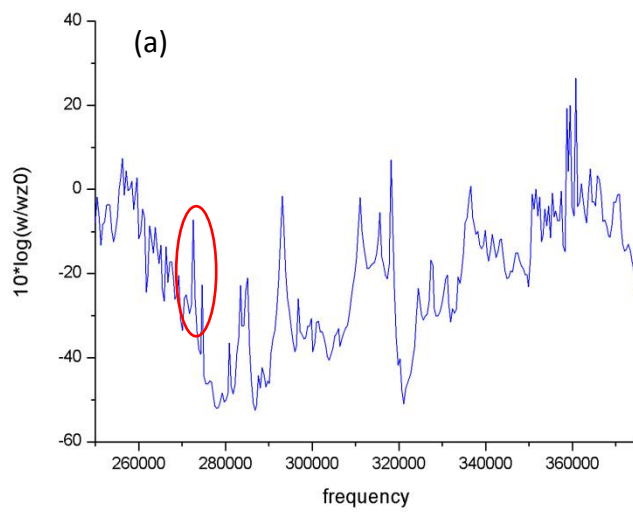
Figure 5.12a: (a) Transmission curve of multi-supercell by removing the first pillar for the third corridor. (b) The geometry result of the resonance peak on freq=2.7174 KHz.

5.2.3.3b. Removing the second pillar
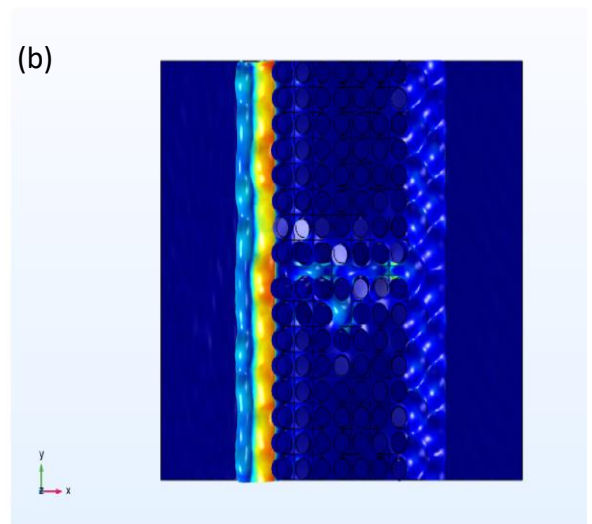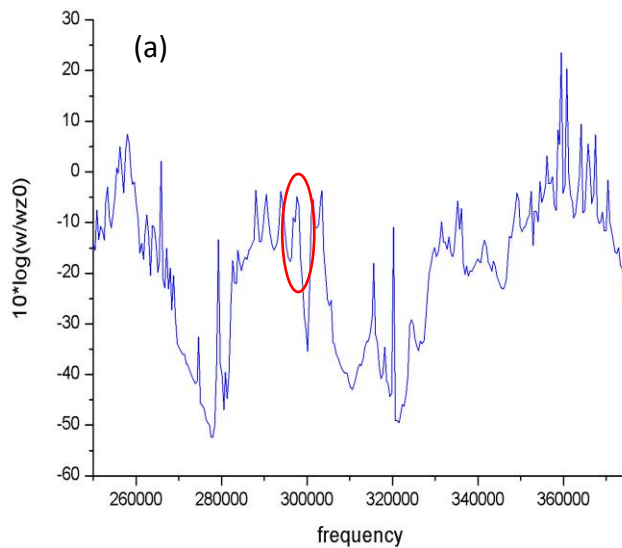
Figure 5.12b: (a) Transmission curve of multi-supercell by removing the second pillar for the third corridor. (b) The geometry result of the resonance peak on freq=2.9822KHz.
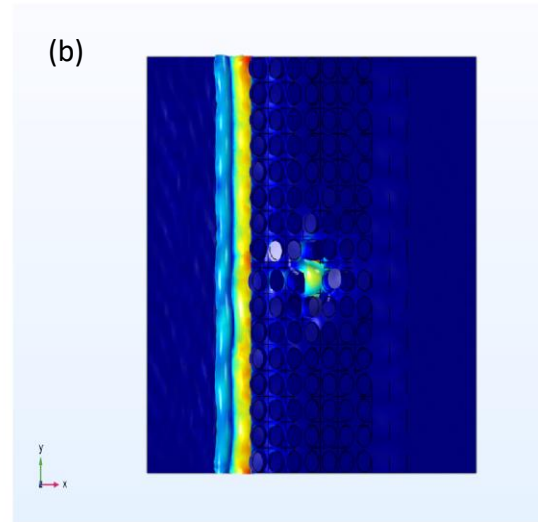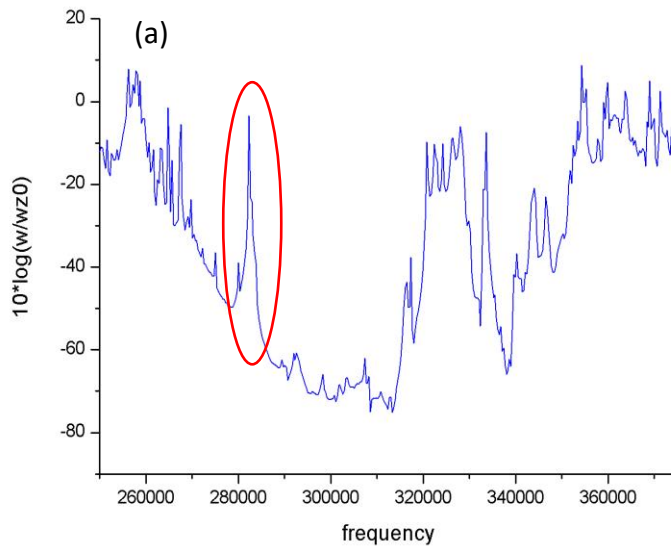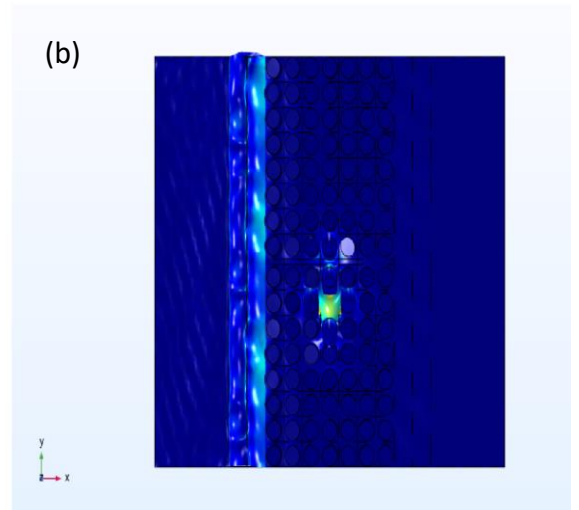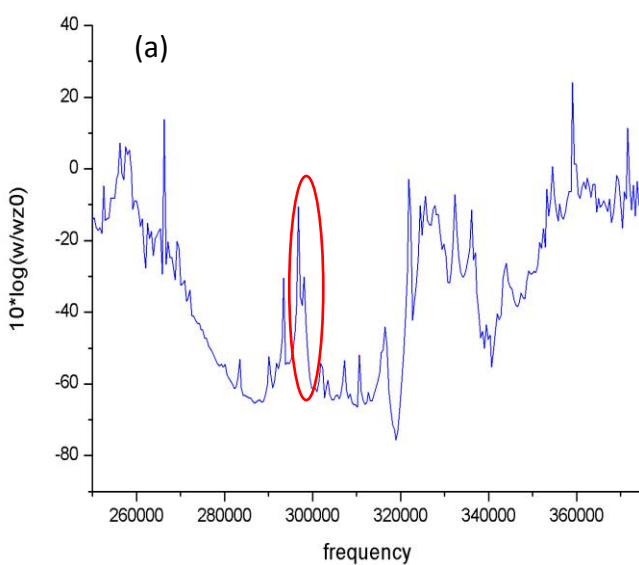
5.2.3.3c. Removing the third pillar
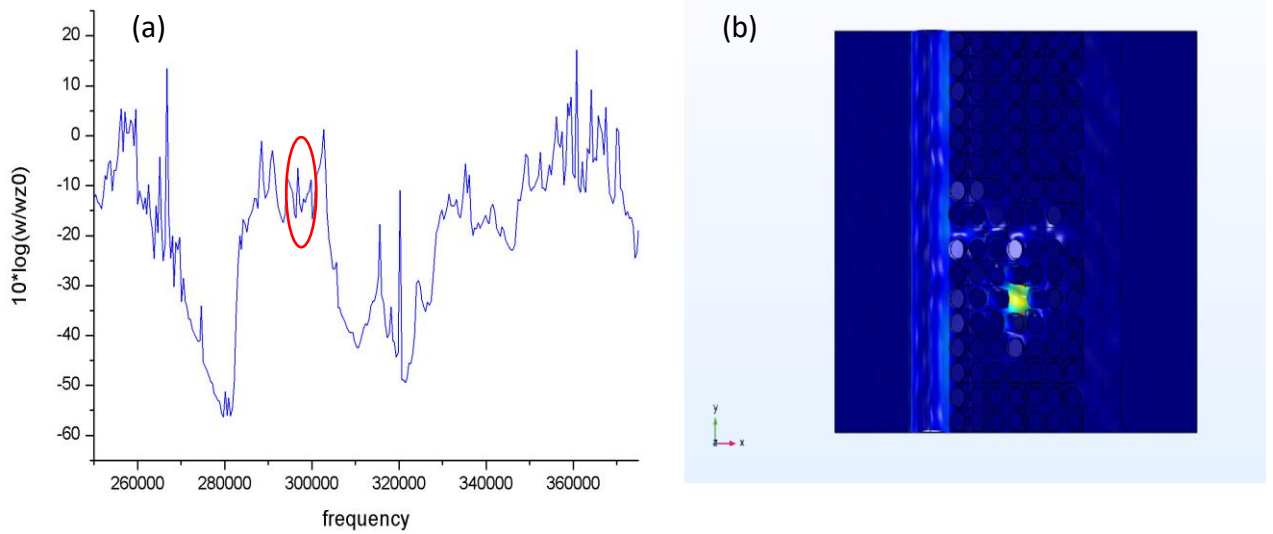
Figure 5.12c: (a) Transmission curve of multi-supercell by removing the third pillar for the third corridor. (b) The geometry result of the resonance peak on freq=2.9798 KHz.

5.2.3.4. Discussion
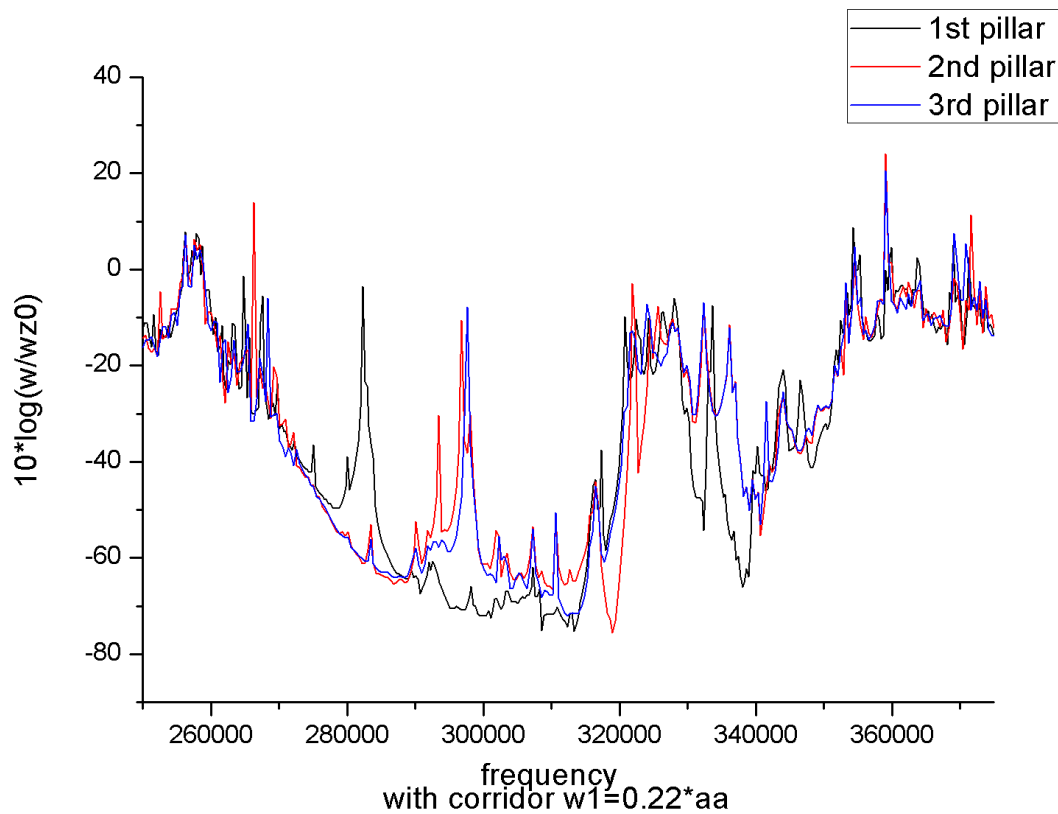
Figure 5.13: Transmission of all multi-super cells with corridor of ww= 0.22*aa by removing one pillar.
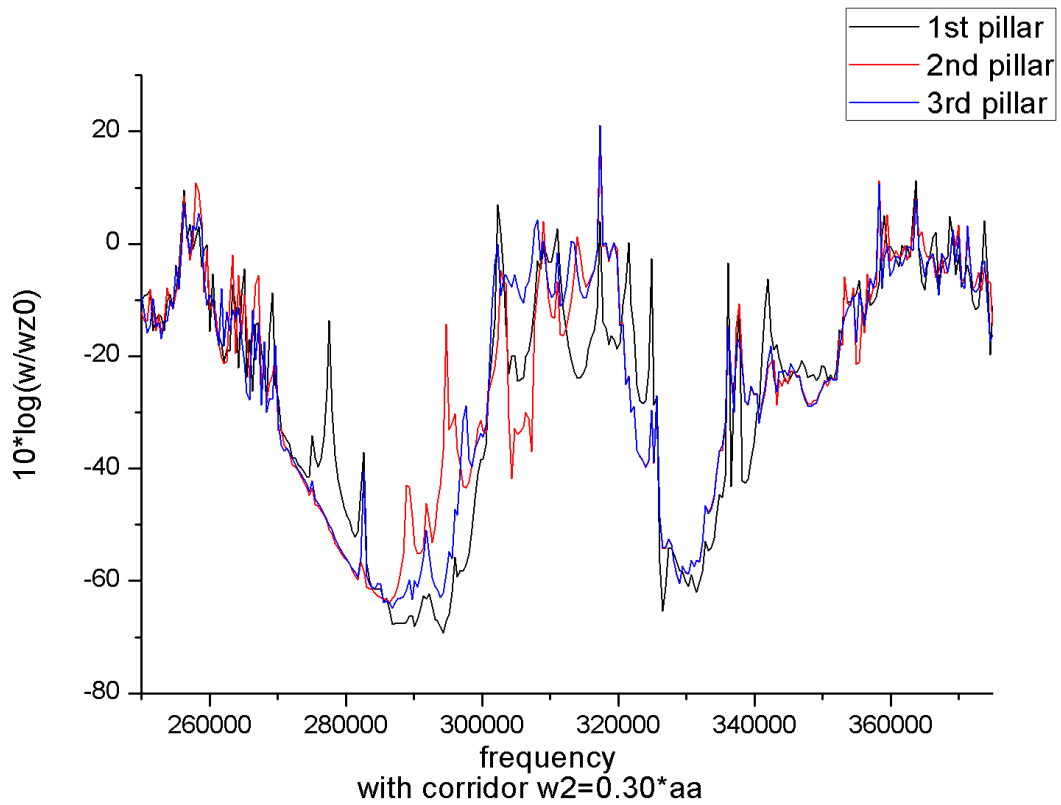
Figure 5.14: Transmission of all multi-super cells with corridor of ww= 0.30*aa by removing one pillar.
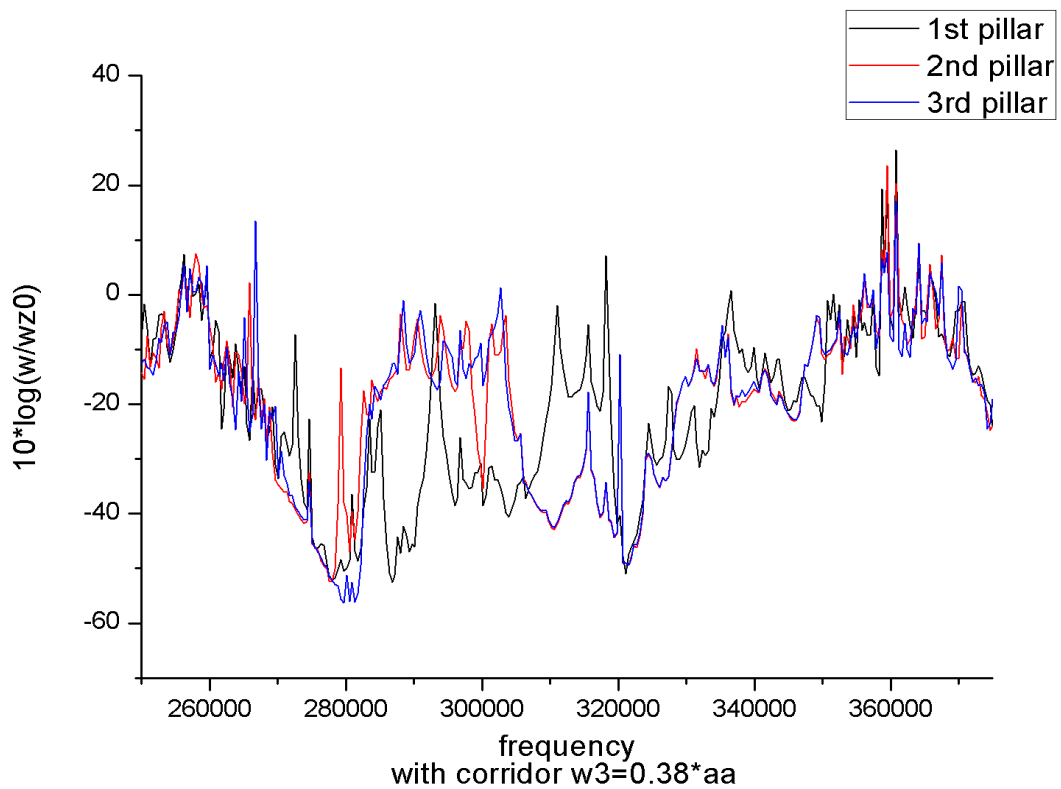
Figure 5.15: Transmission of all multi-super cells with corridor of ww= 0.38*aa by removing one pillar.

Figures (5.10a, 5.10b, 5.10c) are resumed in (Figure 5.13), and Figures (5.11a, 5.11b, 5.11c) are resumed in (Figure 5.14), and Figures (5.12a, 5.12b, 5.12c) are resumed in (Figure 5.15).

In these previous transmission curves we notice that when we're going deeper in removing pillars the band-gap become thinner for ww= 0.22*aa. For example; when we remove the first pillar the band-gap is between [261000Hz – 325000Hz], and when we remove the second and the third pillar the band-gap is between [263000Hz – 314000Hz]. Also, we remark a resonance peak when we remove a pillar; we can see that the resonance peak is moving to the right when we go deeper when removing pillars. For example; when we remove the first pillar the resonance peak is freq=2.8133e5 Hz, for the second pillar it's freq=2.9348e5 Hz, for the third pillar it's freq=2.9682e5 Hz.

For ww= 0.30*aa and ww= 0.38*aa we observe the same behavior when we remove a pillar inside our structure. The band-gap is between [270000Hz – 300000Hz] for ww= 0.30*aa, and for the ww= 0.38*aa the band-gap is between [270000Hz – 282000Hz]. We conclude that more the corridor's width is large more the band-gap is thin. And for the resonance peak of ww=0.30*aa is moving to the right each time we remove a pillar. For example; when we remove the first pillar the resonance peak is freq=2.7634e5 Hz, for the second pillar it's freq=2.8888e5 Hz, for the third pillar it's freq=2.9766e5 Hz. Finally, for ww=0.38*aa the resonance peak has also the same behavior of the previous corridors but appear in strange positions. For example; for the first pillar the resonance peak is freq=2.7174e5 Hz, for the second pillar it's freq=2.9222e5 Hz, for the third pillar it's freq=2.9766e5 Hz.

For ww= 0.22*aa the attenuation of the incident wave is very strong when we remove the first pillar, and it's almost -80dB. But for the other two, it's between -70dB and -68dB. But when ww= 0.30*aa and ww= 0.38*aa the attenuation is very weak when we compare it to the first corridor.

More the width of the corridor is large more the Q factor is very high, and we get a perfect selectivity that leads to a better transmission of the information.

General conclusion

For over twenty years, scientists have been structuring and manufacturing Phononic crystals for their ability to prohibit the propagation of acoustic/elastic waves in frequency ranges called Phononic forbidden bands.

In the first part of this viva, we especially highlighted the research work carried out in the field of wave propagation in composite structures. Depicted in Chapter 1, we have inspected a portion of the significant issues concerning the disclosure and hypothetical and exploratory exhibit of a few astounding practices showed by these crystals.

In chapter 2, we mentioned some theoretical formulations that control the Phononic crystals behavior and we finished this chapter by identifying the FEM and general principal.

In the second part of our viva, we used (Comsol Multiphysics 5.4) and we made different structures with different condition, and we studied the dispersion part and the transmission part, these simulations allowed us to predict "Lane" waveguides that dispose only for specific frequencies and this frequency separation makes it possible to have the highly demultiplexing function that we need in our RFMEMS.

Finally, this work will be more developed in the future by using it in particle sorting that will allow us to separate particles who has specific directional vibrations, also we can use it in drug deliveries and drug manufacturing by controlling particle by particle in injecting or creating medicines and many other things.

In this work, we have treated many structures using few different conditions, this work should be continued in order to get more properties using different shapes and different conditions and different materials to apply it in the real life.

References

[1]   J. D. Joannopoulos, S. G. Johnson, J. N. Winn, and R. D. Meade, "Photonic crystals molding the flow of light Second edition introduction," *Photonic Cryst. Molding Flow Light.*, pp. 1–5, 2008.

[2]   Z. Zhang and S. Satpathy, "Electromagnetic wave propagation in periodic structures: Bloch wave solution of Maxwell's equations," *Phys. Rev. Lett.*, vol. 65, no. 21, p. 2650, 1990.

[3]   R. D. Meade, K. D. Brommer, A. M. Rappe, and J. D. Joannopoulos, "Existence of a photonic band gap in two dimensions," *Appl. Phys. Lett.*, vol. 61, no. 4, pp. 495–497, 1992.

[4]   U. Grüning, V. Lehmann, and C. M. Engelhardt, "Two- dimensional infrared photonic band gap structure based on porous silicon," *Appl. Phys. Lett.*, vol. 66, no. 24, pp. 3254–3256, 1995.

[5]   T. F. Krauss, M. Richard, and S. Brand, "Two-dimensional photonic-bandgap structures operating at near-infrared wavelengths," *Nature*, vol. 383, no. 6602, pp. 699–702, 1996.

[6]   S. I. Tamura, D. C. Hurley, and J. P. Wolfe, "Acoustic-phonon propagation in superlattices," *Phys. Rev. B*, vol. 38, no. 2, p. 1427, 1988.

[7]   M. M. Sigalas and E. N. Economou, "Elastic and acoustic wave band structure," *J. Sound Vib.*, vol. 158, no. 2, pp. 377–382, 1992.

[8]   M. Sigalas and E. N. Economou, "Band structure of elastic waves in two dimensional systems," *Solid State Commun.*, vol. 86, no. 3, pp. 141–143, 1993.

[9]   M. S. Kushwaha, P. Halevi, L. Dobrzynski, and B. Djafari-Rouhani, "Acoustic band structure of periodic elastic composites," *Phys. Rev. Lett.*, vol. 71, no. 13, p. 2022, 1993.

[10]   M. S. Kushwaha, P. Halevi, G. Martinez, L. Dobrzynski, and B. Djafari-Rouhani, "Theory of acoustic band structure of periodic elastic composites," *Phys. Rev. B*, vol. 49, no. 4, p. 2313, 1994.

[11]   M. M. Sigalas and E. N. Economou, "Attenuation of multiple-scattered sound," *EPL (Europhysics Lett.*, vol. 36, no. 4, p. 241, 1996.

[12]   M. M. Sigalas and E. N. Economou, "Elastic waves in plates with periodically placed inclusions," *J. Appl. Phys.*, vol. 75, no. 6, pp. 2845–2850, 1994.

[13]   M. M. Sigalas, "Elastic wave band gaps and defect states in two-dimensional composites," *J. Acoust. Soc. Am.*, vol. 101, no. 3, pp. 1256–1261, 1997.

[14]   J. B. Pendry and A. MacKinnon, "Calculation of photon dispersion relations," *Physical Review Letters*, vol. 69, no. 19. pp. 2772–2775, 1992, doi: 10.1103/PhysRevLett.69.2772.

[15] M. M. Sigalas and N. García, "Theoretical study of three dimensional elastic band Design, fabrication and characterization of Phononic crystals in macro and micro scale gaps with the finite-difference time-domain method," *J. Appl. Phys*, vol. 87, p. 3122, 2000.

[16] Y. Tanaka, Y. Tomoyasu, and S. I. Tamura, "Band structure of acoustic waves in phononic lattices: Two-dimensional composites with large acoustic mismatch," *Phys. Rev. B - Condens. Matter Mater. Phys.*, vol. 62, no. 11, pp. 7387–7392, 2000, doi: 10.1103/PhysRevB.62.7387.

[17] T. Miyashita and C. Inoue, "Numerical investigations of transmission and waveguide properties of sonic crystals by finite-difference time-domain method," *Jpn. J. Appl. Phys.*, vol. 40, no. 5S, p. 3488, 2001.

[18] A. Khelif, B. Djafari-Rouhani, V. Laude, and M. Solal, "Coupling characteristics of localized phonons in photonic crystal fibers," *J. Appl. Phys.*, vol. 94, no. 12, pp. 7944–7946, 2003, doi: 10.1063/1.1627946.

[19] A. Khelif, A. Choujaa, S. Benchabane, B. Djafari-Rouhani, and V. Laude, "Guiding and bending of acoustic waves in highly confined phononic crystal waveguides," *Appl. Phys. Lett.*, vol. 84, no. 22, pp. 4400–4402, 2004, doi: 10.1063/1.1757642.

[20] Z.-Z. Yan and Y.-S. Wang, "Wavelet-based method for calculating elastic band gaps of two-dimensional phononic crystals," *Phys. Rev. B*, vol. 74, no. 22, p. 224303, 2006.

[21] A. Khelif, B. Aoubiza, S. Mohammadi, A. Adibi, and V. Laude, "Complete band gaps in two-dimensional phononic crystal slabs," *Phys. Rev. E - Stat. Nonlinear, Soft Matter Phys.*, vol. 74, no. 4, pp. 1–5, 2006, doi: 10.1103/PhysRevE.74.046610.

[22] J. H. Page, P. Sheng, H. P. Schriemer, I. Jones, X. Jing, and D. A. Weitz, "Group velocity in strongly scattering media," *Science (80-.).*, vol. 271, no. 5249, pp. 634–637, 1996.

[23] H. P. Schriemer, M. L. Cowan, J. H. Page, P. Sheng, Z. Liu, and D. A. Weitz, "Energy velocity of diffusing waves in strongly scattering media," *Phys. Rev. Lett.*, vol. 79, no. 17, p. 3166, 1997.

[24] M. M. Sigalas, "Defect states of acoustic waves in a two-dimensional lattice of solid cylinders," *J. Appl. Phys.*, vol. 84, no. 6, pp. 3026–3030, 1998.

[25] J. O. Vasseur *et al.*, "Waveguiding in two-dimensional piezoelectric phononic crystal plates," *J. Appl. Phys.*, vol. 101, no. 11, 2007, doi: 10.1063/1.2740352.

[26] A. Khelif, M. Wilm, V. Laude, S. Ballandras, and B. Djafari-Rouhani, "Guided elastic waves along a rod defect of a two-dimensional phononic crystal," *Phys. Rev. E - Stat. Physics, Plasmas, Fluids, Relat. Interdiscip. Top.*, vol. 69, no. 6, p. 4, 2004, doi: 10.1103/PhysRevE.69.067601.

[27] C. Qiu and Z. Liu, "Acoustic directional radiation and enhancement caused by band-edge states of two-dimensional phononic crystals," *Appl. Phys. Lett.*, vol. 89, no. 6, p. 63106, 2006.

[28] Z. Liu *et al.*, "Locally resonant sonic materials," *Science (80-.).*, vol. 289, no. 5485, pp. 1734–1736, 2000.

[29] W. Xiao, G. W. Zeng, and Y. S. Cheng, "Flexural vibration band gaps in a thin plate containing a periodic array of hemmed discs," *Appl. Acoust.*, vol. 69, no. 3, pp. 255–261, 2008.

[30] J. B. Pendry, "Negative refraction makes a perfect lens," *Phys. Rev. Lett.*, vol. 85, no. 18, p. 3966, 2000.

[31] M. Oudich, "Contribution à l'étude des cristaux phononiques à résonance locale dans les régimes sonique et hypersonique: approches théorique et expérimentale." Université Henri Poincaré-Nancy 1, 2011.

[32] A. Amrane, "PERSPECTIVES D'UTILISATION DES RESEAUX PERIODIQUES POUR L'ISOLATION DE STRUCTURES SOUMISES AUX VIBRATIONS D'ORIGINE SISMIQUES OU MECANIQUES," p. 178, 2019.

[33] R. P. MOISEYENKO, "DIFFRACTION DANS LES CRISTAUX PHONONIQUES."

[34] "Lord Rayleigh, Proc. London Math. Soc. 17, 4 (1885)." .

[35] C. Droit, "Système d'interrogation à distance de grandeurs physiques à base de capteurs à ondes élastiques de surface pour mesures paramétriques sur une gamme de température étendue (-196/+ 650ºC)." 2013.

[36] B. A. Auld, *Acoustic fields and waves in solids*. Volume II, 1973.

[37] H. Maillou, C. D. E. Cours, H. Maillou, and B. T. S. Aeronautique, "Les Procédés de Mesures Et De Contrôle," pp. 0–14.

[38] N. Omar, "Etude théorique et numérique d'une structure périodique pour l'isolation phonique," p. 87, 2017.

[39] T. Tsutaoka, T. Tokunaga, T. Umeda, and T. Maehara, "Observation of the two-dimensional reciprocal lattice by use of lattice grating sheets and a laser pointer," *Eur. J. Phys.*, vol. 35, no. 5, 2014.

[40] Sedik KHEFFACHE, "Propagation d'ondes élastiques dans les cristaux phononiques bidimensionnels," p. 52, 2011.

[41] A. Khelif and A. Adibi, *Phononic Crystals*. Springer, 2015.

[42] Z. Liu *et al.*, "Locally resonant sonic materials," *Science (80-.).*, vol. 289, no. 5485, pp. 1734–1736, 2000, doi: 10.1126/science.289.5485.1734.

[43] P. Sheng, X. X. Zhang, Z. Liu, and C. T. Chan, "Locally resonant sonic materials," *Phys. B Condens. Matter*, vol. 338, no. 1–4, pp. 201–205, 2003.

[44] Z. Liu, C. T. Chan, and P. Sheng, "Analytic model of phononic crystals with local resonances," *Phys. Rev. B*, vol. 71, no. 1, p. 14103, 2005.

[45] G. Wang, D. Yu, J. Wen, Y. Liu, and X. Wen, "One-dimensional phononic crystals with locally resonant structures," *Phys. Lett. A*, vol. 327, no. 5–6, pp. 512–521, 2004.

[46] Z. Liu, C. T. Chan, and P. Sheng, "Three-component elastic wave band-gap material," *Phys. Rev. B*, vol. 65, no. 16, p. 165116, 2002.

[47] D. R. Smith, W. J. Padilla, D. C. Vier, S. C. Nemat-Nasser, and S. Schultz, "Composite medium with simultaneously negative permeability and permittivity," *Phys. Rev. Lett.*, vol. 84, no. 18, p. 4184, 2000.

[48] H. Kosaka *et al.*, "Superprism phenomena in photonic crystals," *Phys. Rev. B*, vol. 58, no. 16, p. R10096, 1998.

[49] J. Chen *et al.*, "Observation of the inverse Doppler effect in negative-index materials at optical frequencies," *Nat. Photonics*, vol. 5, no. 4, pp. 239–242, 2011.

[50] áM Notomi, "Theory of light propagation in strongly modulated photonic crystals: Refractionlike behavior in the vicinity of the photonic band gap," *Phys. Rev. B*, vol. 62, no. 16, p. 10696, 2000.

[51] X. Hu, C. T. Chan, and J. Zi, "Two-dimensional sonic crystals with Helmholtz resonators," *Phys. Rev. E*, vol. 71, no. 5, p. 55601, 2005.

[52] G. W. Milton and J. R. Willis, "On modifications of Newton's second law and linear continuum elastodynamics," *Proc. R. Soc. A Math. Phys. Eng. Sci.*, vol. 463, no. 2079, pp. 855–880, 2007.

[53] M. Hirsekorn, "Addendum:'Small-size sonic crystals with strong attenuation bandsin the audible frequency range'[Appl. Phys. Lett. 84, 3364 (2004)]," *Appl. Phys. Lett.*, vol. 85, no. 6, p. 1088, 2004.

[54] H. Khales, A. Hassein-Bey, and A. Khelif, "Evidence of ultrasonic band gap in aluminum phononic crystal beam," *J. Vib. Acoust. Trans. ASME*, vol. 135, no. 4, pp. 1–4, 2013, doi: 10.1115/1.4023827.

[55] A. Khelif, A. Choujaa, B. Djafari-Rouhani, M. Wilm, S. Ballandras, and V. Laude, "Trapping and guiding of acoustic waves by defect modes in a full-band-gap ultrasonic crystal," *Phys. Rev. B*, vol. 68, no. 21, p. 214301, 2003.

[56] J. Sánchez-Dehesa and A. Krokhin, "Introduction to acoustics of phononic crystals. Homogenization at low frequencies," in *Phononic Crystals*, Springer, 2016, pp. 1–21.

[57] F. R. M. De Espinosa, E. Jimenez, and M. Torres, "Ultrasonic band gap in a periodic two-dimensional composite," *Phys. Rev. Lett.*, vol. 80, no. 6, p. 1208, 1998.

[58] J. O. Vasseur, P. A. Deymier, G. Frantziskonis, G. Hong, B. Djafari-Rouhani, and L. Dobrzynski, "Experimental evidence for the existence of absolute acoustic band gaps in two-dimensional periodic composite media," *J. Phys. Condens. Matter*, vol. 10, no. 27, p. 6051, 1998.

[59] F.-C. Hsu, C.-I. Lee, J.-C. Hsu, T.-C. Huang, C.-H. Wang, and P. Chang, "Acoustic band gaps in phononic crystal strip waveguides," *Appl. Phys. Lett.*, vol. 96, no. 5, p. 51902, 2010.

[60] G. L. Chahine, K. M. Kalumuck, J.-Y. Cheng, and G. Frederick, "Validation of bubble distribution measurements of the ABS acoustic bubble spectrometer with high speed video photography," *http//resolver. caltech. edu/cav2001 Sess. 004*, 2001.

[61] "https://webcache.googleusercontent.com/search?q=cache:SxgzJV01gNsJ:https://www.yumpu.com/fr/document/view/16515719/des-materiaux-composites-pour-de-nouveaux-isolants-cnrs+&cd=1&hl=fr&ct=clnk&gl=dz." .

[62] A. Khelif, S. Mohammadi, A. A. Eftekhar, A. Adibi, and B. Aoubiza, "Acoustic confinement and waveguiding with a line-defect structure in phononic crystal slabs," *J. Appl. Phys.*, vol. 108, no. 8, p. 84515, 2010.

[63] Y. Pennec, J. O. Vasseur, B. Djafari-Rouhani, L. Dobrzyński, and P. A. Deymier, "Two-dimensional phononic crystals: Examples and applications," *Surf. Sci. Rep.*, vol. 65, no. 8, pp. 229–291, 2010.

[64] Y. Pennec, "Propagation et localisation des ondes élastiques et électromagnétiques dans les matériaux phononiques, photoniques et plasmoniques." 2010.

[65] Y. Pennec and B. Djafari-Rouhani, "Fundamental properties of phononic crystal," in *Phononic Crystals*, Springer, 2016, pp. 23–50.

[66] S. Mohammadi, A. Khelif, and A. Adibi, "Future Prospects of Phononic Crystals and Phononic Metamaterials," in *Phononic Crystals*, Springer, 2016, pp. 239–245.

[67] C. Coste, "Ondes élastiques dans les solides isotropes," 2016.

[68] K. Billon, M. Ouisse, E. Sadoulet-Reboul, and M. Collet, "Outils Numériques pour la Simulation de Propagation d'Ondes dans les Structures Périodiques Amorties," 2015.

[69] S. Benchabane, "Guidage et filtrage des ondes dans les cristaux phononiques." 2006.

[70] D. ROYER and E. DIEULESAINT, "Acoustique-Propagation dans un solide," 2001.

[71] G. Qiu, F. Lin, and Y. P. Li, "Complete two-dimensional bandgap of photonic crystals of a rectangular Bravais lattice," *Opt. Commun.*, vol. 219, no. 1–6, pp. 285–288, 2003.

[72] T.-C. Wu, T.-T. Wu, and J.-C. Hsu, "Waveguiding and frequency selection of Lamb waves in a plate with a periodic stubbed surface," *Phys. Rev. B*, vol. 79, no. 10, p. 104306, 2009.

[73] "T.B.Y.Comsol,"No Title", P.Comsol AB (2009,April). [Online]. Available: http, 2009." .

[74] "I.Management, 'APPLICATIONS OF COMSOL MULTIPHYSICS SOFTWARE TO', 2010." .

[75] "A.C.M.H. COMSOL AB (2009). COMSOL AB (2009,April). COMSOL Multiphysics Handbook, 2009." .

[76] G. Mahfoud, "Immobilized enzyme In PDMS substrate reaction modeling and Simulation for specific protein detection in biosensor," p. 78, 2019.

[77] "M.Hanke, 'Short Introduction to Comsol Multiphysics Starting Comsol Multiphysics', pp. 1-6, 2006." .

[78] "Q. Li, K. Ito, Z. Wu, C. S. Lowry, and S.P.L.li, 'COMSOL Multiphysics : A Novel Approach to Ground Water Modeling', vol. 47, no. 4, 2009." .

[79] "COMSOL AB, Multiphysics COMSOL QUICK START AND QUICK REFERENCE." .

[80] "Q. W. Thesis, 'Mathematical Methods for Biosensor Models'." .

[81] "O. Š. M. Sapagovas, A. Štikonas, 'Alternating direction method for the Poisson equation with variable weight coefficients in an integral'." .

[82] "Xia,Y. & Whitesides, G. M. Soft Lithography. Angew. Chem. Int. Ed. 37, 550-575 (1998)." .

[83] "Piruska, A. et al. The autofluorescence of plastic materials and chips measured under laser irradiation. Lab. Chip 5, 1348-1354 (2005)." .

[84] "Hua, F. et al. Polymer Imprint Lithography with Molecular-Scale Resolution. Nano Lett. 4, 2467-2471 (2004)." .

[85] "Yoo E.H, Lee S.Y. Glucose biosensors: an overview of use in clinical practice. Sensors. 2010;10:4558-4576." .

[86] "COMSOL Multiphysics 4.3a, 'COMSOL Documentation'. (2012)." .